STUDIES ON SOME METAL COMPLEXES OF BIOLOGICALLY IMPORTANT LIGANDS

A thesis submitted to the
Cochin University of Science and Technology
in partial fulfilment
of the requirements for the degree of

DOCTOR OF PHILOSOPHY

in

CHEMISTRY

under the Faculty of science

By

R - SREEKALA

DEPARTMENT OF APPLIED CHEMISTRY

COCHIN UNIVERSITY OF SCIENCE AND TECHNOLOGY

KOCHI - 682 022, KERALA

JULY 1991

CERTIFICATE

This is to certify that the thesis bound herewith is an authentic record of research work carried out by the author under my supervision in partial fulfilment of the requirements for the degree of Doctor of Philosophy of Cochin University of Science and Technology, and further that no part thereof has been presented before for any other degree.

DR. K. K. MOHAMMED YUSUFF
(Supervising Teacher)

PREFACE

The thesis deals with our studies on the synthesis and characterization of new metal complexes of some biologically important ligands such as substituted benzimidazoles, quinoxaline-2-carboxalideneglycine and quinoxaline-2-carboxaldehyde thiosemicarbazone.

The thesis is divided into nine chapters: Chapter I presents an introduction to the chemistry of the metal complexes of substituted benzimidazoles, Schiff bases derived from amino acids, and thiosemicarbazones, with emphasis on recent literature and on aspects relevant to the theme of the present work. The scope of the present investigation is outlined at the concluding section of this chapter.

The details of the preparation and purification of the ligands employed in the study are given in Chapter II. Furthermore, the various characterization techniques employed are also described in this chapter.

Chapters III and IV of the thesis deal with studies on the metal complexes of 1-benzyl-2-phenylbenzimidazole (BPBI) and 1-(2'-hydroxybenzyl)-2-(2'-hydroxyphenyl)-benzimidazole (HBHPBI) respectively. These ligands are interesting from the point of view of their bulkiness

and the consequent steric effects they might cause during complexation. While Chapter III describes the synthesis and characterization of cobalt(II) complexes of BPBI, those of iron(III), cobalt(II), nickel(II) and copper(II) complexes of HBHPBI are described in Chapter IV.

The thermal behaviour of the complexes mentioned in Chapters III and IV was investigated by the techniques of non-isothermal thermogravimetry (TG), derivative thermogravimetry (DTG) and differential thermal analysis (DTA). The main decomposition steps in TG were subjected to mathematical analysis for evaluating the kinetic parameters of the decomposition process. Details of these studies are given in Chapter V. Chapter VI of the thesis describes the synthesis and characterization of some lanthanide complexes of HBHPBI.

In an attempt to study the influence of polymer back bone on the donor properties of benzimidazole, we have synthesized a benzimidazole based Schiff base by condensing 2-aminobenzimidazole with polystyrene bound aldehyde. Some mixed ligand cobalt(II) complexes containing this polymer ligand and BPBI or *meso*-tetraphenylporphyrin have been synthesized and characterized. Studies on these complexes are presented in Chapter VII.

Chapters VIII and IX of the thesis deal with the studies on some other complexes of Schiff bases derived from the condensation of quinoxaline-2-carboxaldehyde with glycine as well as with thiosemicarbazide. Synthesis and characterization of some new iron(III), cobalt(II), nickel(II) and copper(II) complexes of quinoxaline-2-carboxalideneglycine are presented in Chapter VIII, while those of cobalt(III), nickel(II) and copper(II) complexes of quinoxaline-2-carboxaldehyde thiosemicarbazone, are presented in Chapter IX.

Results described in this thesis have been published/are under publication as indicated below:

1. "Thermal and spectral studies of 1-benzyl-2-phenylbenzimidazole complexes of cobalt(II)", K. K. M. Yusuff and R. Sreekala, *Thermochim. Acta,* 159, 357 (1990).

2. "Thermal and spectral studies of 1-(2'-hydroxybenzyl)-2-(2'-hydroxyphenyl)benzimidazole complexes of iron(III), cobalt(II), nickel(II) and copper(II)", K. K. M. Yusuff and R. Sreekala, *Thermochim. Acta,* 179, 313(1991).

3. "New complexes of iron(III), cobalt(II), nickel(II) and copper(II) with Schiff base derived from

quinoxaline-2-carboxaldehyde and glycine", K. K. M. Yusuff and R. Sreekala, *Synth. React. Inorg. Met.-Org. Chem.*, (in press).

4. "Synthesis and characterization of lanthanide(III) complexes of 1-(2'-hydroxybenzyl)-2-(2'-hydroxyphenyl)benzimidazole", K. K. M. Yusuff and R. Sreekala, *Synth. React. Inorg. Met.-Org. Chem.*, (in press).

5. "New complexes of cobalt(III), nickel(II) and copper(II) with quinoxaline-2-carboxaldehyde thiosemicarbazone", (communicated).

CONTENTS

		Page No.
CHAPTER I	INTRODUCTION	1
	1.1 Metal complexes of benzimidazoles	6
	1.1.1 *Introduction*	6
	1.1.2 *X-Ray crystallographic studies*	7
	1.1.3 *Magnetic susceptibility measurements*	16
	1.1.4 *Electronic spectra*	26
	1.1.5 *EPR spectra*	27
	1.1.6 *Infrared spectra*	28
	1.1.7 *Biological importance*	34
	1.2 Metal complexes of Schiff bases derived from amino acids	40
	1.3 Metal complexes of thiosemicarbazones	48
	1.3.1 *Introduction*	48
	1.3.2 *X-Ray crystallographic studies*	50
	1.3.3 *Magnetic susceptibility measurements*	57
	1.3.4 *Electronic spectra*	66
	1.3.5 *EPR spectra*	67
	1.3.6 *Infrared spectra*	71
	1.3.7 *Biological importance*	72
	1.4 Scope of the present investigation	77
CHAPTER II	EXPERIMENTAL TECHNIQUES	80
	2.1 Reagents	80
	2.2 Preparation of ligands	82
	2.2.1 *1-Benzyl-2-phenylbenzimidazole*	82
	2.2.2 *1-(2'-hydroxybenzyl)-2-(2'-hydroxyphenyl)benzimidazole*	83
	2.2.3 *Polymer bound Schiff base*	83

2.2.4 *meso-Tetraphenylporphyrin* 83

2.2.5 *Quinoxaline-2-carboxaldehyde thiosemicarbazone* 84

2.3 **Analytical methods** 85

2.3.1 *Estimation of metals* 85

2.3.2 *CHN analyses* 87

2.3.3 *Estimation of halogen and sulphur* 87

2.4 **Physico-chemical methods** 88

2.4.1 *Conductance measurements* 88

2.4.2 *Magnetic susceptibility measurements* 88

2.4.3 *Electronic spectra* 89

2.4.4 *Infrared spectra* 89

2.4.5 ^{1}H *NMR spectra* 90

2.4.6 *EPR spectra* 90

2.4.7 *Thermogravimetry* 90

2.4.8 *Differential thermal analysis* 91

CHAPTER III 1-BENZYL-2-PHENYLBENZIMIDAZOLE COMPLEXES OF COBALT(II) 92

3.1 **Introduction** 92

3.2 **Experimental** 93

3.2.1 *Materials* 93

3.2.2 *Synthesis of the complexes* 93

3.2.3 *Analytical methods* 94

3.3 **Results and discussion** 94

3.3.1 *Magnetic susceptibility measurements* 97

3.3.2 *Electronic spectra* 97

3.3.3 *Infrared spectra* 99

3.3.4 ^{1}H *NMR spectra* 103

CHAPTER IV 1-(2'-HYDROXYBENZYL)-2-(2'-HYDROXYPHENYL)-BENZIMIDAZOLE COMPLEXES OF IRON(III), COBALT(II), NICKEL(II) AND COPPER(II) 104

4.1 Introduction 104

4.2 Experimental 105

4.2.1 *Materials* 105

4.2.2 *Synthesis of the complexes* 105

4.2.3 *Analytical methods* 105

4.3 Results and discussion 106

4.3.1 *Magnetic susceptibility measurements* 106

4.3.2 *Electronic spectra* 109

4.3.3 *Infrared spectra* 111

CHAPTER V THERMAL STUDIES OF 1,2-DISUBSTITUTED BENZIMIDAZOLE COMPLEXES OF IRON(III), COBALT(II), NICKEL(II) AND COPPER(II) 116

5.1 Introduction 116

5.2 Experimental 117

5.3 Results and discussion 119

5.3.1 *Thermal studies of the cobalt(II) complexes of 1-benzyl-2-phenylbenzimidazole* 119

5.3.2 *Thermal studies of the Fe(III), Co(II) Ni(II) and Cu(II) complexes of 1-(2'-hydroxybenzyl)-2-(2'-hydroxyphenyl)-benzimidazole* 126

APPENDIX 133

CHAPTER VI LANTHANIDE(III) COMPLEXES OF 1-(2'-HYDROXYBENZYL)-2-(2'-HYDROXYPHENYL)-BENZIMIDAZOLE 138

6.1 Introduction 138

6.2 Experimental 138

6.2.1 *Materials* 138
6.2.2 *Synthesis of the complexes* 139
6.2.3 *Analytical methods* 139

6.3 Results and discussion 139

6.3.1 *Electronic spectra* 140
6.3.2 *Infrared spectra* 144

CHAPTER VII STUDIES ON SOME POLYMER BOUND COBALT(II) COMPLEXES 150

7.1 Introduction 150

7.2 Experimental 152

7.2.1 *Materials* 152
7.2.2 *Synthesis of the complexes* 153
7.2.3 *Analytical methods* 153

7.3 Results and discussion 154

7.3.1 *Magnetic susceptibility measurements* 156
7.3.2 *EPR spectra* 158
7.3.3 *Electronic spectra* 160
7.3.4 *Infrared spectra* 162

CHAPTER VIII COMPLEXES OF IRON(III), COBALT(II), NICKEL(II) AND COPPER(II) WITH THE SCHIFF BASE DERIVED FROM QUINOXALINE-2-CARBOXALDEHYDE AND GLYCINE 167

8.1 Introduction 167

8.2 Experimental 168

8.2.1 *Materials* 168
8.2.2 *Synthesis of the complexes* 168
8.2.3 *Analytical methods* 169

8.3 Results and discussion 169

8.3.1 *Magnetic susceptibility measurements* 171
8.3.2 *Electronic spectra* 171
8.3.3 *Infrared spectra* 174
8.3.4 *Thermal analysis* 177

CHAPTER IX COMPLEXES OF COBALT(II), NICKEL(II) AND COPPER(II) WITH QUINOXALINE-2-CARBOXALDEHYDE THIOSEMICARBAZONE 180

9.1 Introduction 180

9.2 Experimental 181

9.2.1 *Materials* 181
9.2.2 *Synthesis of the complexes* 181
9.2.3 *Analytical methods* 182

9.3 Results and discussion 182

9.3.1 ^{1}H *NMR spectra* 186
9.3.2 *Magnetic susceptibility measurements* 187
9.3.3 *Electronic spectra* 188
9.3.4 *Infrared spectra* 190

SUMMARY 195

REFERENCES 200

CHAPTER I

INTRODUCTION

Over the last decade or so there has been a growing awareness of the role of a wide range of metallic and non-metallic elements in biological systems. Metal ions are a key factor in the structural organization of biochemical molecules and the functional processes operating in the genetic and metabolic apparatus[1]. When a small molecule is coordinated to a metal ion, it undergoes several changes which can dramatically alter its reactivity[2,3]. Since the appearance of water on Earth, aqua complex ions of metals must have existed. The subsequent appearance of life depended on, and may even have resulted from interaction of metal ions with organic molecules. Studies on these aspects are now part of the emerging field, bioinorganic chemistry.

The scope of bioinorganic chemistry is very broad, stretching from chemical physics to clinical medicine. The general upsurge of interest in this field is connected with (1) improved analytical methods, (2) less time-consuming preparative techniques, (3) the successful application of spectroscopy and diffraction techniques, (4) the improved synthesis of simple

inorganic complexes used to model or mimic various aspects of biological molecules, (5) the increased concern about the environmental hazards caused by some metal ions, (6) the use of metal ions or complexes as therapeutic agents and (7) the recognition of the importance of an increasing number of trace elements in plant, animal and human nutrition.

In recent years it has been recognized that bioinorganic chemistry is a bridge between the academic disciplines of biochemistry and inorganic chemistry. In 1975, Wood made the salient point that "biochemistry is the coordination chemistry of living systems"[4]. This dependence is well exemplified by the observation that one third of all enzymes have a metal ion as an essential component[5]; besides, it has been reported that almost all globular proteins bind a wide range of metal ions[6]. Studies on simple metal complexes of biologically active ligands are important since they can sometimes be considered as models of the more complex biological systems[7-11]. The living cell is so complex that its functions can be understood only by studying simple model systems. The literature relevant to this topic was first reviewed[12] by Guard and Wilcox in 1956.

The quest of a coordination chemist is directed at acquiring a deeper understanding of the natural

processes in which metal ions act as catalysts as well as at acquiring the competence to design more effective catalysts for a variety of metal catalysed ligand reactions. With this in view, a large number of metal complexes of biologically important ligands have been synthesized and studied. The most prominent among them, are the complexes of porphyrins[13-15].

Porphyrins are tetrapyrrole macrocycles which lose two protons on coordination to metal ions. The tetradentate dianionic ligand forms metal complexes which are basically planar; but because of some flexible nature of the ligand, the complexes may be slightly distorted. One of the most widespread porphyrin complex from the point of view of occurence in a variety of organisms and partcipation in a variety of functions is heme, an iron(II) porphyrin. Attached to proteins, heme is involved in an array of physiological processes: Hemoglobin and myoglobin act as oxygen carriers and the cytochromes are involved in redox systems. Chlorophyll occuring in green plants is a magnesium-porphyrin complex containing a modified ring system. These metalloporphyrin complexes are biologically accessible compounds whose functions can be varied by changing the metal ion, its oxidation state, or the nature of the organic substituents on the porphyrin structure. Reviews on the various aspects of porphyrin and

metalloporphyrin chemistry have appeared in the literature[16-18].

Metal complexes find wide applications not only in the field of biochemistry and catalysis, but also in the field of medicine[19]. The empirical use of inorganic substances in medicine has its origin in antiquity. For example, in the 4th century B. C., Hippocrates recommended the medicinal use of metallic salts. Nevertheless it is only in recent times, following the advances in chemistry, biochemistry and related disciplines, that logical bases have been established for understanding the role of inorganic species in medicine.

In many cases it is known that metal complexes of ligands which have biological activity are more active than free ligands[20,21]. The activity of some of the antimicrobial drugs is dependent upon the complexing ability of these drugs with metal ions. Metal complexes of the drugs are often more lipophilic than the drugs themselves and thus facilitate the transportation of the drugs across the cell membrane. For antibacterial and antifungal activity it is often advantageous if the metal chelate is lipid soluble so that penetration of the cell is enhanced[22]. 8-Hydroxyquinoline has antifungal and antibacterial properties only when

chelated to Fe(III). Albert has shown that this ligand and Fe(III) are both inactive when separated from each other, but are highly effective together, particularly when present in 1:1 molar ratio. It appears that the metal ion is necessary for the entry of the oxine molecule into the cell[23]. Similar type of metal ion involvement has been noticed in the activity of tetracyclines. The metal ion itself might be the toxic agent. An excess of toxic metal ion in the living system can be removed using a chelating agent. D-Pencillamine is known to be a good chelating agent for the excretion of Cu ions in patients with Wilson's disease, and hence finds use in controlling this disease. Earliest reviews on chelating agents in medicine date back to 30 years[24] and have continued to appear ever since with fluctuating frequency[25-30].

METAL COMPLEXES OF SOME BIOLOGICALLY IMPORTANT LIGANDS

We wish to review here some aspects of the metal complexes of biologically important ligands. We shall limit our interest to the iron, cobalt, nickel and copper complexes of benzimidazoles, Schiff bases derived from amino acids, and thiosemicarbazones as our present study is on these types of complexes.

1.1 METAL COMPLEXES OF BENZIMIDAZOLES

1.1.1 Introduction

Benzimidazoles play a significant role in determining the function of a number of biologically important metal complexes[31]. Benzimidazole is a planar molecule, as expected for an aromatic system. The resonance energies of benzimidazole and naphthalene are comparable. The benzimidazoles contain a phenyl ring fused to an imidazole ring as shown in Fig. 1.1. Benzimidazoles which contain a hydrogen atom attached to nitrogen readily tautomerise.

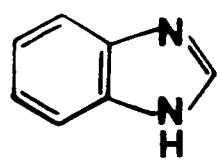

Fig. 1.1 Structure of benzimidazole

Imidazole and benzimidazole are amphoteric in nature. They are moderately strong organic bases capable of accepting protons at N-3 as well as weak acids capable of losing a proton from N-1. Therefore in neutral solutions the unprotonated molecule usually functions as a unidentate ligand through the unshared pair of electrons on N-3. The probability of participation of the pair of electrons on N-1 in

coordination is very small, because these electrons are delocalized throughout the π-system. However, neutral imidazole undergoes deprotonation at N-1 in strongly basic solution, and the resulting aromatic imidazolate ion possesses two equivalent sites for coordination[32,33].

Fusion of benzene ring at position 4 and 5 in benzimidazole does not perturb the electronic configuration of the heterocyclic ring or alter the properties considerably from that of imidazole. However, due to the increased size of the ligand, the maximum number of benzimidazole molecules that has been reported to coordinate with a metal ion is four[34]. A very large number of research papers have been published on transition metal complexes of benzimidazole derivatives. While some of the reports are on the applied aspects of these complexes such as their role in the protection of metals from corrosion, their use as antifungal, antibacterial, antiviral and antifouling agents etc., a large number of papers deal with the syntheses and structural studies of these complexes.

1.1.2 X-Ray crystallographic studies

The results of X-ray studies are described first because they yield conclusive information about structure of the complexes. Due to the large angular distortion of nitrogen atom of benzimidazole

derivatives, most of the metal complexes adopt highly distorted structures. Several studies have been carried out to establish the crystal structure of transition metal complexes containing benzimidazole ligands (Table I.1).

Nickel halides and benzimidazole (L) form a series of solid complexes of composition $[NiL_4X_2]$. These complexes are unstable in solution losing two benzimidazole molecules[49]. The complex, $[NiL_4Cl_2]$ has been subjected to X-ray crystal structure analysis[50]. The four benzimidazole molecules occupy octahedral sites in a binuclear cation in which one chloride bridges two nickel ions. The coordination position trans to the chloride bridge is occupied by a chloride ion. The benzimidazole rings are tilted out of the plane defined by the coordinating nitrogens minimizing steric repulsions[51-53].

Nickel(II) complexes with 2-α-hydroxy-benzimidazole contain strongly hydrogen bonded dimers[38], with a Ni-Ni bond length of 4.77 Å. In the complex, $[CuL_2(NO_3)_2]$ (where L = 2-(2'-thienyl)-1-(2'-thienyl-methyl)benzimidazole), the copper coordination is tetragonal (compressed octahedral) in which two oxygen atoms of the nitrate group appear to coordinate symmetrically to the metal; however, it has unusually

Table I.1
X-Ray crystallographic data

Compound	Ligand, L	Space group	Z	a(Å) b(Å) c(Å)	α(°) β(°) γ(°)	Other data		Ref.
$[CuL_2(NO_3)_2]$	2-(2'-thienyl)-1-(2'-thienylmethyl)benzimidazole	$P2_1/c$	2	9.884(4) 9.892(4) 18.732(8)	90 114.89(2) 90	Cu-N Cu-O	1.970(6) 2.318(7) 2.246(9)	35
$[CuL_2Cl_2]$	2-(2'-thienyl)benzimimidazole	Pbcn	4	14.835(1) 8.193(1) 20.493(1)	90 90 90	Cu-N Cu-Cl Cu-S	1.950(3) 2.270(1) 3.370(2)	35
$[CoL(DH)_2CHX_2]$	1,5,6-trimethylbenzimidzole X = Cl/Br DH = monoanion of DMG	P1	2	8.867(2) 10.719(2) 13.345(2)	94.81(2) 90.89(1) 105.63(2)	Co-N Co-C	2.043(2) 1.983(2)	36
$[CoL_2Cl_2]$	2-(ethylthiomethyl)-benzimidazole	$P2_1/c$	2	9.707(1) 14.977(2) 8.525(1)	90 112.03(1) 90	Cu-N Cu-Cl Cu-S	2.000(5) 3.222(2) 3.001(2)	37

Table I.1 (continued)

$[NiL_2L'(ClO_4)]$	1-n-propyl-2-α-hydroxy-	$P2_1/c$	4	14.549(2)	90	O-H-O	2.560	38
	benzylbenzimidazole			19.812(3)	96.05(1)		2.620	
	L' = deprotonated L			16.988(3)	90	Ni-Ni	4.770	
$[CoL_2I_2].2H_2O$	2-α-methoxybenzylbenz-	P1	2	10.619(2)	110.39(1)	Co-N	2.097(5)	39
acetone	imidazole			11.934(2)	92.95(1)			
				14.940(1)	98.91(2)			
$[CuL]BF_4$	2,2'-bis(2-(N-propyl-	$P2_1/c$	4	9.865(3)	90	Cu-S	2.469(9)	40
	benzimidazolyl))diethyl-			17.614(5)	104.93(2)	N-Cu-S	98.3(2)°	
	sulphide			15.242(3)	90		99.4(2)°	
$[CuL(H_2O)X]X$	2,2'-bis(2-(5,6-di-	P1	2	7.909(4)	103.10(6)	Cu-S	2.322(2)	40
	methylbenzimidazolyl)-			10.972(1)	96.56(6)	$Cu-OH_2$	2.045(5)	
	diethylsulphide			16.650(1)	103.98(5)	$Cu-OClO_3$	2.346(6)	
	X = ClO_4							
$[CuLCl]Cl.2C_2H_5OH$	1,6-bis(2-benzimidazol-	$P2_1/c$	4	14.930(3)	90	Cu-N	1.961(6)	41
	yl)-2,5-dithiahexane			17.109(4)	97.23(2)		1.968(6)	
				10.774(2)	90	Cu-Cl	2.241(2)	
						Cu-S	2.434(2)	
							2.561(2)	

Table I.1 (continued)

$[Cu_4(\mu_3\text{-}I)_4L_4]\cdot$ 3diglyme	benzimidazole	$I4_1/a$	4	22.838(2)	90	Cu-I	2.688(3)	42
				22.838(2)	90		2.720(2)	
				11.970(1)	90	Cu-Cu	2.740(3)	
							2.757(3)	
$[Cu(\mu_3\text{-}I)L]_n$	benzimidazole	$P2_1/c$	4	4.337(1)	90	Cu-I	2.631(2)	42
				11.999(2)	97.94(1)		2.738(2)	
				16.120(2)	90	Cu-Cu	2.958(2)	
							2.989(2)	
$[CuIL_2]\cdot THF$	1-benzyl-2-phenyl-	C2/c	4	10.844(2)	90	Cu-I	2.512(3)	42
	benzimidazole			20.778(4)	92.23(2)			
				17.104(3)	90			
$[Cu_2(\mu\text{-}I)_2L_2]\cdot$ 2THF	1-benzyl-2-phenyl-	P1	1	9.278(2)	96.99(1)	Cu-I	2.554(2)	42
	benzimidazole			10.947(2)	109.64(1)		2.598(2)	
				9.191(2)	89.63(1)	Cu-Cu	2.546(3)	
$[Cu_2LF_2](BF_4)_2\cdot$ $2H_2O\cdot H_2OBF_3$	1,8-bis(1'-methylbenzi-	Pccn	4	12.159(2)	90	Cu-F	1.861(6)	43
	midazole-2'-ylmethyl)-			16.909(2)	90	Cu-O	2.350(2)	
	amino-3,6-dioxaoctane			25.654(5)	90		2.410(2)	
						Cu-N	1.945(9)	

Table I.1 (continued)

$[CuLCl_2]Cl_2.6H_2O$	1,8-bis(1'-methylbenzi-	P1	2	14.006(3)	105.97(3)	Cu-Cl	2.232(6)	43
	midazole-2'-ylmethyl)-			15.204(6)	110.89(20		2.220(6)	
	amino-3,6-dioxaoctane			15.756(3)	96.72(3)	Cu-O	2.410(2)	
							2.460(1)	
						Cu-N	2.090(2)	
							2.140(2)	
$[CuLBr_2](CF_3SO_3)_2.$	1,8-bis(1'-methylbenzi-	P1	2	13.954(5)	78.16(3)	Cu-Br	2.370(2)	43
C_2H_5OH	midazole-2'-ylmethyl)-			14.420(5)	75.90(3)		2.385(2)	
	amino-3,6-dioxaoctane			15.539(6)	61.85(3)	Cu-O	2.400	
							2.584(8)	
						Cu-N	2.097(8)	
							1.950(9)	
$[CuL(NO_3)_2].$	N,N'-bis(benzimidazol-	Pbca	8	16.136(5)	90	Cu-N	1.953(4)	44
CH_3OH	2-ylmethyl)isopropyl-			15.316(5)	90		2.102(5)	
	amine			18.901(3)	90	Cu-O	2.390(5)	
							1.982(4)	
$[CuL(NO_3)_2]$	N,N'-bis(benzimidazol-	$P2_1/c$	4	14.497(3)	90	Cu-N	1.942(5)	44
	2-ylmethyl)n-butylamine			14.401(3)	137.51(2)		2.068(7)	
				15.613(4)	90	Cu-O	1.987(7)	
							2.631(5)	

Table I.1 (continued)

$[CuL(NO_3)_2]$	N,N'-bis(benzimidazol-2-ylmethyl)isobutylamine	Pbca	8	29.550(1) 16.366(3) 9.380(2)	90 90 90	Cu-N Cu-O	1.928(6) 2.087(6) 2.038(6) 2.482(7)	44
$[CuL(NO_3)_2]\cdot CH_3OH$	N,N'-bis(benzimidazol-2-ylmethyl)t-butylamine	Pbca	8	16.635(3) 18.768(4) 15.548(5)	90 90 90	Cu-N Cu-O	1.932(6) 2.138(6) 2.461(6) 1.965(6)	44
$[CuL(CH_3CN)X]X$	2,6-bis(benzimidazol-2'-yl)pyridine X = ClO_4	$P2_1/c$	4	14.061(1) 20.638(1) 8.273(1)	90 101.11(8) 90	Cu-N	1.96-2.03	45
$[CuL_2](ClO_4)_2\cdot H_2O$	2,6-bis(benzimidazol-2'-yl)pyridine	$P2_1/c$	4	8.482(2) 29.196(2) 16.739(2)	90 95.83(1) 90	Cu-N	2.510	45
$[CuL'CuL](PF_6)X\cdot(CH_3)_2CO$	tris(2-(N-ethylbenzimidazolyl)methyl)amine L' = 1:1:1 condensation product of acetylacetone, ethylenediamine and 1-formylimidazole, X = ClO_4	P1	2	13.131(5) 19.285(6) 10.878(4)	93.89(2) 92.83(2) 114.64(2)	Cu-N	1.957	46

Table I.1 (continued)

$[CuL_2(HCHO)_2(H_2O)]$	benzimidazole	C2/c	4	12.940(4)	90	Cu-O	1.997(5)	47
				12.700(4)	96.00(3)	Cu-N	2.017(6)	
				10.400(2)	90	$Cu-OH_2$	2.625(2)	
						Cu-O-Cu	164.2(5)°	
$[CoLX_2(CHClCN)]$	1,5,6-trimethyl-benzimidazole X = dimethylglyoxime	$P2_1/c$	4	9.587(2)	90	Co-C	2.000(5)	48
				15.683(2)	102.44(2)	Co-N	2.010(3)	
				16.163(2)	90			
$[CoLX_2(C_{10}H_{15})]$	1,5,6-trimethyl-benzimidazole X = dimethylglyoxime	$P2_1/c$	4	12.162(2)	90	Co-C	2.179(5)	48
				13.035(2)	92.54(2)	Co-N	2.137(4)	
				18.558(5)	90			

large thermal motion which suggests a fluxional behaviour[35]. Juen *et al.* reported a copper(II) complex with a bidentate ligand, 2-(ethylthiomethyl)-benzimidazole, which has a distorted octahedral geometry with two benzimidazole nitrogen atoms and two chlorine atoms occupying equatorial positions and two thioether sulphur atoms in the two axial positions[37].

Daddigian *et al.* studied the differences in the intrinsic structural preferences of copper(I) and copper(II) within the constraints of a tridentate benzimidazole thioether chelating ligand[40]. A three coordinate T-shaped copper(I) cation is formed with the NNS donor ligand, 2,2'-bis(2-(N-propylbenzimidazolyl)di-ethylsulphide. The 4th and 5th ligands bound to copper(II) are an equatorial water molecule and an axial monodentate perchlorate ion.

The reaction of CuI with benzimidazole (L)) in a constant 1:2 molar ratio led to compounds having different structures depending on the solvent used[42]. In THF, a binuclear compound, $[Cu_2(\mu\text{-}I)_2L_4]$ was isolated. The same reaction carried out under a CO atmosphere in the presence of $NaBPh_4$ (where BPh_4 = tetraphenylborate ion) gave $[CuL_3(CO)](BPh_4)$. When this reaction was performed in diglyme, a tetranuclear complex, $[Cu_4(\mu_3\text{-}I)_4L_4]$.3diglyme, was isolated. Its

X-ray analysis showed a cubane type structure having crystallographically imposed 4-fold symmetry. The benzimidazole adduct, $[Cu(\mu_3\text{-}I)L]_n$, isolated from methanol, has a polymeric structure containing tetracoordinate copper atoms. Substituted benzimidazoles like 1-benzyl-2-phenylbenzimidazole and 2-phenylbenzimidazole form mononuclear and binuclear adducts with CuI in THF, containing three coordinate copper atoms.

1.1.3 Magnetic susceptibility measurements

Room temperature magnetic moments of some benzimidazole complexes are given in Table I.2. A number of benzimidazole complexes have been studied over a temperature range. Kennedy *et al.* reported the magnetic properties of a range of five coordinated cobalt(II) complexes of benzimidazole[54]. A variety of benzimidazoles have been used and have been shown to influence the electronic states of the cobalt(II) atom in a sensitive manner. In some cases, it results in a spin-crossover between the high-spin (quartet) and low-spin (doublet) states of this d^7 system. The high-spin complex, [CoL'L] (where L' = N,N'-ethylenebis-(3-methoxysalicylaldimine) and L = 5,6-dimethylbenz-imidazole), has a room temperature magnetic moment value of 4.45 BM which decreases very rapidly below 50 K,

Table I.2

Magnetic moment and electronic spectral data

Compound	Ligand,L	$\mu_{eff.}$ BM	Abs. max. cm^{-1}	Proposed structure	Ref.
$[CoLCl_2]$	2-(4'-methyl-2'-pyridyl)benzimidazole	4.80	5800,9200 11500,16100 16700,17500 18900	pseudo tetrahedral	55
$[NiL_2Cl_2]$	2-(4'-methyl-2'-pyridyl)benzimidazole	3.19	8500,10000 12500,16000 18700	distorted octahedral	55
$[Cu_2L(OH)Cl_3]$. DMF	3,6-bis(N-ethyl-2-benzimidazolyl)-thiopyridazine	1.38	12050-12190	dimeric trigonal bipyramidal	56
$[NiL_2(NO_3)_2]$	1-n-propyl-2-α-hydroxybenzyl-benzimidazole	3.28	9250,12800 15200,23000 25650	octahedral	38

Table I.2 (continued)

$[CoL_2(NO_3)_2]$	1-n-propyl-2-α-hydroxybenzyl-benzimidazole	4.73	6700,10500 15400,19600 21000	octahedral	38
$[CoL_2Cl_2]$	2-α-methoxybenzyl-benzimidazole	4.57	6200,7150 8600,15700 17000,19600 23000	tetrahedral	39
$[CoL_2Br_2]$	2-α-methoxybenzyl-benzimidazole	4.80	4600,6000 6670,8200 10750,15150 15600,17100	distorted tetrahedral	39
$[CoL_2(NCS)_2]$	2-α-methoxybenzyl-benzimidazole	4.60	7200,8100 17200,20400	tetrahedral	39
$[CuL_2(NCO)_2]$	2-methylbenzimid-azole	1.83	17600	elongated octahedral	57
α-$[CuL_2(NCO)_2]$	2-ethylbenzimid-azole	1.82	18800	elongated octahedral	57

Table I.2 (continued)

β-$[CuL_2(NCO)_2]$	2-ethylbenzimid-azole	1.85	16100	elongated octahedral	57
$[CuLX(NO_3)_2]$	tris(2-benzimid-azolylmethyl)amine X = Cl/Br	1.8-2.0	8000,12500 22000-33000	pseudo octahedral	58
$[CoLBr_2]$	tris(2-benzimid-azolyl-5'-methyl)-ethane	4.43	6300,7500 9000,15000 16000,16800	tetrahedral	59
$[CoLI_2]$	tris(2-benzimid-azolyl-5'-methyl)-ethane	4.58	6060,7100 8600,14700 15400,16300	tetrahedral	59
$[CoLCl_2]_2$	2-β-pyridylbenz-imidazole	4.56	4000,6500 16000	dimeric tetrahedral	60
$[CoLBr_2]_2$	2-β-pyridylbenz-imidazole	4.50	4000,6500 16000	dimeric tetrahedral	60
$[CoL_2Cl_2]$	2-o-aminophenyl-benzimidazole	4.9	9000,20000	octahedral	60

Table I.2 (continued)

$[NiL_2L'_2]$	2-methylbenzimidazole L' = N-phenyl-N'-benzothiazol-2-yl-thiocarbamide	4.10	8700,13880 25000	octahedral	61
$[CoL_2L'_2]$	2-methylbenzimidazole L' = N-phenyl-N'-benzothiazol-2-yl-thiocarbamide	5.00	9430,19610 21740	octahedral	61
$[Cu_2LL']X_2$	2-(2'-pyridyl)benzimidazole, L'=N,N'-ethylenebis-(salicylaldiminate) X = ClO_4	1.20	30000-48000	dimeric	62
$[CoL_2]$	2-(p-toluenesulphonamido)methylbenzimidazole	5.07	10640,17610 19800	octahedral	63
$[NiL_2]$	2-(benzenesulphonamido)-β-ethylbenzimidazole	3.38	12900,20000	distorted octahedral	63

Table I.2 (continued)

$[CuL_2]$	2-(benzenesulph-onamido)-β-ethyl-benzimidazole	1.91	13510,24390 25640	distorted octahedral	63
$[CoL_2X_2]$	1-(2-thienyl)meth-yl-2-(2-thienyl)-benzimidzole X = Cl/Br/I	4.39-4.76	14500-17000	tetrahedral	64
$[CuL_2X_2]$	1-(2-thienyl)meth-yl-2-(2-thienyl)-benzimidzole X = Cl/Br	1.78-1.87	11000	tetrahedral	64
$[CoL_2]$	2-(benzenesulph-onamido)methyl-benzimidazole	5.03	10000	octahedral	65
$[NiL_2]$	2-(benzenesulph-onamido)methyl-benzimidazole	3.33	13300,15150 18180,25640	octahedral	65
$[CuL_2]$	2-(benzenesulph-onamido)methyl-benzimidazole	1.82	11000-16660	octahedral	65

Table I.2 (continued)

$[CoL_2]$	2-(benzenesulph-onamido)-β-ethyl-benzimidazole	5.02	11430,16260 17540,18180 20610	octahedral	63
$[NiL_2]$	2-(p-toluenesulph-onamido)methyl-benzimidazole	3.26	13610,18020 20410,24270	octahedral	63
$[CuL_2]$	2-(p-toluenesulph-onamido)methyl-benzimidazole	1.91	15150,25320	octahedral	63

reaching 3.8 BM at 4.2 K. It is known that the doublet/quartet separation in these types of five-coordinated complexes is small, often leading to spin-crossover behaviour.

The complex [CoL"L] (where L" = N, N'-ethylenebis-(salicylaldimine)) also exhibits typical spin-crossover behaviour[54]. The corresponding magnetic moment value is found to decrease rapidly between 300 and 200 K from the room temperature value of 3 BM to the low-spin value of 1.9 BM. The influences of the benzimidazole group and the in-plane ligand on the spin state of the central metal ion in terms of σ and π bonding capacities have also been studied[66]. The magnetic properties of the complex, [CoL"'L] (where L"' = N,N'-phenylenebis-salicyaldimine) show a sharp transition in magnetic moment at 110 K. Above and below this temperature, the susceptibilities follow Curie-Weiss behaviour but with different slopes. The moment does not level off to a low-spin value even at 4.2 K, which suggests that the sharp transition may be due to a structural phase transition, an incomplete spin state change, or a combination of both.

Thompson *et al.* reported binuclear copper(I) and copper(II) complexes of a series of N-alkyl substituted derivatives of the tetradentate ligand,

3,6-bis(2-benzimidazolylthio)pyridazine[56]. In these complexes, the two trigonal bipyramidal copper(II) centres are antiferromagnetically coupled (-2J = 260 cm^{-1}). The variable temperature magnetic susceptibility studies of a variety of benzimidazolate bridged dicopper(II) complexes reveal that the benzimidazolate group can mediate moderate antiferromagnetic interactions.

For $[FeL_2]Cl_2.CH_3OH$ (where L = 2,6-bis(benzimidazol-2'-yl)pyridine), the magnetic moment varies gradually from 0.8 BM at 10 K to 2.2 BM at 300 K, which can be attributed to the effects of temperature independent paramagnetism and to the presence of some paramagnetic impurity[67]. It is interesting to compare this with the magnetic behaviour of the bromide complex, $[FeL'_3]Br_2$ (where L' = 2-pyridylbenzimidazole), for which Sams *et al.*[68] found an incomplete, gradual spin-crossover (with a magnetic moment varying from 3.6 to 5.3 BM between 100 and 300 K). One could account for the higher moment of this latter compound as resulting from the ligands being bidentate; while for the chloro complex, L is a tridentate ligand and should have a stronger coordination to the iron and greater ligand field strength.

The magnetic moment values of the complexes, $[FeL_3](ClO_4)_3.xH_2O$ (where L = 2-pyridylbenzimidazole), depend on the amount of water present in the lattice: The $\mu_{eff.}$ value for the compound with one molecule of water is 2 BM at 80 ^{o}C, while that for the compound with 2 molecules of water is 1.2 BM. Both compounds exhibit a moment of 5.4 BM at 300 K. The complex, $[FeL'_3](ClO_4)_3$ (where L' = 1-methyl-2-pyridylbenzimidazole), also shows evidence of spin-crossover behaviour; the magnetic moment varies from 0.84 BM at 125 K to 2.0 BM at 300 K. The generally lower paramagnetism of the methylated compound has been attributed to the increase in basicity caused by the methyl group on the benzimidazole nitrogen[69].

Magnetic behaviour of iron(II) complexes of 1-methyl-2-(pyridin-2-yl)imidazole and 1-methyl-2-(pyridin-2-yl)benzimidazole have been studied. They are diamagnetic and show an anomalous temperature dependence, which indicates population of quintet electronic states at elevated temperature[70]; however, only slight dependence was observed for the imidazole complex. The spin-crossover in these systems is displayed to higher temperatures compared to that in the complexes of unsubstituted imidazole and benzimidazole ligands.

1.1.4 Electronic spectra

Electronic spectra of a large number of benzimidazole complexes have been studied. Spectral data of some of these complexes are given in Table I.2.

Mixed ligand complexes of copper(II) containing benzimidazole and thiolate exhibit intense blue, brown or green colour on lowering the temperature. Charge transfer transitions are responsible for these colours[71]. The blue band at 16700 cm^{-1} originates from the S^{-}——>Cu charge transfer transitions. This band is seen almost at the same position in blue copper proteins. At -78°C, $S^{-}(\pi)$——>Cu and $S^{-}(\sigma)$——>Cu charge transfer transitions are observed around 15880 cm^{-1} and 18520 cm^{-1} respectively.

Changes in the electronic spectra are observed for [CoL'L] (where L = N,N'-ethylenebis(salicylaldimine) and L' = 5,6-dimethylbenzimidazole), as the temperature is lowered from 295 to 8 K. The bands that occur between 13000 and 26000 cm^{-1} generally decrease markedly in intensity on lowering the temperature to 8 K. The spectral variations are attributed to a change in the spin state[66].

1.1.5 EPR spectra

Most of the EPR studies are centered on the copper(II) complexes. The limited number of studies with other metal complexes might be due to the complicated nature of their spectra, probably because of the presence of more than one unpaired electron. Furthermore, the spectra are not observed in many cases even at liquid nitrogen temperature due to fast spin-lattice relaxation.

The observed crystal g values for the copper(II) complexes depend on the symmetry of ligand field and the alignment of tetragonal axes present in the unit cell. Three types of spectra are generally observed: isotropic spectra, axial spectra and rhombic spectra. Isotropic spectra are expected for copper(II) ion in regular static octahedral or tetrahedral stereochemistry. As copper(II) complexes are unlikely to have regular octahedral or tetrahedral geometry due to Jahn-Teller distortions, isotropic spectra are not observed for solid complexes in practice. However, such type of spectra can occur with a dynamically distorted octahedral structure[72].

Axial spectra are most commonly observed with tetragonal copper(II) ion environments in which tetragonal axes are aligned parallel. Two g values, $g_{\parallel}$

and $g_{\perp}$, are observed in such cases. If the lowest g value is smaller than 2.04, the copper(II) ion may be in an elongated tetragonal stereochemistry, whereas g values greater than 2.03 indicate a compressed tetragonal stereochemistry[73]. The EPR studies indicate that these two types of structures are commonly observed for the benzimidazole complexes of copper(II). Rhombic spectra are also seen in a few cases. This type of spectra can arise from the slight misalignment of rhombic or axial local copper(II) environments. In such cases three g values, g_1, g_2 and g_3 are obtained. Table I.3 lists the observed Spin-Hamiltonian parameters of some benzimidazole complexes of copper(II).

1.1.6 Infrared spectra

The infrared spectra of benzimidazoles are very complex. Benzimidazoles are known to be strongly associated through intermolecular hydrogen bonding. The spectra of all compounds studied show strong broad bands around 3300-2800 cm^{-1} which indicate polymeric association through intermolecular hydrogen bonding. The C-H stretching vibrations of the ring also occur in this range and cannot be distinguished from the N-H stretching frequencies. The 1650-1500 cm^{-1} region is a very characteristic region of the benzimidazole spectrum. The spectra of most substituted

Table I.3
EPR spectral data

Compound	Ligand, L	g values	A* values	Ref.
$[CuL(NO_3)].H_2O$	tris(benzimidazol-2-ylmethyl) amine	$g_{\parallel}$ 2.01 $g_{\perp}$ 2.23	$A_{\parallel}$ 72 $A_{\perp}$ 98	74
$[CuL(NO_3)]NO_3.$ $2H_2O$	tris(1-methyl-benzimidazol-2-ylmethyl)amine	$g_{\parallel}$ 2.01 $g_{\perp}$ 2.24	$A_{\parallel}$ 72 $A_{\perp}$ 98	74
$[CuL(NO_3)]NO_3.$ $0.5H_2O$	tris(1-ethyl-benzimidazol-2-ylmethyl)amine	$g_{\parallel}$ 2.01 $g_{\perp}$ 2.23	$A_{\parallel}$ 74 $A_{\perp}$ 95	74
$[CuL(NO_3)]NO_3.$	tris(1-benzyl-benzimidazol-2-ylmethyl)amine	$g_{\parallel}$ 2.01 $g_{\perp}$ 2.24	$A_{\parallel}$ 72 $A_{\perp}$ 95	74
$[CuL(NO_3)]NO_3.$	tris(1-*o*-methylbenzylbenzimidazol-2-ylmethyl) amine	$g_{\parallel}$ 2.01 $g_{\perp}$ 2.24	$A_{\parallel}$ 74 $A_{\perp}$ 93	74
$[CuLCl]Cl$	1,6-bis(benzimidazol-2-yl)-2,5-dithiahexane	$g_{\parallel}$ 2.22 $g_{\perp}$ 2.06	$A_{\parallel}$ 130	75
$[CuLBr]PF_6$	N-(2-benzimidazolylmethyl)-N,N'-bis(2-methylthioethyl)amine	g_1 2.18 g_2 2.10 g_3 1.98	A_1 127 A_2 80 A_3 114	76

Table I.3 (continued)

$[CuLCl]PF_6$	N-(2-pyridylmethyl-N-(2-benzimidazolylmethyl)-N,N'-bis(2-methylthioethyl)amine	$g_{\parallel}$	2.248	$A_{\parallel}$	168	76
$[CuLCl]ClO_4$	N,N-bis(2-benzimidazolylmethyl)ethanolamine	$g_{\parallel}$	2.253	$A_{\parallel}$	168	76
$[CuLBr]ClO_4$	N,N-bis(2-benzimidazolylmethyl)ethanolamine	$g_{\parallel}$	2.247	$A_{\parallel}$	172	76
$[CuL(H_2O)](NO)_3$	N,N-bis(2-benzimidazolylmethyl)ethanolamine	$g_{\parallel}$	2.279	$A_{\parallel}$	160	76
$[CuL_2(NCO)_2]$	2-methylbenzimidazole	g_0	2.06		-	57
α-$[CuL_2(NCO)_2]$	2-ethylbenzimidazole	$g_{\parallel}$ $g_{\perp}$	2.23 2.04		-	57
β-$[CuL_2(NCO)_2]$	2-ethylbenzimidazole	$g_{\parallel}$ $g_{\perp}$	2.18 2.05		-	57
$[CuLCl_2]H_2O$	1,6-bis(2-benzimidazolyl)-2,5-dithiahexane	g_1 g_2 g_3	2.21 2.06 2.00		-	41
$[CuL(ClO_4)_2]H_2O$	1,6-bis(2-benzimidazolyl)-2,5-dithiahexane	g_1 g_2 g_3	2.21 2.13 2.00		-	41

Table I.3 (continued)

$[CuL(BF_4)_2]H_2O$	1,6-bis(2-benzimidazolyl)-2,5-dithiahexane	g_1	2.27	-		41
		g_2	2.08			
		g_3	2.02			
$[CuLBr_2]H_2O$	1,6-bis(2-benzimidazolyl)-2,5-dithiahexane	g_1	2.14	-		41
		g_2	2.08			
		g_3	2.04			
$[CuLCl]PF_6.H_2O$	tris(2-benzimidazolylmethyl) amine	$g_{\parallel}$	1.99	$A_{\parallel}$	60	58
		$g_{\perp}$	2.23	$A_{\perp}$	84	
$[CuLBr]PF_6.$ $1.5H_2O$	tris(2-benzimidazolylmethyl) amine	$g_{\parallel}$	1.97	$A_{\parallel}$	53	58
		$g_{\perp}$	2.21	$A_{\perp}$	97	
$[CuLBr]ClO_4$	tris(2-benzimidazolylmethyl) amine	$g_{\parallel}$	1.97	$A_{\parallel}$	58	58
		$g_{\perp}$	2.22	$A_{\perp}$	100	
$[CuL(NCS)]BF_4.$ H_2O	tris(2-benzimidazolylmethyl) amine	$g_{\parallel}$	2.01	$A_{\parallel}$	69	58
		$g_{\perp}$	2.22	$A_{\perp}$	99	
$[CuL(N_3)]N_3.$ $3CH_3OH$	tris(2-benzimidazolylmethyl) amine	$g_{\parallel}$	2.00	$A_{\parallel}$	69	58
		$g_{\perp}$	2.11	$A_{\perp}$	89	
$[CuLCl(NO_3)]$	tris(2-benzimidazolylmethyl) amine	$g_{\parallel}$	2.00	$A_{\parallel}$	60	58
		$g_{\perp}$	2.24	$A_{\perp}$	85	
$[CuLBr(NO_3)]$	tris(2-benzimidazolylmethyl) amine	$g_{\parallel}$	2.01	$A_{\parallel}$	70	58
		$g_{\perp}$	2.12	$A_{\perp}$	98	

Table I.3 (continued)

$[CuLBr(H_2O)]BF_4$	tris(2-benzimidazolylmethyl) amine	$g_{\parallel}$ $g_{\perp}$	2.02 2.22	$A_{\parallel}$ $A_{\perp}$	80 100	58
$[CuLBr(ClO_4)]$	tris(2-benzimidazolylmethyl) amine	$g_{\parallel}$ $g_{\perp}$	1.98 2.21	$A_{\parallel}$ $A_{\perp}$	75 100	58
$[Cu_2LCl_2]Cl_2 \cdot 6H_2O$	1,8-bis(bis(1'-methylbenzimidazole-2'-ylmethyl)-amino)3,6-dioxaoctane	g	2.09	-		43
$[CuL_2](ClO_4)_2 \cdot H_2O$	2,6-bis(1'-methylbenzimidazol-2'-yl)pyridine	$g_{\parallel}$ $g_{\perp}$	2.23 2.03	$A_{\parallel}$	167 -	45
$[CuLCl_2]H_2O$	1,6-bis(2'-benzimidazolyl)-2,5-dithiahexane	g_1 g_2 g_3	2.21 2.06 2.00		-	77

* values are in Gauss

benzimidazoles have only two bands in this region, one around 1620 cm^{-1} and the other around 1590 cm^{-1}. The band around 1590 cm^{-1} is in general fairly intense, because of the conjugation between the benzene and imidazole rings. These bands vary in position and intensity with the nature and position of the substituent[78]. Substitution at the 2-position is accompanied by the appearance of a rather intense band around 1550 cm^{-1}.

Heterocyclic compounds show a series of characteristic bands in the 1250-1000 cm^{-1} region which may be assigned to in-plane C-H deformations and ring breathing modes. Substituted benzimidazoles also show a number of bands in this region which are similarly located. Out-of-plane C-H deformations and in-plane ring deformations cause absorption in the 1000-650 cm^{-1} region. The out-of-plane C-H bending frequencies of substituted benzenes also fall in this region[79].

In addition to the vibrations typical of benzimidazole ring, vibrations of the groups attached to the ring must also be considered. In general, substituents show the same characteristic bands regardless of whether they are attached to a benzene or benzimidazole ring[80,81]. On complex formation, most of the bands do not undergo frequency shifts. However,

there will be slight shifts in the vibrational frequencies of bands at the coordination positions. Further, new bands due to metal-ligand vibrations appear in the far IR spectra of metal complexes. The far IR spectral data for some benzimidazole complexes are given in Table I.4.

1.1.7 Biological importance

The imidazole nucleus is found in a number of important natural products such as histidine and the purines while 5,6-dimethyl-1-(α-D-ribofuranosyl)benzimidazole is an integral part of the structure of vitamin B_{12}. Consequently a massive research effort has been expended upon the chemistry of imidazoles and benzimidazoles with particular emphasis on the synthesis of new compounds for pharmacological screening. The discovery of new antibacterial and anthelmintic agents has added momentum to investigations in these areas.

It is rather difficult to accumulate definite information about commercial uses of benzimidazoles. Several benzimidazole derivatives have been marketed in the past decade as anthelmintic and antimicrobial agents for both human and veterinary purposes (Table I.5).

Copper(II) complexes of benzimidazoles are reported to have herbicidal and growth regulating activity[82].

there will be slight shifts in the vibrational frequencies of bands at the coordination positions. Further, new bands due to metal-ligand vibrations appear in the far IR spectra of metal complexes. The far IR spectral data for some benzimidazole complexes are given in Table I.4.

1.1.7 Biological importance

The imidazole nucleus is found in a number of important natural products such as histidine and the purines while 5,6-dimethyl-1-(α-D-ribofuranosyl)benzimidazole is an integral part of the structure of vitamin B_{12}. Consequently a massive research effort has been expended upon the chemistry of imidazoles and benzimidazoles with particular emphasis on the synthesis of new compounds for pharmacological screening. The discovery of new antibacterial and anthelmintic agents has added momentum to investigations in these areas.

It is rather difficult to accumulate definite information about commercial uses of benzimidazoles. Several benzimidazole derivatives have been marketed in the past decade as anthelmintic and antimicrobial agents for both human and veterinary purposes (Table I.5).

Copper(II) complexes of benzimidazoles are reported to have herbicidal and growth regulating activity[82].

Table I.4
Far IR absorption frequencies (cm^{-1})

Compound	Ligand,L	ν(M-N)	ν(M-X)	Ref.
$[CoLCl_2]$	2-(4'-methyl-2'-pyridyl)benzimidazole	255s	285s	55
$[NiL_2Cl_2]$	2-(4'-methyl-2'-pyridyl)benzimidazole	252m	283s	55
$[CuL_2Cl_2]$	2-(2'-thienyl)benzimidazole	-	295s	35
$[CuL(NCO)_2]$	2-methylbenzimidazole	253s	-	57
α-$[CuL(NCO)_2]$	2-ethylbenzimidazole	276s	-	57
β-$[CuL(NCO)_2]$	2-ethylbenzimidazole	258s	-	57
$[CuLCl]PF_6.H_2O$	tris(2-benzimidazolylmethyl)amine	-	290s	58
$[CuLBr]PF_6.H_2O$	tris(2-benzimidazolylmethyl)amine	-	230s	58
$[CuLBr]ClO_4$	tris(2-benzimidazolylmethyl)amine	-	235s	58
$[CuLCl]NO_3$	tris(2-benzimidazolylmethyl)amine	-	270s	58
$[CuLBr]NO_3$	tris(2-benzimidazolylmethyl)amine	-	219s	58

Table I.4 (continued)

$[CuL_2]$	2-(p-toluenesul-phonamido)methyl-benzimidazole	637w	-	63
$[NiL_2]$	2-(p-toluenesul-phonamido)methyl-benzimidazole	635w	-	63
$[NiL_2(NH_3)]$	2-(p-toluenesul-phonamido)methyl-benzimidazole	622w	-	63
$[CoL_2]$	2-(p-toluenesul-phonamido)methyl-benzimidazole	635w	-	63
$[CuL_2]$	2-(benzenesul-phonamido)-β-ethyl-benzimidazole	629w	-	63
$[NiL_2]$	2-(benzenesul-phonamido)-β-ethyl-benzimidazole	628w	-	63
$[CoL_2]$	2-(benzenesul-phonamido)-β-ethyl-benzimidazole	631w	-	63
$[CoL_2]$	2-(benzenesul-phonamido)methyl-benzimidazole	590w	-	65

Abbreviations: s = strong, m = medium, w = weak

Table I.5
Benzimidazoles of biological importance

Approved name	Chemical name	Structure	Use
Thiabendazole	2-(3-tiazolyl)benzimidazole	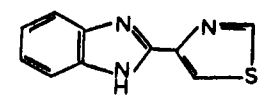	anthelmintic
Mebendazole	methyl 5-benzoyl-2-benzimidazole carbamate	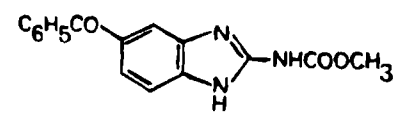	anthelmintic
Bezitramide	1-(3-cyano-3,3-diphenylpropyl)-4-(2-oxo-3-propionyl-1-benzimidazolinyl)piperidine	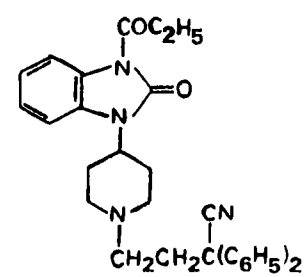	analgesic

Table I.5 (continued)

Clemizole	1-(*p*-chlorobenzyl)-2-(1-pyrrolidinylmethyl)-benzimidazole	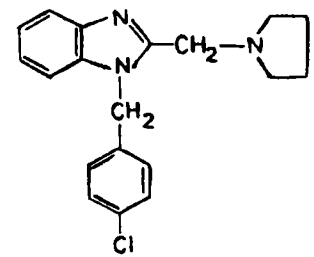	antihistamine
Fuberidazole	2-(2-furanyl)benzimidazole	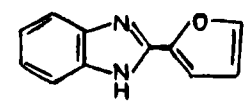	fungicide
Cambendazole	5-isopropoxycarbonylamino-2-(4-thiazolyl)-benzimidazle	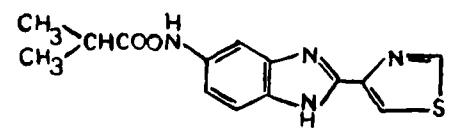	anthelmintic

Some metal complexes of benzimidazoles were screened for antibacterial activity against gram-negative and gram-positive bacteria. A majority of compounds were found to be effective at moderate to high concentration levels[83]. Milanino *et al.* prepared copper(II) chelates of some bis(2-benzimidazolyl)thioethers and orally administered to rats. They found that these chelates were most effective as anti-inflammatory agents[84].

Benzimidazoles and imidazoles as axial bases facilitate oxygen binding by heme iron[85-87]. Such complexes can be considered as models for myoglobin. The oxygen binding constant is at least 3800 times greater for the imidazole compound than that for the pyridine analogue. The π-donor ability of the imidazole ring is suggested as an explanation for its increased binding capacity[88].

Cobaloximes are the most studied models[89] of vitamin B_{12}. Interaction of cobaltous acetate and dimethylglyoxime in the presence of cyanide ion and benzimidazoles produces cobaloximes having cyanide ion and benzimidazole ligands at axial positions. Similar complexes having halide in place of cyanide have been prepared from cobaltous halides, dimethylglyoxime and benzimidazoles. The possible role of cobaloximes in the

mechanism of corrinoid based enzymatic reactions has been a subject of considerable discussion[90].

1.2 METAL COMPLEXES OF SCHIFF BASES DERIVED FROM AMINO ACIDS

Schiff bases are those compounds containing the azomethine group (-RC=N-) and are usually formed by the condensation of a primary amine with an active carbonyl compound. Bases which are effective as coordinating ligands bear a functional group, usually -OH, sufficiently near the site of condensation that a five- or six- membered chelate ring can be formed upon reaction with a metal ion. Because of the great synthetic flexibility of Schiff base formation, many ligands of diverse structural type have been synthesized[91].

Aldehydes condense with amino acids to form Schiff bases, which can be represented by the general formula, $R-CH=N-CH(R')-COO^-$ where R and R' are various substituents. They coordinate through imino and carboxylate groups. Metal binding is favoured by the strong electron donor character of N(amino) atoms, the relatively strong ligand field effect of N (imino) compared with other potential donor atoms in transition metal complexes and also by the fact that an O(carboxyl)

atom is capable of forming a chelate ring. The role of the metal ion in these complexes seems to involve both stabilization or trapping of the Schiff base, and in addition it also ensures the planarity of the conjugated π-system. The stabilities of Schiff base complexes depend primarily on the strength of the C=N bond, the basicity of the imino group and steric factors.

Transition metal complexes of Schiff bases derived from various aldehydes and amino acids were prepared and studied by several workers. Some of these are given in Table I.6. Crystallographic studies have been done in a few cases and the data are given in Table I.7.

The Schiff base derived from pyridoxal and amino acids forms complexes of type I which are in tautomeric equilibrium with II (Fig. 1.2).

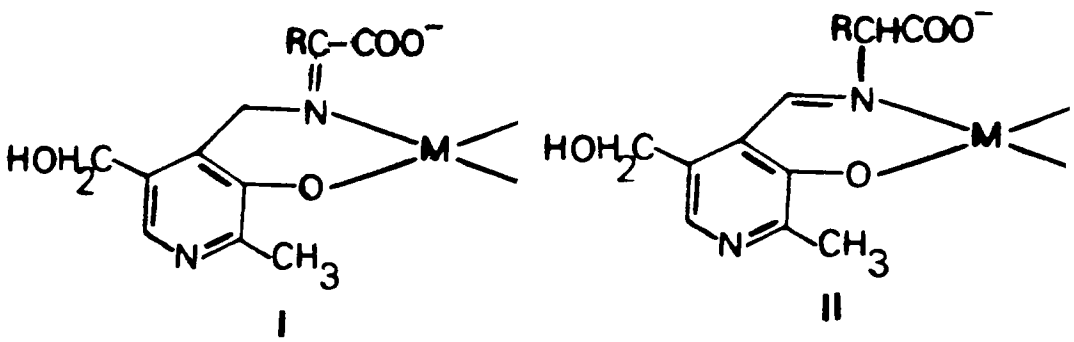

Fig. 1.2 Tautomeric structures of the complexes

Table I.6
Metal complexes of Schiff bases derived from amino acids

Metal	Schiff base ligands derived from		Ref.
	Aldehyde/ketone	Amino acids	
Fe(II)	N-(2-hydroxy-1-naphth-aldehyde)	glycine	97
Co(II)	N-(2-hydroxy-1-naphth-aldehyde)	glycine	97,98
	furan-2-carbaldehyde	glycine α-alanine α-valine	99
	L-menthyl-3-(o-hydr-oxybenzoyl)propionate	alanine valine leucine phenylalanine	100
	cholesteryl-3-(o-hydr-oxybenzoyl)propionate	alanine valine leucine phenylalanine	100
	salicylaldehyde	glycine valine threonine	101
	3-methylsalicylalde-hyde	glycine valine threonine	101
	isatin	β-alanine	102
Ni(II)	N-(2-hydroxy-1-naphth-aldehyde)	glycine alanine valine leucine isoleucine norleucine serine aspartic acid	103,97
	furan-2-carbaldehyde	glycine α-alanine α-valine	99

Table I.6 (continued)

	salicylaldehyde	DL-2-aminobutyric acid β-alanine 3-aminobutyric acid DL-asparagine L-glutamine	104
	salicylaldehyde	S(+)cystein	105
	aceyl acetone	S(+)cystein	105
Cu(II)	salicylaldehyde	glycine histamine serine cystein tryptophan	106
	N-(2-hydroxy-1-naphthaldehyde)	serine histidine tryptophan	107
	1R-3-hydroxymethylene camphor	S-phenylalanine	108
	7-hydroxy-5-methoxy-2-methyl-chromonaldehyde	glycine valine leucine asparagine glutamine arginine histidine serine	109
	furan-2-carbaldehyde	glycine α-alanine α-valine	99
	N-(2-hydroxy-1-naphthaldehyde)	glycine	97
	o-aminobenzaldehyde	N-benzyl-S-proline	110
	o-aminoacetophenone	N-benzyl-S-proline	110
	benzene-1,3-dicarbaldehyde	1-histidine methyl ester	111

Table I.7
X-Ray crystallographic data

Compound	Space group	Z	a(Å) b(Å) c(Å)	α(°) β(°) γ(°)	Other data		Ref.
((R,S)-N,N'-ethylenebis-	$P2_1/c$	4	10.516(3)	90	Cu-N	2.006	112
(serinato))copper(II)-			12.204(3)	143.88		2.001	
monohydrate			15.631(3)	90	Cu-O	1.961	
						2.181	
diaqua(n-salicylidene-L-	$P2_1$	4	6.681(4)	90	Cu-O	1.951	113
threoninato)copper(II)			13.640(8)	90.88		1.921	
			16.646(8)	90	Cu-N	1.951	
N-salicylideneglycinato-	C2/c	8	10.721	90			114
aquocopper(II)tetra-			17.769	94.71	-		
hydrate			13.895	90			
N-salicylideneglycinato-	C2/c	-	17.160	90	Cu-O	1.953	115
aquocopper(II)hemi-			6.840	111.29		1.928	
hydrate			17.570	90		2.234	
						2.016	
					Cu-N	1.949	
pyruvidene-β-alaninato-	$P2_1/c$	4	6.860	90	Cu-O	1.906	116
aquocopper(II)dihydrate			11.398	106.93		1.963	
			13.358	90	Cu-N	1.963	

This tautomeric equilibrium leads to transamination; thus the same metal complexes can be obtained when either pyridoxal and alanine or pyridoxamine and pyruvic acid are allowed to react together in the presence of a metal ion. The Schiff bases derived from amino acids and pyridoxal have attained considerable attraction due to the biochemical significance of vitamin B_6 and the realization that many of the enzymic reactions involving vitamin B_6 could be brought about in the absence of enzyme by using pyridoxal and various metal ions.

The Schiff base complexes derived from amino acids are particularly stable towards hydrolysis and dissociation in aqueous solution. The high thermodynamic stability associated with these complexes is attributed to their greater chelation over the bidentate nature of the amino acids, a feature which is attributed, in part, to their ability to undergo ketoimine and aldimine tautomerism[117].

In the complexes of Schiff bases derived from a tridentate amino acid, histidine, and pyruvate, histidine binding occurs through the N(imino) and N(imidazole); whereas in other complexes of Schiff bases derived from histidine, glycine like chelation occurs. These different modes can be readily distinguished by their CD spectra[118].

Casella and Gullotti studied a number of cobalt(II) complexes of the imines of the L-amino acids derived from salicylaldehyde and pyridoxal[119]. The complexes are high-spin and have five or six coordinated structure. Their stereochemical properties were deduced from the CD spectra and by preparing some representative adducts with donor bases. Further the complexes have the capacity to bind with molecular oxygen. The histidine derivatives react readily with molecular oxygen in any solvent; but, the derivatives of amino acids with non-polar side chains require the presence of additional base molecules. The reactivity of the histidine complexes is determined essentially by the glycine-like mode of binding of the amino acid residue. However, the histidine complex derived from pyruvate, in which the amino acid is bound as a substituted histamine, is completely unreactive to dioxygen. In some cases, the presence of bulky, non-polar side chains on the amino acid residues sterically hinders dimerization of the 1:1 dioxygen adducts and provides a reversible oxygenation behaviour at room temperature. Complimentary information on the evolution of the 1:1 and 2:1 dioxygen species during the oxygenation reactions are obtained by combined ESR and CD measurements.

Okawa *et al.* reported cobalt(III) complexes of amino acid Schiff bases of l-menthyl-3-(*o*-hydroxybenzoyl)propionate and cholesteryl-3-(*o*-hydroxybenzoyl)-propionate in solution[100]. The intensity of the CD peak induced at 520 nm changes with the solvent used for the precipitation of the complex, decreasing in the order: ethanol > methanol > DMSO > DMF > acetonitrile.

Belokon *et al.* describe the search for universal chiral reagents for the asymmetric synthesis, resolution and retroracemization of amino acids[110]. Reaction of N-benzyl-S-proline with *o*-aminobenzaldehyde or *o*-aminoacetophenone has given S-2-N-(N'-benzylprolyl)-aminobenzaldehyde or S-2-N-(N'-benzylprolyl)acetophenone. These chiral reagents on interaction with α-amino acids and copper(II) ions form complexes in which Schiff bases act as tetradentate ligands and coordinate to the copper ion by the nitrogen atom of the pyrrolidene fragment, the deprotonated amide group, the amino acid fragment and by the oxygen atom of the carboxylate. Several chiral cobalt(III) complexes with Schiff bases of amino acids (glycine, valine or threonine) with salicylaldehyde or 3-methylsalicylaldehyde have also been studied. Diastereoisomers of complexes formed from the Schiff base derived from valine or threonine were separated on Al_2O_3 and enantiomers of complexes formed

from the glycine Schiff base were resolved with brucine and strychnine.

Nickel(II) complexes of Schiff bases of 2-N-benzylprolylaminobenzophenone with amino acids were prepared[120] and were reacted with the appropriate alkyl halide in DMF at 25°C using solid NaOH as a catalyst. The alkylated products thus formed on cleavage with HCl solution regenerated the ketone and produced the α-methyl amino acids. This method can be used for the asymmetric synthesis of α-amino acids under a variety of conditions.

By the condensation of salicylaldehyde or acetylacetone with S(+)cystein ester in the presence of Ni^{2+} ions, diamagnetic, binuclear, square planar Schiff base complexes were obtained[105]. Their CD spectra show negative Cotton effect due to the stereospecific coordination of the chiral ligand. Their PMR spectra have also been studied, and these studies show that complexes in solution exists in preferred δ conformation with the axial -COOR group. From the electronic spectra and magnetic moment it was deduced that in donor solvents like pyridine or water, complexes exist as monomeric hexacoordinate ones. In addition, alkoxycarbonyl group undergo ester exchange which is facilitated by the inductive effect of the -CH=N- group.

Although complexes were prepared in the presence of base, they did not undergo racemization. Increased optical stability was ascribed to unfavourable conformation of the complex.

The electron spin resonance studies of frozen solutions of a range of copper complexes have been carried out at 110 K. The complexes have distorted square planar structure with two N and two O coordinating groups[106]. They are sufficiently flexible, and the degree of planarity is seen to be affected by the coordinated solvent. Since the compounds are of low symmetry, two components of $g_{\perp}$ are observed. The values obtained for $g_{\parallel}$ and $A_{\parallel}$ are both solvent dependent; probably because DMSO and DMF replace water from the copper coordination sphere. The most planar complexes have the highest $A_{\parallel}$ to $g_{\parallel}$ ratios and these values decrease with increasing distortion.

1.3 METAL COMPLEXES OF THIOSEMICARBAZONES

1.3.1 INTRODUCTION

A large number of thiosemicarbazone ligands have been derived by simply condensing aliphatic, aromatic or heterocyclic aldehydes or ketones with thiosemicarbazide compounds. Thiosemicarbazones exist probably as an

equilibrium mixture of thione and thiol tautomers (Fig. 1.3).

(a) (b)

Fig. 1.3 Tautomeric structures of thiosemicarbazones

Thione form (a) can act as a neutral bidentate ligand, while the deprotonated thiol form (b) can act as a singly charged bidentate ligand. Therefore, cationic, neutral or anionic complexes will result depending upon the preparative conditions, especially by changing the pH of the solution. In most cases, thiosemicarbazone complexes are formed with ligands in the uncharged form.

A review on the important developments in the structural chemistry of transition metal complexes of thiosemicarbazones has appeared[121] in 1985. Prior to this, a very comprehensive review by Campbell on the coordination chemistry of thiosemicarbazides and thiosemicarbazones provides details of the thermodynamic, structural, magnetic, and vibrational and electronic spectral properties of their metal complexes[122]. Campbell has pointed out that the nature of the sulphur donor atom is the most important single

factor affecting the behaviour of these ligands. This leads to a high degree of thermodynamic stability for complexes formed with `soft' or `marginally soft' metal ions. The stereochemistries of N-substituted complexes are largely influenced by steric effects involving the sulphur atoms. Developments prior to Campbell's review have been dealt with adequately by Livingstone[123]. The analytical applications of thiosemicarbazones have also been reviewed[124,125]. Our aim, here, is to present a brief survey of recent literature of the complexes of thiosemicarbazones.

1.3.2 X-Ray crystallographic studies

Crystal structure data are now available for some thiosemicarbazone complexes and are given in Table I.8. The most common stereochemistries encountered in thiosemicarbazone complexes are octahedral and square planar. On rare occasions five coordinated structures are also obtained.

Divjakovic and Leovac reported[126] the crystal structure data of the five coordinate complex, $[CoL_2(CH_3COO)]I$ (where L = acetone-S-methylthiosemicarbazone). The coordination around cobalt is found to be close to that of a trigonal bipyramid formed by four nitrogen atoms and one oxygen atom of the acetyl group.

Table I.8
X-Ray crystallographic data

Compound	Ligand, L	Space group	Z	a(Å) b(Å) c(Å)	α(°) β(°) γ(°)	Other data		Ref.
$[CuL(H_2O)]Cl.H_2O$	pyridoxal thiosemicarbazone	P1	2	9.732(2) 9.491(3) 7.894(2)	95.73(3) 101.65(3) 79.30(2)	Cu-Cu Cu-N Cu-OH_2 Cu-S	3.549(2) 1.943(6) 1.941(5) 2.226(2)	132
$[CuL(CH_3COO)]_2$	2-formylpyridine thiosemicarbazone	P1	1	8.827(3) 8.813(3) 8.997(3)	117.49(2) 110.9693) 91.65(3)	Cu-S	2.274(1)	133
$[CuL(SO_4)]_2$	2-formylpyridine thiosemicarbazone	C2/c	4	14.751(3) 9.138(2) 17.468(4)	90 104.91(2) 90	Cu-S	2.279(1)	133
$[Cu(HL)(NO_3)].2H_2O$	pyridoxal thiosemicarbazone	$P2_1/n$	4	16.126(1) 7.267(1) 12.466(1)	90 108.60(1) 90	-		134
$[CoL_2(CH_3COO)]I$	acetone-S-methyl thiosemicarbazone	P1	2	8.323(3) 9.971(3) 13.128(4)	82.28(2) 89.55(2) 87.56(2)	Co-N Co-O	2.165(6) 2.041(5)	126

Table I.8 (continued)

$[CoL_2Cl_2].H_2O$	acetone thiosemi-carbazone	$P2_1$	4	11.373(3) 8.875(3) 17.817(6)	90 101.35(2) 90	Co-Cl Co-S Co-N	2.292(3) 2.281(3) 2.230(1)	135
$[CoL_2I_2]$	acetone thiosemi-carbazone	C2/c	4	11.969(8) 11.547(9) 18.883(7)	90 106.10(9) 90	Co-I Co-S	2.578(1) 2.304(2)	136
$[NiL_2Cl].H_2O$	acetone thiosemi-carbazone	Pca2/1	4	21.934(3) 6.920(1) 11.762(2)	90 90 90	Ni-N Ni-S Ni-Cl	2.135 2.291 2.305	128
$[NiL_2].H_2O$	isoquinoline-1-carb-oxaldehyde thiosemi-carbazone	C2/c	8	17.884(3) 17.567(3) 15.901(6)	90 101.57(2) 90	Ni-S	2.424(2) 2.412(2)	130

The compound thus constitutes a rare example of a series of thiosemicarbazone complexes wherein the sulphur atom does not take part in coordination.

McCleverty and coworkers have determined[127] the structures of the two square planar diamagnetic nickel(II) complexes formed with the bisthiosemicarbazones of hexane-2,5-dione (L_1) and phthalaldehyde (L_2). Both of the complexes contain a seven-membered chelate ring as well as the two five membered rings involving thiosemicarbazide moieties. Although no information is available on the geometries of the free ligands, it is worthnoting that the C-S and N-N as well as the Ni-N and Ni-S bond lengths are similar to those found in the square planar nickel(II) complexes of thiosemicarbazide. In NiL_1, the coordination about the nickel atom involves a distortion from square planarity such that the Ni, the two S and one of the coordinated N atoms are approximately coplanar, while the other coordinated nitrogen is 0.66 Å away from this mean plane. On the other hand, in NiL_2, chelate planes are mutually inclined at an angle of 33° and are symmetrically oriented with respect to the mean coordination plane of the nickel.

In the complex, $[NiL_2Cl_2]$ (where L = acetone thiosemicarbazone), the nickel atom is pentacoordinated

with the donor atom set N_2S_2Cl, the two sulphur atoms being in the axial positions of an approximately trigonal bipyramidal coordination polyhedron[128]. The geometries of the coordinated thiosemicarbazone ligands are not identical; but, apart from the longer C-S bond lengths they are not very different from that of the free ligand. As expected, the Ni-S bond lengths are intermediate between those found for 4- and 6-coordinated nickel(II) complexes of thiosemicarbazones, but the Ni-Ni distances are longer than those in both 4- and 6- coordinated species. In the corresponding nitrate complex, $[NiL_2(NO_3)_2]$, the nickel atom is coordinated with the donor atom set, $N_2S_2O_2$, but only one of the nitrate groups is found to be coordinated and is therefore necessarily bidentate. However, the coordination polyhedron is distorted towards an approximately trigonal bipyramidal shape, with the coordinated bidentate nitrate effectively occupying a single coordination position. The two Ni-O bond lengths are appreciably different as are the Ni-S and Ni-N bond lengths[129].

The structures of two six coordinated nickel(II) complexes with thiosemicarbazones have been determined. The ligands are the thiosemicarbazones of isoquinoline-1-carboxaldehyde and pyridine-2-carbox-

aldehyde, which are tridentate, the third donor atom being the heterocyclic nitrogen. Because of the coplanarity of the three ligand donor atoms, NNS, the two sulphur atoms are necessarily *cis*. In each case there are significant differences in the parameters found for the two ligand molecules in the complex[130]. The Ni-S bond lengths are appreciably longer than those in the 4- and 5- coordinated complexes and are similar to the values found for the paramagnetic six coordinated nickel(II) complexes of thiosemicarbazide. The Ni-N (hydrazinic) bond lengths are intermediate between those in the 4- and 5- coordinated species and are appreciably shorter than the Ni-N (heterocyclic N) bond lengths.

Crystal structure of 3-ethoxy-2-oxo-butyraldehyde thiosemicarbazone, its copper complex, and the benzylbis(thiosemicarbazone)copper(II) complex were investigated by Bushnell and Tasang in order to investigate the antitumour mechanism at the molecular level[131]. Comparison of their structures led these authors to suggest that bonding of sulphur to the axial copper site is probably not totally dominant over the forces of double hydrogen bonding and that hydrogen bonding may be an important factor in their antitumour mechanism. Adenine, guanine and cytosine, all have amino groups adjacent to unprotonated ring nitrogen

atoms and are thus well suited to form double hydrogen bonds with the bis(thiosemicarbazone)copper(II) complex. The authors have pointed out the striking structural similarity between the copper complex of 3-ethoxy-2-oxo-butyraldehyde thiosemicarbazone and the nucleoside formed from guanine and ribose (or deoxyribose), which is in some way related to their antitumour activity.

Ferrari *et al.* studied[132] the crystal structure of the complex, $[Cu(HL)(H_2O)]Cl.H_2O$ (where H_2L = pyridoxal thiosemicarbazone). In this compound, the copper(II) ion has a square planar geometry with phenolic oxygen, imine nitrogen, sulphur and a water molecule as the basal donors. A sulphur atom of a centrosymmetrically related molecule occupying the axial position serves as a bridging element to form a dimeric structure.

Crystal structure studies of copper(II) complexes of pyridine-2-carboxaldehyde thiosemicarbazone (HL), $[CuLX]_2$ (where X = acetate or sulphate) have been reported[133]. These complexes consist of discrete centrosymmetric dimers; the monomeric units being bridged by two acetate and sulphate ligands. The copper atoms have a distorted square pyramidal coordination geometry with three donor atoms (NNS) coming from L or HL to form a tricyclic ligating system. The fourth

donor atom comes from the bridging acetate or sulphate ion. The fifth coordination position is occupied by a less strongly bound oxygen from the second bridging anion.

1.3.3 Magnetic susceptibility measurements

Magnetic behaviour of only a few thiosemicarbazone complexes have been studied over a temperature range. However, even room temperature moments are often useful in assigning the stereochemistry about the metal ion. The room temperature magnetic moments of some thiosemicarbazone complexes are shown in Table I.9. In a few cases, the room temperature magnetic moments were found to be much lower than those expected on the basis of the spin-only formula; however, magnetic behaviour of these complexes have not been investigated in detail.

In a series of papers, Zelentsov and coworkers have described the magnetic properties of iron(III) complexes of substituted salicylaldehyde thiosemicarbazone ligands of the type $M[Fe(R\text{-}L)_2].nH_2O$ (where M = Cs, NH_4 or K; R = H, 5-Cl, 5-Br, 3,5-di-Cl or 3,5-di-Br; n = 0 or 1.5 and L = salicylaldehyde thiosemicarbazone)[137,138]. It has been observed that the crystal field splitting energy of these systems corresponds to the energy region of crossover of electronic terms $^6A_1$ and $^2T_2$ on

Table I.9

Magnetic moment and electronic spectral data

Compound	Ligand,L	$\mu_{eff.}$ BM	Abs. max. cm^{-1}	Proposed structure	Ref.
$[CuL_2Cl_2]$	indane-1,2,3-trione monothiosemicarbazone	1.81	15500,23200	square planar	140
$[FeL_2(H_2O)_2]Br_2$	p-anisaldehyde thiosemicarbazone	5.12	11010	octahedral	141
$[CoL_2(H_2O)_2]Br_2$	p-anisaldehyde thiosemicarbazone	4.85	10000,19300	octahedral	141
$[NiL_2(H_2O)_2]Br_2$	p-anisaldehyde thiosemicarbazone	3.10	11030,18800 31000	octahedral	141
$[CuL_2(CH_3COO)].(CH_3COO)2H_2O$	4-(methoxybenzaldehyde)-4-phenyl-3-thiosemicarbazone	1.74	14860,19120 29400	octahedral	142
$[NiL_2SO_4)].2H_2O$	4-(methoxybenzaldehyde)-4-phenyl-3-thiosemicarbazone	2.62	15500,27020 35700	octahedral	142

Table I.9 (continued)

$[NiL_2]$	hydrazine-S-methyl-dithiocarboxylate thiosemicarbazone	diamag.	17700,22200 25000	square planar	143
$[FeLSO_4]$	1-formylisoquinoline thiosemicarbazone	5.16	5400,9100 20000	distorted trigonal bipyramidal	144
$[FeLCl_3]$	1-formylisoquinoline thiosemicarbazone	2.07	16500,20000	distorted octahedral	144
$[FeLSO_4]$	4-methyl-5-amino-1-formylisoquinoline thiosemicarbazone	5.18	5400,9100 20000	distorted trigonal bipyramidal	144
$[FeLCl_3]$	4-methyl-5-amino-1-formylisoquinoline thiosemicarbazone	2.09	5400,9100 20000	distorted octahedral	144
$[FeLSO_4]$	4-(m-aminophenyl)-2-(formylpyridine) thiosemicarbazone	5.21	5400,9100 20000	distorted trigonal bipyramidal	144
$[FeLCl_3]$	4-(m-aminophenyl)-2-(formylpyridine) thiosemicarbazone	2.11	16500,20000	distorted octahedral	144

Table I.9 (continued)

$[CuL_2Cl]$	*O*-aminobenzaldehyde thiosemicarbazone	diamag.	26810,32470	square planar	145
$[FeL_2]$	2,4-dihydro-5-methyl-2-phenyl-3H-pyrazol-3-one thiosemicarbazone	5.93	15600	octahedral	146
$[CoL_2]$	2,4-dihydro-5-methyl-2-phenyl-3H-pyrazol-3-one thiosemicarbazone	2.65	9000,15000 20000,23000	trigonal bipyramidal	146
$[CuL_2]$	2,4-dihydro-5-methyl-2-phenyl-3H-pyrazol-3-one thiosemicarbazone	1.74	15800,19000 21000	square planar	146
$[NiL_2]$	2,4-dihydro-5-methyl-2-phenyl-3H-pyrazol-3-one thiosemicarbazone	diamag	15700,18460 28000	square planar	146
$[CoL_2X_3]$	thiophene-2-carboxaldehyde thiosemicarbazone	diamag.	16000,20000	octahedral	147

Table I.9 (continued)

$[NiL_2]$	benzylmethyl-ketone thiosemi-carbazone	diamag.	17000,20000 23000	square planar	148
$[CoL_2]$	benzylmethyl-ketone thiosemi-carbazone	4.80	8700,16000 21000	distorted octahedral	148
$[CuL_2]$	benzylmethyl-ketone thiosemi-carbazone	1.82	15400,21500	square planar	148
$[CoL_2X_2]$	2-furfuraldehyde thiosemicarbazone X = NO_3/Cl/Br/I/NCS	4.65-4.90	8600,19000 26000	octahedral	149
$[CoLX_2].2H_2O$	2-furfuraldehyde thiosemicarbazone X = NO_3/Cl/Br/I/NCS	4.55-4.90	8000,17000 25000	octahedral	149
$[CoL_2]$	2-furfuraldehyde thiosemicarbazone	4.85	7790,16750 25250	square planar	149
$[NiL_2(NCS)_2]$	benzylmethylketone thiosemicarbazone	3.10	9090,17400 26600	octahedral	150

Table I.9 (continued)

$[NiL_2X_2]$	benzylmethylketone thiosemicarbazone X = Cl/Br/I	3.18	6350,8300 16000,23500	trigonal bipyramidal	150
$[NiL_2(CH_3COO)_2]$	benzylmethylketone thiosemicarbazone	diamag.	18100,20000 23500	square planar	150
$[NiL_2SO_4]$	benzylmethylketone thiosemicarbazone	4.00	5060,9090 15300	tetrahedral	150
$[CoL_2]$	propiophenone thiosemicarbazone	4.75	8000,16100 21200	polymeric octahedral	151
$[NiL_2]$	propiophenone thiosemicarbazone	diamag.	17500,21800 23400	square planar	151
$[CuL_2]$	propiophenone thiosemicarbazone	1.82	17500,21800 23400	square planar	151
$[NiL(CH_3COO)].H_2O$	1-(*o*-aminoacetophenone)-4-phenyl thiosemicarbazone	diamag.	12430,17240 20200	square planar	152
$[NiLCl].3H_2O$	1-(*o*-aminoacetophenone)-4-phenyl thiosemicarbazone	2.69	16600,20400 26500	square planar and octahedral isomers	152

Table I.9 (continued)

$[CoL_2]$	4-(2-thiazolyl)- 1-(2-acetylfuran) thiosemicarbazone	3.8	9760,17390 20620	octahedral	153
$[CoL_2Cl_2]$	4-(2-thiazolyl)- 1-(2-acetylfuran) thiosemicarbazone	4.8	10000,16130 22990	octahedral	153
$[NiL_2]$	4-(2-thiazolyl)- 1-(2-acetylfuran) thiosemicarbazone	diamag.	10260,16530 23250	square planar	153
$[CuL_2]$	4-(2-thiazolyl)- 1-(2-acetylfuran) thiosemicarbazone	1.2	16200	octahedral	153
$[CoL_2X]$	2-pyridine carbox- aldehyde thiosemi- carbazone X = Cl/NCS/NO_3/N_3/CN	3.89	16900,23820 31270	rhombic	154
$[CoLCl_2]$	4-(*m*-aminophenyl)- 2-formylpyridine thiosemicarbazone	4.43	4490,4835 5810,12690 17240,19230	trigonal bipyramidal	155
$[NiLCl_2]$	4-(*m*-aminophenyl)- 2-formylpyridine thiosemicarbazone	3.25	7220,10530 12500,14390 19230,21740	trigonal bipyramidal	155

Table I.9 (continued)

$[CuLCl_2]$	4-(*m*-aminophenyl)-2-formylpyridine thiosemicarbazone	1.84	10100,13335	trigonal bipyramidal	155
$[CoL_2]$	piperonaldehyde (3,4-methylenedioxybenzaldehyde thiosemicarbazone	2.00	9090,10000	square planar	156
$[CoL_2]Cl_2$	piperonaldehyde (3,4-methylenedioxybenzaldehyde thiosemicarbazone	4.52	14290,14600	tetrahedral	156

Tanabe-Sugano diagrams. As a result, these compounds offer excellent opportunities for coordination chemists to examine correlations between structural and magnetic features. Cryomagnetic studies have indicated that for $Cs[FeL_2]$ and $NH_4[Fe(5\text{-}Cl\text{-}L)]$ the spin state as well as the coordination geometry of the iron atom remain unchanged between 103 and 298 K, while for $NH_4[Fe(5\text{-}Br\text{-}L)]$ there are two morphologically different types of microcrystals, each exhibiting a peculiar magnetic behaviour. Thus the tablet-shaped species, which is low-spin at room temperature ($\mu_{eff.}$ = 2.16 BM), undergoes a sharp transition in magnetic moment ($\mu_{eff.}$ = 5.10 BM) at 400 K, while black mica-like crystals, which are high-spin compounds at room temperature ($\mu_{eff.}$ = 5.06 BM), exhibit a similar transition at 220 K ($\mu_{eff.}$ = 2.29 BM). These two modifications are isostructural and probably represent rather rare examples of spin isomers that are established in crystals.

The complexes $NH_4[FeL_2].1.5H_2O$ and $K[FeL_2]$ (where L = 3,5-dichlorosalicylaldehyde thiosemicarbazone) are crossover complexes of the spin-equilibrium type with $\mu_{eff.}$ values that are intermediate between high-spin and low-spin values. The characteristic features of these isostructural compounds are the two crystallographically independent positions for the iron atoms and the

magnetic properties which are determined by the site distributions of Fe(III) atoms within the crystals. Whether this distribution is static or dynamic needs to be investigated.

Magnetic behaviour of a pentacoordinated iron(III) complex with a square pyramidal configuration and S = 3/2, derived from the 2-hydroxy-1-naphthaldehyde thiosemicarbazone ligand, has been described by Bhoon[139]. The powdered samples at different temperatures, yield magnetic moments for this complex that rise continuously from near 3 BM at 4.2 K to 4.46 BM at 143.4 K. The slightly higher magnetic moment of 4.47 BM at room temperature has been thought to be due to contributions from the closely lying excited states.

1.3.4 Electronic spectra

Electronic spectral bands of some thiosemicarbazone complexes are given in Table I.9.

Very intense bands above 33000 cm^{-1} shown by some thiosemicarbazone complexes were assigned as the ligand $\pi \longrightarrow \pi^*$ transition. The spectra of a number of closely related copper(II) bisthiosemicarbazone complexes have two bands, often only partially resolved[157,158], at about 20000 cm^{-1} and another pair of bands, again often only partially resolved, at about 30000 cm^{-1}. Blumberg

and Peisach have proposed[159], by analogy with certain intensely absorbing copper proteins, that in spite of the high intensity, the 20000 cm^{-1} bands are d-d transitions. A semiempirical molecular orbital treatment using the Wilfsberg-Helmholtz approximation has been carried out[122] in order to try and fit the observed spectrum of diacetylbis(thiosemicarbazone)-copper(II). Taking the plane of the molecule as the xy-plane, the ground state ($^2B_2$ in C_{2v} symmetry) has been shown to be an antibonding σ combination of copper d_{xy} and ligand σ orbitals. The most important result of the calculation is that regardless of the input assumptions very large ligand orbital contributions to the ground state are found.

1.3.5 EPR spectra

Most of the EPR studies are focussed on the copper(II) complexes. Table I.10 lists the EPR parameters of some copper(II) complexes containing thiosemicarbazone ligands.

Raina and Srivastava have described the EPR spectra of low-spin iron(III) complexes of the type $[FeL_2X]$ (where L = 2-acetylpyridine thiosemicarbazone and X = NO_3, OH, Cl. N_3, NCS or NO_2)[160]. The broad isotropic signal (g = 2.120) observed for the azide complex is

Table I.10
EPR spectral data

Compound	Ligand,L	g values	A* values	Ref.
$[CuLCl_2]$	2-formylpyridine thiosemicarbazone	$g_{\parallel}$ 2.18 $g_{\perp}$ 2.03	$A_{\parallel}$ 155 A_{iso} 72	163
$[CuL(CH_3COO)]$	2-formylpyridine thiosemicarbazone	$g_{\parallel}$ 2.18 $g_{\perp}$ 2.03	$A_{\parallel}$ 175 A_{iso} 75	163
[CuLCl]	2-formylpyridine thiosemicarbazone	$g_{\parallel}$ 2.17 $g_{\perp}$ 2.03	$A_{\parallel}$ 163 A_{iso} 75	163
[CuL(SCN)]	2-formylpyridine thiosemicarbazone	$g_{\parallel}$ 2.18 $g_{\perp}$ 2.03	$A_{\parallel}$ 165 -	163
$[CuLCl_2]$	2-acetylpyridine thiosemicarbazone	$g_{\parallel}$ 2.18 $g_{\perp}$ 2.03	$A_{\parallel}$ 155 A_{iso} 75	163
$[CuL(CH_3COO)]$	2-acetylpyridine thiosemicarbazone	$g_{\parallel}$ 2.16 $g_{\perp}$ 2.03	$A_{\parallel}$ 180	163
$[CuL_2]$	4,5-dimethylpyrazole-3-carboxaldehyde thiosemicarbazone	$g_{\parallel}$ 2.16 $g_{\parallel}$ 2.03	-	164
[CuLCl]	4,5-dimethylpyrazole-3-carboxaldehyde thiosemicarbazone	$g_{\parallel}$ 2.16 $g_{\perp}$ 2.04	$A_{\parallel}$ 175	164

Table I.10 (continued)

[CuLBr]	4,5-dimethylpy-razole-3-carbox-aldehyde thio-semicarbazone	$g_{\parallel}$ $g_{\perp}$	2.17 2.04	$A_{\parallel}$	182	164
[CuL(NO_3)]	4,5-dimethylpy-razole-3-carbox-aldehyde thio-semicarbazone	$g_{\parallel}$ $g_{\perp}$	2.18 2.05	$A_{\parallel}$	186	164
[CuL(NCS)]	4,5-dimethylpy-razole-3-carbox-aldehyde thio-semicarbazone	$g_{\parallel}$ $g_{\perp}$	2.17 2.04	$A_{\parallel}$	189	164
[CuL_2]	benzylmethyl-ketone thiosemi-carbazone	g_x g_y g_z	2.17 2.05 2.08	-		148
[CuL_2]	propiophen-one thiosemi-carbazone	g_x g_y g_z	2.03 2.03 2.12	-		151
[CuL_2]	butyrophen-one thiosemi-carbazone	g_x g_y g_z	2.03 2.03 2.12	-		151
[CuL_2Cl_2]	4-(2-thiazol-yl)-1-(2-acetyl-furan)thiosemi-carbazone	$g_{\parallel}$ $g_{\perp}$	2.17 2.01	$A_{\parallel}$ $A_{\perp}$	67 30	153
[CuL_2]	4-(2-thiazol-yl)-1-(2-acetyl-furan)thiosemi-carbazone	$g_{\parallel}$ $g_{\perp}$	2.16 2.04	$A_{\parallel}$ $A_{\perp}$	153 21	153
[CuL_2(NO_3)]	2-pyridine carb-oxaldehyde thio-semicarbazone	g	3.86	-		154

* values are in Gauss

possibly due to spin-spin relaxation *via* dipolar interactions, which seems to suggest that the anions in these complexes are capable of influencing the environment of the iron(III) ion in the solid state.

Blumberg and Peisach have studied[159] the X-band EPR spectrum of a copper complex of 3-ethoxy-2-oxobutanone bis(thiosemicarbazone) in DMF at 1.4 K. Unfortunately the sample they used contained isotopically normal copper (69% ^{63}Cu, 31% ^{65}Cu) with the result that anomalous lines appeared in the ligand hyperfine structure because of the non-coincidence of the two sets of lines arising from the two copper isotopes. As a result they erroneously interpreted the ^{14}N hyperfine structure as arising from the interaction of the unpaired spin with four equivalent ^{14}N nuclei. But the crystal structure study shows that copper is coordinated to only two N and two S atoms. Hatfeild and coworkers examined the solution spectra of two analogous compounds which had been prepared from ^{63}Cu ions[161]. They found that the ^{14}N ligand hyperfine structure superimposed on each of the copper hyperfine lines consisted of only five lines showing that the unpaired spin interacts with only two nitrogen nuclei. Getz and Silver also examined[162] the X-band spectrum of Cu(II) doped into the diamagnetic nickel(II) analogue of Hatfeild's compound, and found a five line ^{14}N superhyperfine structure.

The EPR spectrum of red solid copper complex of 3-ethoxy-2-oxobutanone bisthiosemicarbazone was studied by Blumberg and Peisach who reported[159] a strong exchange interaction with the lowest lying singlet state (S = 0). From their data they calculated the singlet-triplet separation to be 23 K. They also reported that addition of acid to the complex gave a yellow species of the same formula which they assumed to be the protonated form. A concentrated solution of this species in DMF showed no EPR signal upto 130 K. To account for this they proposed a dimeric structure for this complex.

1.3.6 Infrared spectra

Assignments of the major bands in the IR spectra of thiosemicarbazides and thiosemicarbazones have been made by Campbell and Grzeskowiak[165]. On complexation most of the bands in the spectrum of thiosemicarbazone undergo frequency shifts and in many cases intensity changes. The most marked change is that of the 805 cm^{-1} band which is shifted almost 100 cm^{-1} to lower frequencies. This band is largely ν(C=S) and a shift of this order would indicate the formation of a strong metal-sulphur bond.

Gingras and coworkers have reported[166-171] the IR spectra of a large number of thiosemicarbazones, both alkyl and aryl N-substituted thiosemicarbazones and bisthiosemicarbazones. In most cases they have prepared the copper(I) complexes of these compounds and they found that the ν(C=S) band is a useful probe for complex formation. Complications can arise when absorption by the aldehyde or ketone part of the ligand occurs in the C=S stretching region. In this case coupling will occur and the assignment becomes difficult.

The far IR spectral data for transition metal complexes of thiosemicarbazone have been reported by several authors. Some of these are given in Table I.11. However in the absence of a full normal coordinate analysis it is not meaningful to assign the bands in this region, as thiosemicarbazone is a non-rigid molecule having low frequency vibrations with which the metal-ligand vibrations can couple[172].

1.3.7 Biological importance

Since Domagk's original report[173] on the antitubercular activity of thiosemicarbazones, the number of papers on the pharmacology of these compounds has expanded dramatically. These compounds were found to be active against influenza, protozoa, small-pox and

Table I.11
Far IR absorption frequencies (cm^{-1})

Compound	Ligand,L	ν(M-N)	ν(M-S)	Ref.
$[CuL_2Cl_2]$	indane-1,2,3-trione mono-thiosemicarbazone	510m	-	140
$[CuL_2(H_2O)_2]Br_2$	*p*-anisaldehyde thiosemicarbazone	480s	340s	141
$[CoL_2(NO_3)_2].H_2O$	4-methoxybenzaldehyde-4-phenyl-3-thiosemicarbazone	520s	420s	142
$[NiL_2SO_4)].2H_2O$	4-methoxybenzaldehyde-4-phenyl-3-thiosemicarbazone	420s	390s	142
$[CuL_2(CH_3COO)].(CH_3COO).2H_2O$	4-methoxybenzaldehyde-4-phenyl-3-thiosemicarbazone	490s	410s	142
$[FeL_2]$	2,4-dihydro-5-methyl-2-phenyl-3H-pyrazol-3-one thiosemicarbazone	510m	375m	146
$[NiLCl].3H_2O$	1-(*o*-aminoacetophenone)-4-phenyl thiosemicarbazone	415s	470s	152
$[CoLCl_2]$	4-(*m*-aminophenyl)-2-formylpyridine thiosemicarbazone	260m	290m	155

Abbreviations: s = strong, m = medium, w = weak

certain kinds of tumour, and further they have been suggested as possible pesticides and fungicides[174-178]. Their activity has frequently been thought to be due to their ability to chelate trace metals. Thus Leibermeister showed[179] that copper ions enhance the antitubercular activity of p-acetamidobenzaldehyde thiosemicarbazone. Petering and coworkers also showed that the active intermediate in the antitumour activity of 3-ethoxy-2-oxobutyraldehyde bisthiosemicarbazone is its copper chelate[180,181].

Springarn and Sartorelli have synthesized[182] pyrazine-2-carboxaldehyde thiosemicarbazone and similar compounds and have evaluated their potential for removing excess iron from iron-loaded mice. These ligands are seen to be capable of removing excess iron accumulated in patients suffering from Cooley's anaemia.

2-Acetylpyridine thiosemicarbazone derivatives have been found to possess inhibitory activity for the RNA-polymerases of the influenza virus, which is thought to be mediated through chelation[183]. Support for this hypothesis has come through recent observations on the enhanced antileukemic properties of 1:1 complexes of Fe(III), Cu(II) and Ni(II) with 2-actylpyridine thiosemicarbazone ligands[184]. Bhoon *et al.* have reported[185] an iron(III) complex of N,N-disubstituted

2-acetylpyridine thiosemicarbazone, which has antimalarial activity.

The nature of the binding of copper(II) complex of pyridine-2-carboxaldehyde thiosemicarbazones with Ehrlich ascites tumour cells has been recently described by Petering and coworkers[186]. The compound is found to inhibit cellular DNA formation at low concentrations, but the RNA formation is seen to be less sensitive. The binding sites are indicated to be glutathione thiol groups, confirming the earlier observations of Bushnell and Tasang[187].

Antitumour activity of Fe(II) and Fe(III) complexes of isoquinoline-1-carboxaldehyde thiosemicarbazone and 4-methyl-5-amino-isoquinoline-1-carboxaldehyde thiosemicarbazone was evaluated against the P388 lymphocytic leukemia test system in mice and have been found to possess significant activity at the dosages employed[144].

Bamgboye *et al.* checked the antifungal behaviour of the ligand, p-anisaldehyde thiosemicarbazone and its transition metal complexes[141]. It was found that the metal chelates were more fungitoxic than the chelating ligand. It was also observed that as the radius of the metal ion decreases, the toxicity of the metal chelate increases. On the premise of the chelation theory, a

probable mode of toxicity may be envisaged. On chelation, the polarity of the metal ion is greatly reduced due to the sharing of its positive charge with the donor group and consequent π electron delocalization over the entire chelate ring manifold. Thus the lipophilic nature of the metal chelate increases and promotes its permeation through fungus membranes. Involvement of the hydrogen bond *via* the N=C group also enhances the activity.

In the case of the acetylpyridine thiosemicarbazones, only the 2-substituted derivative shows any appreciable antiviral activity. The absence of any significant antiviral activity in the 3- and 5-substituted derivatives supports the hypothesis that a metal chelate is formed between the ring nitrogen atom and thiosemicarbazone moiety[188]. Investigatons of the mode of action of 1-methylisatin-β-thiosemicarbazone, the prophylactic used successfully in the treatment of people who had been exposed to small-pox infected patients, indicate that its copper(II) chelate binds to nucleic acids *in vitro* under conditions in which there is no significant binding of aquated copper(II) ions[189]. It is possible that the copper chelate is bound to a m-RNA which is synthesized late in the infective cycle. It is also known that the thiosemicarbazone acts only in

the final process of infection and is active even after the synthesis of viral DNA has ceased. As the small-pox virus contains appreciable amounts of copper(II), it is possible that its chelation is part of the mode of action[190]. The other thiosemicarbzones are less well studied and as yet the link between antiviral action and chelation is not fully established.

1.4 Scope of the present investigation

Metal complexes of biologically important ligands are receiving increasing attention because of their wide applications in the field of biochemistry and medicine. In many cases, it has been found that the biological activity of ligands are increased by complexation with metal ions. Furthermore, such type of ligands are part of many biological coordination compounds, which are so complex that the function of metal ions can be understood only by studying simple model systems. Owing to these applications, there is a continuing interest in the synthesis of such complexes.

The aim of the present investigation was to synthesize and characterize some new metal complexes of biologically important ligands. The following ligands were selected for the study:

i) 1-Benzyl-2-phenylbenzimidazole (BPBI)

ii) 1-(2'-Hydroxybenzyl)-2-(2'-hydroxyphenyl)benzimidazole (HBHPBI)

iii) Schiff base derived from quinoxaline-2-carboxaldehyde and glycine

iv) Quinoxaline-2-carboxaldehyde thiosemicarbazone

The compulsions that prompted a study on metal complexes of these ligands were:

1. Benzimidazoles play an important role in the structure and function of a number of biological coordination compounds. Further, the ligands, BPBI and HBHPBI, are interesting from the structural point of view because of their bulky nature and steric effects.

2. The Schiff bases derived from amino acids are capable of forming mononuclear as well as polynuclear metal complexes which may serve as models for metalloproteins.

3. Pronounced anticancer activity is seen for the thiosemicarbazones which have a nitrogen heterocyclic ring system and are capable of NNS coordination with a metal ion.

4. Many of the complexes of thiosemicarbazones and benzimidazoles have catalytic as well as biological activities (*vide* sections 1.1.7 and 1.3.7), and it was expected that the complexes of the ligands selected for the present study would find application in the fields of medicine and catalysis.

CHAPTER II

EXPERIMENTAL TECHNIQUES

Details about the general reagents used, preparation of ligands and various analytical and physico-chemical methods employed for the characterization of the metal complexes are discussed in this chapter. Procedural details regarding the synthesis of metal complexes are given in the appropriate chapters.

2.1 REAGENTS

The following metal salts were used: $FeCl_3$ (Aldrich, 98% pure); $CoNO_3.6H_2O$ (E. Merck, GR); $CoCl_2.6H_2O$ (E. Merck, GR); $CoBr_2$ (Aldrich, 98% pure); $NiCl_2.6H_2O$ (BDH, GPR); $NiBr_2$ (Aldrich, 98% pure) $CuCl_2.2H_2O$ (E. Merck, GR); Rare Earth Oxides (Indian Rare Earths Ltd., 99% pure).

Glycine (BDH, GPR), thiosemicarbazide (Merck, GR), 2-aminobenzimidazole (Merck, GR) and 2% cross-linked chloromethylated polystyrene (Fluka) were used for the present work.

Quinoxaline-2-carboxaldehyde was prepared[191] by adopting the following procedure: Glacial acetic acid

(6 mL), *o*-phenylenediamine (21.6 g, 0.2 mol), hydrazine hydrate (5 mL, 0.1 mol) and a pinch of sodium bicarbonate were added to a solution of D-glucose (36 g, 0.2 mol) in water (54 mL), and the mixture was heated under reflux for 5 h on a boiling water bath. The solution was then cooled in ice, and the precipitated product 2-(D-arabinotetrahydroxybutyl)quinoxaline was filtered and washed with water. This product was further purified by recrystallization from hot water. The recrystallized 2-(D-arabinotetrahydroxybutyl)-quinoxaline (5.0 g, 0.02 mol) was mixed with sodium metaperiodate (13 g, 0.06 mol) in water (300 mL) and glacial acetic acid (10 mL), and the mixture was kept at room temperature with occasional shaking for 16 h. It was then filtered, and the filtrate was neutralized with sodium bicarbonate. The neutral solution was extracted with ether. The ether extract was then dried with anhydrous sodium sulphate, filtered and evaporated to dryness. The resulting residue was recrystallized from petroleum ether to give pure quinoxaline-2-carboxaldehyde.

(Yield = 60%, m. p. =107 ^{o}C)

The polymer bound benzaldehyde was prepared[192] in the following way: A mixture of poly(chloromethyl-styrene) (20.0 g, 3.8 mequiv Cl/g), dimethyl sulphoxide

(300 mL), and sodium bicarbonate (19 g) was stirred at 138-140 ^{o}C for 12 h. The resultant resin was filtered, washed with hot ethanol, methylene chloride and benzene, and dried *in vacuo* over anhydrous calcium chloride.

Unless otherwise specified, all other reagents used were of analytical reagent grade. The solvents employed were either of 99% purity or purified[193] by known laboratory procedures.

2.2 PREPARATION OF LIGANDS

2.2.1 1-Benzyl-2-phenylbenzimidazole

This ligand was prepared by adopting the procedure reported in the literature[194], with slight modifications. Details about the preparation are given below:

o-Phenylenediamine (10.8 g, 0.1 mol) and benzaldehyde (21.2 g, 0.2 mol) were separately dissolved in glacial acetic acid (50 mL), and mixed. The mixture was kept aside for 12 h. It was then filtered and the filtrate was poured into crushed ice. After 2 h, the mother liquor was decanted off. The product formed was washed several times with water by decantation and was recrystallized from 50% ethanol.

(Yield = 60%, m. p = 134 ^{o}C)

2.2.2 1-(2'-Hydroxybenzyl)-2-(2'-hydroxyphenyl)benzimidazole

This ligand was prepared in the same way as 1-benzyl-2-phenylbenzimidazole using *o*-phenylenediamine (10.8 g, 0.1 mol) and salicylaldehyde (24.6 g, 0.2 mol). (Yield = 60%, m. p. = 215 ^{o}C)

2.2.3 Polymer bound Schiff base

The Schiff base was prepared by condensing polymer bound benzaldehyde with 2-aminobenzimidazole. For the condensation, the following procedure was adopted: Polymer bound benzaldehyde (10 g) was swollen in dioxan (50 mL) for 24 h. Afterwards dioxan was decanted off, and 2-aminobenzimidazole (4 g) in absolute ethanol was added. This mixture was then refluxed on a water bath for 10 h. The polymer bound Schiff base formed was filtered, washed several times with dioxan and ethanol, and dried *in vacuo* over anhydrous calcium chloride.

2.2.4 *meso*-Tetraphenylporphyrin[195]

Propionic acid (150 mL) was taken in a 500 mL R. B. flask, and heated to gentle reflux. A protective asbestos-centered gauze was placed between flame and the flask. While the acid was being heated, freshly distilled pyrrole (2.70 g, 0.04 mol) and benzaldehyde

(4.25 g, 0.04 mol) were added slowly through the condenser using a little propionic acid as a rinse. The mixture was gently refluxed for 30 minutes and cooled to room temperature by keeping the flask in a pan of water. The purple crystals separated was filtered, washed with ethanol and then with water, and finally air dried.

The product thus obtained was passed through a column packed with alumina. The porphyrin was then eluted with chloroform. The residue obtained by evaporation of the chloroform eluate is pure *meso*-tetraphenylporphyrin.
(Yield = 60%)

2.2.5 Quinoxaline-2-carboxaldehyde thiosemicarbazone

Thiosemicarbazide (0.91 g, 0.01 mol) and crystallized sodium acetate (1 g) were dissolved in water (50 mL). To this mixture, quinoxaline-2-carboxaldehyde (1.58 g, 0.01 mol) in ethanol (50 mL) was added, shaken for 30 minutes and allowed to stand for 2-3 h. Quinoxaline-2-carboxaldehyde thiosemicarbazone formed was filtered, washed with cold water and ethanol, and dried *in vacuo* over anhydrous calcium chloride.
(Yield = 60%, m. p. = 241 ^{o}C)

2.3 ANALYTICAL METHODS

2.3.1 Estimation of metals

Lanthanides in the complexes were estimated by igniting a known weight of the complexes (0.2-0.3 g) at red hot temperature for nearly 2 h and weighed as their oxides.

In all the cases, the organic part of the transition metal complexes was completely eliminated before estimation of metals. In the case of the polymer bound cobalt complexes, this was done by treating with aqua regia for 24 h at 100 ^{o}C and then estimating the cobalt concentration in the filtered solution spectrophotometrically[196] using nitroso-R-salt.

The following procedure was used for eliminating the organic part of the thiocyanate and thiosemicarbazone complexes: A known weight of the metal complex (0.2-0.3 g) was treated with concentrated nitric acid (25 mL) and bromine in carbon tetrachloride (20 mL). This mixture was kept for about 3 h. It was then evaporated to dryness on a water bath and converted to its sulphate by fuming with a few drops of concentrated sulphuric acid several times. The

resulting metal sulphate was dissolved in water, and was used for the estimation of the metal.

A uniform procedure was adopted for eliminating the organic part of all other complexes. A known weight of the metal complex (0.2-0.3 g) was treated with concentrated sulphuric acid (5 mL) followed by concentrated nitric acid (20 mL). After the reaction subsided, perchloric acid (5 mL, 60%) was added. This mixture was maintained at the boiling temperature for 3 h on a sand bath. The clear solution thus obtained was evaporated to dryness. After cooling, concentrated nitric acid (5 mL) was added and evaporated to dryness on a water bath. The residue was dissolved in water and this neutral solution was used for the estimation of metals.

Gravimetric procedures[196] were adopted for the estimation of iron, cobalt and nickel. Iron in the complex was estimated by precipitating the metal with ammonia solution and igniting the resulting hydroxide to ferric oxide. Cobalt was estimated by precipitating it as $[Co(C_5H_5N)_4](SCN)_2$ using ammonium thiocyanate and pyridine. Nickel was precipitated as nickel dimethylglyoximate complex by the addition of an alcoholic solution of dimethylglyoxime and excess of

ammonia solution. Iodometric method[196] was employed for the estimation of copper in the complex.

2.3.2 CHN analyses

Microanalyses for carbon, hydrogen and nitrogen were done on a Perkin Elmer 2400 CHN elemental analyser or on a Heraeus CHN elemental analyser.

2.3.3 Estimation of halogen and sulphur[196]

Halogen content was determined by peroxide fusion of the sample, followed by volumetric estimation using Volhard's method. For sulphur estimation, the complexes were fused with Na_2CO_3 and Na_2O_2 and the resulting sulphate was determined gravimetrically as barium sulphate.

For the estimation of chlorine in the polymer sample, the following procedure was adopted: The polymer supported sample (3 g) was digested with pyridine (5 mL) for 2 h at 100 ^{o}C. Then the mixture was quantitatively transferred to a conical flask containing 50% acetic acid (30 mL) and concentrated nitric acid (5 mL). To this solution, standard silver nitrate solution was added with stirring and then the mixture was allowed to stand for 5 minutes. Afterwards about 50 mL of water was added to this followed by toluene. The solution was

mixed thoroughly, using a stirrer. The excess of silver nitrate was back titrated with standard ammonium thiocyanate solution.

2.4 PHYSICO-CHEMICAL METHODS

2.4.1 Conductance measurements

The molar conductance of the complexes were determined at 28±2 ^{o}C using a Thoshniwal or Elico PR 9500 conductivity bridge with a dip type cell and a platinized platinum electrode.

2.4.2 Magnetic susceptibility measurements

The magnetic susceptibility measurements were done at room temperature (28±2°C) using EG&G PARC Model 155 vibrating sample magnetometer or on a simple Gouy-type magnetic balance. Due lack of facilities, variations of magnetic susceptibility with temperature could not be studied. The Gouy tube was standardized using [Hg(Co(CNS)$_4$)] as recommended by Figgis and Nyholm[197]. The effective magnetic moment was calculated using the equation,

$$\mu_{eff} = 2.84\ (X_m^{corr}\ T)^{1/2}\ BM$$

where T is the absolute temperature and X_m^{corr} is the

molar susceptibility corrected for diamagnetism of other atoms in the complex using Pascal's constants[198-201].

2.4.3 Electronic spectra

Electronic spectra were taken in solution (wherever solubility permitted this) or in the solid state by a mull technique following a procedure recommended by Venanzi[202]. The procedure is briefly described below.

Small filter paper strips were impregnated with a paste of the sample in nujol mull. These were placed over the entrance to the photocell housing. A nujol treated filter paper strip of similar size and shape was used as the blank.

The spectra were recorded on a Hitachi U-3410 spectrophotometer or on a Shimadzu UV-160A spectrophotometer.

2.4.4 Infrared spectra

Infrared spectra of the ligand and complexes in the region 4000-600 cm^{-1} were taken both in nujol mull and as KBr discs with a Carl Zeiss UR-10 recording spectrophotometer or with a Perkin Elmer 781 spectrophotometer.

The IR spectra of the complexes in the region 600-200 cm^{-1} were taken in a polyethylene matrix on a Polytech FIR-30 Fourier far IR spectrophotometer or on a Perkin Elmer 983 spectrophotometer.

2.4.5 ^{1}H NMR spectra

The proton nuclear magnetic resonance spectra of complexes were taken in $CDCl_3$ or D_2O (wherever solubility permitted this) using Hitachi R-600 FT NMR spectrophotometer. Tetramethylsilane (TMS) was employed as the internal reference.

2.4.6 EPR spectra

The EPR spectra of powdered samples of the polymer bound metal complexes were recorded at room temperature as well as at -140 ^{o}C using Varian E-109 X/Q band EPR spectrophotometer. The calibrations were done using 1,1-diphenyl-2-picrylhydrazyl (DPPH) as a field marker.

2.4.7 Thermogravimetry (TG)

The TG curves were obtained on a Ulvac Sinku-Riko TA-1500 thermal analyser or on a Perkin Elmer 3700 thermal analyser, at a heating rate of 10 ^{o}C min^{-1} in an air atmosphere using a platinum crucible. The mass of the samples used was in the range 5-10 mg.

2.4.8 Differential thermal analysis (DTA)

The DTA curves were obtained on the Ulvac Sinku-Riko TA-1500 thermal analyser simultaneously with TG under the operational conditions mentioned above. The reference substance used for DTA measurements was α-Al_2O_3.

CHAPTER III

1-BENZYL-2-PHENYLBENZIMIDAZOLE COMPLEXES OF COBALT(II)

3.1 INTRODUCTION

Benzimidazoles play a significant role in the structure and function of a number of biologically important molecules[1-3]. For example, 5,6-dimethylbenzimidazole supplies one of the five nitrogen atoms coordinated to cobalt in vitamin B_{12} and, in fact this has created an interest in the study of coordination compounds of benzimidazole and its derivatives[34]. Furthermore, benzimidazoles have been reported to possess wide range of biological responses, such as antibacterial, antifungal and antiviral[203-206]. The derivative, 1-benzyl-2-phenylbenzimidazole (BPBI) (Fig. 3.1) is interesting from the structural point of view because of its bulky nature and steric effects.

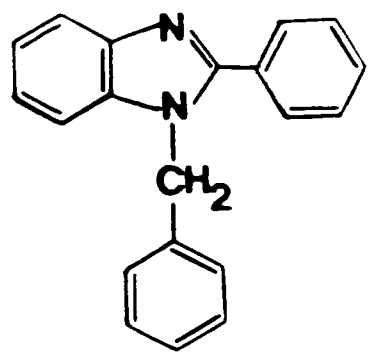

Fig. 3.1 Structure of BPBI

The results of our studies on the synthesis and characterization of this ligand are described in this chapter.

3.2 EXPERIMENTAL

3.2.1 Materials

Details regarding the preparation and purification of the ligand BPBI are given in Chapter II.

3.2.2 Synthesis of the complexes

The chloro and bromo complexes were prepared by the same general procedure. A solution containing cobaltous halide (0.005 mol- 1.19 g of $CoCl_2.6H_2O$ or 1.08 g of $CoBr_2$) in ethanol (25 mL) was added to a solution of BPBI (0.01 mol, 2.84 g) in ethanol (25 mL). The complex slowly separated out on scratching the sides of the beaker with a glass rod. It was filtered off, washed with ethanol and dried *in vacuo* over anhydrous calcium chloride.
(Yield = 60-70%)

For the synthesis of the iodo and thiocyanato complexes, the following procedure was used: First, $Co(NO_3)_2.6H_2O$ (0.005 mol, 1.45 g) and KSCN/KI (0.01 mol - 0.97 g of KSCN or 1.66 g of KI) were separately dissolved in the minimum quantity of ethanol and mixed.

The precipitated KNO_3 was filtered off and washed with ethanol. The filtrate was concentrated to a small volume and then added to a solution of BPBI (0.01 mol, 2.84 g) in ethanol (25 mL). The complex that separated out was filtered off, washed with ethanol and dried *in vacuo* over anhydrous calcium chloride.
(Yield = 70-80%)

3.2.3 Analytical methods

Details about the analytical methods and other characterization techniques are given in Chapter II.

3.3 RESULTS AND DISCUSSION

All the complexes are crystalline and non-hygroscopic, and are quite stable to atmospheric oxidation. The complexes are soluble in methanol, acetone, nitrobenzene, chloroform, DMF and DMSO. The analytical data of the complexes are presented in Table III.1. The data show that the complexes have the general empirical formula, $[Co(BPBI)_2X_2]$ (where X = Cl, Br, I or NCS). The molar conductance values suggest that the complexes are non-electrolytes in nitrobenzene (Table III.2). But, the conductance value of the iodo complex is higher than that of the other BPBI complexes, which may be due to the partial dissociation of the

Table III.1

Analytical data

Compound (Empirical formula)	Colour	C(%) Found (Calc.)	H(%) Found (Calc.)	N(%) Found (Calc.)	Co(%) Found (Calc.)	Anion(%) Found (Calc.)
$[Co(BPBI)_2Cl_2]$	Blue	67.98	4.32	8.01	8.31	10.08
$(C_{40}H_{32}N_4CoCl_2)$		(68.78)	(4.59)	(8.02)	(8.34)	(10.15)
$[Co(BPBI)_2Br_2]$	Greenish	60.51	4.01	7.08	7.37	20.24
$(C_{40}H_{32}N_4CoBr_2)$	blue	(61.01)	(4.07)	(7.08)	(7.48)	(20.30)
$[Co(BPBI)_2I_2]$	Bluish	53.87	3.41	6.42	6.59	28.72
$(C_{40}H_{32}N_4CoI_2)$	green	(54.50)	(3.63)	(6.42)	(6.68)	(28.79)
$[Co(BPBI)_2(NCS)_2]$	Deep	67.01	4.08	7.51	7.81	15.69
$(C_{42}H_{32}N_6CoS_2)$	blue	(67.84)	(4.31)	(7.51)	(7.92)	(15.63)

Table III.2
Molar conductance and magnetic moment data

Compound	Molar conductance $ohm^{-1}\ cm^{2}\ mol^{-1}$	Magnetic moment BM
$[Co(BPBI)_2Cl_2]$	1.3	4.6
$[Co(BPBI)_2Br_2]$	2.1	4.6
$[Co(BPBI)_2I_2]$	14.1	4.7
$[Co(BPBI)_2(NCS)_2]$	8.1	4.5

complex in nitrobenzene. However the value is lower than that expected for a 1:1 electrolyte.

3.3.1 Magnetic susceptibility measurements

The distinction of octahedral and tetrahedral complexes of cobalt(II) from the magnetic moment values is possible to a certain extent. Usually the moments of tetrahedral complexes are in the range 4.4-4.8 BM and those of octahedral high spin complexes of cobalt(II) are around 5 BM. All the present BPBI complexes (Table III.2) exhibit $\mu_{eff.}$ values around 4.6 BM suggesting a tetrahedral structure for the complexes[207].

3.3.2 Electronic spectra

The electronic spectral data are given in Table III.3. All the complexes exhibit an absorption band with fine structure around the region 15000-20000 cm^{-1} (Fig. 3.2). This band can be assigned to the $^4A_2 \longrightarrow {}^4T_1(P)$ electronic transition. The fine structure observed for the complexes in this region is characteristic of the tetrahedral complex, and arises due to spin-orbit coupling of the T-state[208]. The broad absorption band in the region 6000-9000 cm^{-1} is assigned to $^4A_2 \longrightarrow {}^4T_1(F)$. The low energy band expected for tetrahedral complexes is seen around 5000 cm^{-1} in the spectra of the present complexes (Fig. 3.2), and is due to the $^4A_2 \longrightarrow {}^4T_2$ transition.

Table III.3
Electronic spectral data

Compound	Abs. max., cm^{-1}	Tentative assignments
$[Co(BPBI)_2Cl_2]$	17260	
	16290	$^4A_2 \longrightarrow {}^4T_1(P)$
	15480	
	6770	$^4A_2 \longrightarrow {}^4T_1(F)$
	5190	$^4A_2 \longrightarrow {}^4T_2$
$[Co(BPBI)_2Br_2]$	16830	
	15880	$^4A_2 \longrightarrow {}^4T_1(P)$
	15070	
	6750	$^4A_2 \longrightarrow {}^4T_1(F)$
	5200	$^4A_2 \longrightarrow {}^4T_2$
$[Co(BPBI)_2I_2]$	16220	
	15200	$^4A_2 \longrightarrow {}^4T_1(P)$
	14310	
	6930	$^4A_2 \longrightarrow {}^4T_1(F)$
	5230	$^4A_2 \longrightarrow {}^4T_2$
$[Co(BPBI)_2(NCS)_2]$	20220	
	17850	$^4A_2 \longrightarrow {}^4T_1(P)$
	16250	
	8180	$^4A_2 \longrightarrow {}^4T_1(F)$
	5160	$^4A_2 \longrightarrow {}^4T_2$

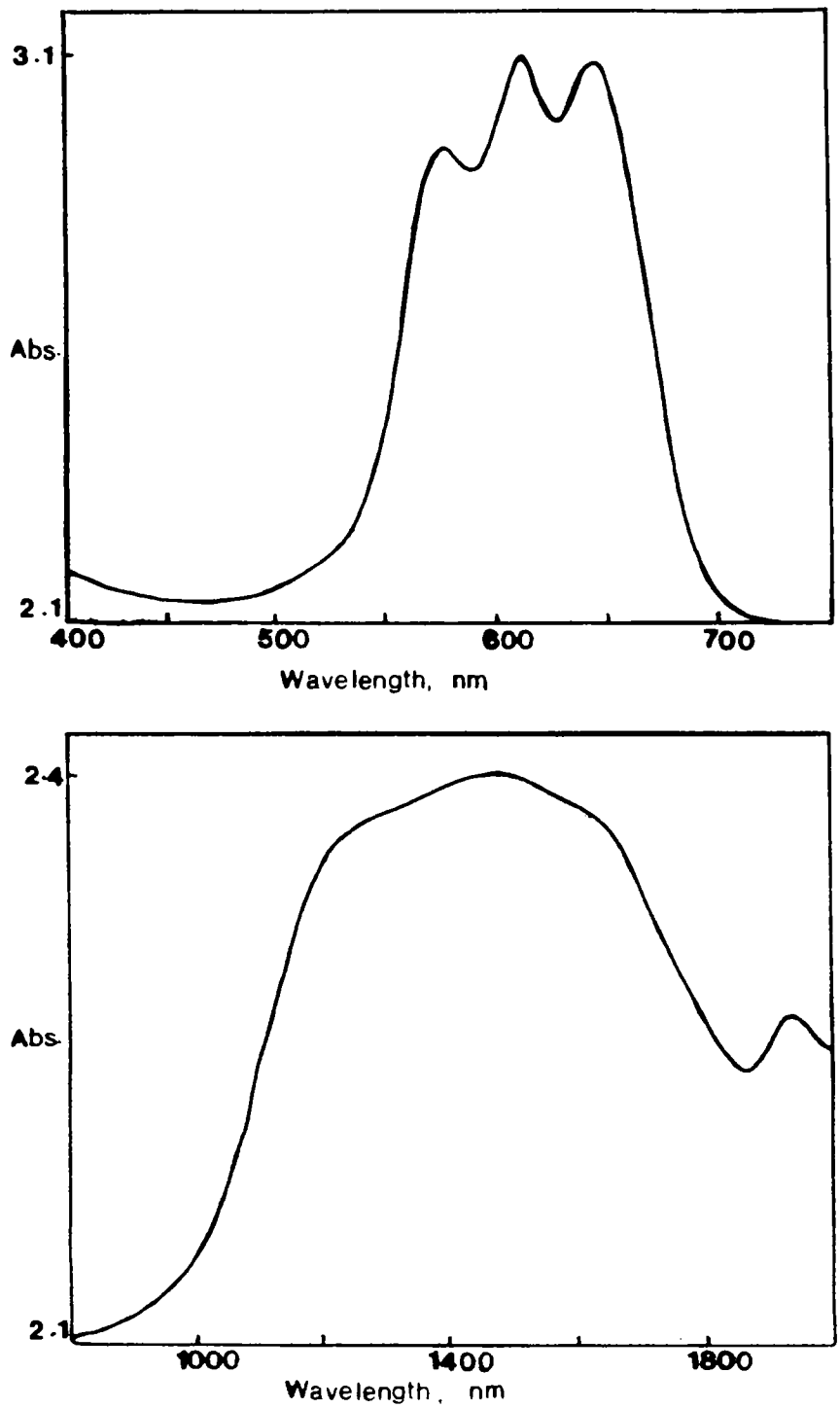

Fig. 3.2 Electronic spectra of $[Co(BPBI)_2Cl_2]$

3.3.3 Infrared spectra

The infrared spectral data of the ligand and complexes are given in Table III.4. The band of medium intensity at 1500 cm^{-1} in the spectrum of the free ligand may be attributed to the C-N stretching vibration. This band is seen at 1485 cm^{-1} in the spectra of the complexes. The shifting of this band to lower frequency on complexation was observed by earlier workers also[209-211], and has been suggested as being due to the coordination of the N-3 atom of BPBI to the metal atom. The thiocyanato complex shows a strong band at 2100 cm^{-1}, which can be assigned to the ν(C-N) of the thiocyanate group[212]. A band around 490 cm^{-1} is usually seen for the thiocyanato complexes in which the NCS group is bonded through nitrogen, and this band has been assigned to the NCS deformation[213]. Presence of a medium band at 490 cm^{-1} in the spectrum of the present thiocyanato complex suggests that bonding of the thiocyanate group to the metal is through its nitrogen atom.

All the complexes show a strong band at 295 cm^{-1} in the far IR region, which may be attributed to the Co-N(benzimidazole) stretching vibration. The bands observed at 320 cm^{-1} for the chloro complex and at

Table III.4

Infrared absorption frequencies (cm^{-1})

L	I	II	III	IV	Assignments
3040w	3040w	3040w	3040w	3040w	
2930w	2930w	2930w	2930w	2930w	
2860w	2860w	2860w	2860w	2860w	
-	-	-	-	2100s	ν(C-N) (thiocyanate)
1610w	1615m	1615m	1610m	1610m	
1520w	1525w	1520w	1520w	1525w	
1500m	1485m	1480m	1485m	1490w	ν(C-N) (benzimidazole)
1475s	1470s	1470s	1470s	1470m	
1460s	1460s	1455s	1455s	1455s	
1400s	1410s	1410s	1410s	1420s	
1380s	1360m	1370m	1360m	1370m	
1340w	1340w	1340w	1340w	1340w	
1320m	1325w	1325w	1320m	1315w	
1290m	1295w	1295w	1295m	1290w	
1260m	1255w	1255w	1250m	1255w	
1230m	1240w	1235w	1235w	1240w	
1190w	1190w	1190w	1180w	1175w	
1080w	1080w	1080w	1080w	1080w	
1040m	1035m	1035w	1030w	1030w	
1010m	1015w	1015w	1005w	1005w	
930m	925m	925w	925w	925w	
850m	845w	860w	855w	850w	

Table III.4 (continued)

800s	790s	790m	790m	790w	
780m	770s	770s	770m	765w	
740s	740s	735s	745s	740m	
720s	720s	720s	720s	720s	
710s	705s	705m	700s	700m	
650w	645w	640w	635w	640w	
580s	580w	580w	580w	590m	
510s	510s	510s	510s	510s	
-	-	-	-	490m	δ(NCS)
420s	420s	420s	420s	420s	
410w	410w	410w	410w	410w	
-	-	-	-	380m	ν(Co-N) (thiocyanate)
370w	370w	370w	370w	370w	
340m	340m	340m	340m	340m	
-	320m	-	-	-	ν(Co-Cl)
-	295s	295s	295s	295s	ν(Co-N) (benzimidazole)
270w	270w	270w	270w	270w	
-	-	260m	-	-	ν(Co-Br)
210m	210m	210m	210m	210m	

Abbreviations: s = strong, m = medium, w = weak,

L = BPBI, I = $[Co(BPBI)_2Cl_2]$, II = $[Co(BPBI)_2Br_2]$
III = $[Co(BPBI)_2I_2]$, IV = $[Co(BPBI)_2(NCS)_2]$

Table III.5

^1H NMR data

Compound	Chemical shift, ppm	
	Aromatic protons	Benzyl protons
BPBI	7.5m	2.3s
$[Co(BPBI)_2Cl_2]$	7.3m, br	1.6s
$[Co(BPBI)_2Br_2]$	7.3m, br	1.5s
$[Co(BPBI)_2I_2]$	7.5m, br	1.7s
$[Co(BPBI)_2(NCS)_2]$	7.4m, br	1.6s

Abbreviations: s = singlet, m = multiplet, br = broad

260 cm^{-1} for the bromo complex may be due to Co-Cl and Co-Br stretching modes respectively, as these bands are unique to these complexes and are not seen in the spectra of other BPBI complexes[214]. In the thiocyanato complex, the band observed at 380 cm^{-1} may be due to the Co-N(thiocyanate) stretching vibration.

3.3.4 ^1H NMR spectra

The ^1H NMR spectra of the complexes in $CDCl_3$ consist of a multiplet centered at δ 7.5 ppm and a singlet at δ 1.6 ppm (Table III.5). The integrated proton ratios were in accordance with the formulae assigned to the complexes. A major change observed on complexation is the upfield shift of the CH_2 (benzyl) proton signal. This signal appears as a singlet at δ 2.3 ppm in the spectrum of the ligand, which gets shifted to δ 1.6 ppm on complexation. This large upfield shift may be attributed to the coordination of the nitrogen atom to the metal ion, which destroys the delocalization of the π-electron system in the imidazole ring. Slight broadening of the signals is observed in the spectra of the complexes, which might have been caused by both dipolar and electron spin-nuclear spin coupling mechanisms[208].

CHAPTER IV

1-(2'-HYDROXYBENZYL)-2-(2'-HYDROXYPHENYL)BENZIMIDAZOLE COMPLEXES OF IRON(III), COBALT(II), NICKEL(II), AND COPPER(II)

4.1 INTRODUCTION

1-(2'-Hydroxybenzyl)-2-(2'-hydroxyphenyl)benzimidazole (HBHPBI) is not only a bulky ligand, but also contains more potential donor sites than BPBI. The synthesis and characterization of HBHPBI (Fig. 4.1) complexes of copper(II), iron(III), iron(II) and cobalt(II) have been reported earlier[215,216]. In these complexes, intramolecularly hydrogen bonded phenolic OH groups of the ligand are not taking part in complexation. But, we were able to synthesize, using a different synthetic procedure, new Fe(III), Co(II),

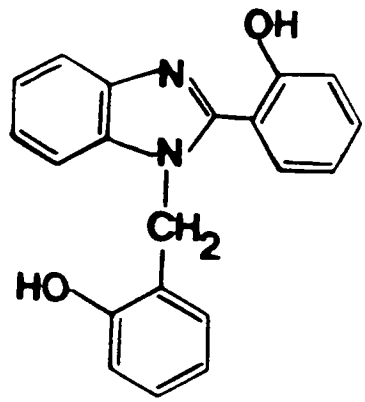

Fig. 4.1 Structure of HBHPBI

Ni(II) and Cu(II) complexes of this ligand, in which one of its phenolic oxygen atoms is coordinated to the metal atom. The results of our studies on these complexes are presented in this chapter.

4.2 EXPERIMENTAL

4.2.1 Materials

Details about the preparation and purification of the ligand, HBHPBI, are given in Chapter II.

4.2.2 Synthesis of the complexes

The ligand, HBHPBI (0.01 mol, 3.18 g), was dissolved in 1% NaOH solution (80 mL). The solution was neutralized with a few drops of 2N acetic acid, and to this was added metal chloride (0.005 mol - 0.81 g of $FeCl_3$, 1.19 g of $CoCl_2.6H_2O$, 1.18 g of $NiCl_2.6H_2O$ or 0.85 g of $CuCl_2.2H_2O$) solution in water (25 mL). The complex separated out was filtered, washed several times with water and dried *in vacuo* over anhydrous calcium chloride.

(Yield = 50-60% for the copper complex and 70-75% for the other complexes).

4.2.3 Analytical methods

Details about the analytical methods and other characterization techniques are given in Chapter II.

4.3 RESULTS AND DISCUSSION

All the complexes are crystalline, non-hygroscopic and coloured substances, which are stable to aerial oxidation. The complexes are slightly soluble in methanol, ethanol and acetone, and are fairly soluble in DMF and DMSO. The analytical data (Table IV.1) show that the complexes have the general formulae $[ML(OH)(H_2O)].H_2O$ for the Co(II), Ni(II) and Cu(II) complexes and $[FeL(OH)_2(H_2O)_2].H_2O$ for the Fe(III) complex (where L=HBHPBI).

4.3.1 Magnetic susceptibility measurements

Magnetic moment values of the complexes are presented in Table IV.2. The iron(III) complex has a magnetic moment value of 5.92 BM which suggests it to be a high spin octahedral complex[217]. The magnetic moment value of 4.3 BM for the Co(II) complex suggests it to have a tetrahedral structure[207]. In the case of the Ni(II) complex also, the magnetic moment value (3.8 BM) is in favour for a tetrahedral structure[218]. The magnetic moments of simple Cu(II) complexes are generally in the range 1.73-2.20 BM regardless of stereochemistry[200]. The present Cu(II) complex has a magnetic moment value of 1.73 BM. This slightly lower

Table IV.1
Analytical data

Compound (Empirical formula)	Colour	C(%) Found (Calc.)	H(%) Found (Calc.)	N(%) Found (Calc.)	M(%) Found (Calc.)
$[FeL(OH)_2(H_2O)_2].H_2O$	reddish	52.06	5.00	6.09	12.10
$(C_{20}H_{23}N_2FeO_7)$	brown	(51.85)	(4.75)	(6.05)	(12.06)
$[CoL(OH)(H_2O)].H_2O$	grey	55.73	4.51	6.62	13.70
$(C_{20}H_{20}N_2CoO_5)$		(55.64)	(4.41)	(6.50)	(13.68)
$[NiL(OH)(H_2O)].H_2O$	light	55.86	4.71	6.54	13.68
$(C_{20}H_{20}N_2NiO_5)$	green	(55.72)	(4.41)	(6.50)	(13.63)
$[CuL(OH)(H_2O)].H_2O$	green	55.61	4.51	6.48	14.70
$(C_{20}H_{20}N_2CuO_5)$		(55.10)	(4.36)	(6.43)	(14.59)

Table IV.2
Molar conductance and magnetic moment data

Compound	Molar conductance $ohm^{-1}\ cm^{2}\ mol^{-1}$	Magnetic moment BM
$[FeL(OH)_2(H_2O)_2].H_2O$	0.69	5.9
$[CoL(OH)(H_2O)].H_2O$	0.57	4.3
$[NiL(OH)(H_2O)].H_2O$	0.62	3.8
$[CuL(OH)(H_2O)].H_2O$	0.55	1.7

magnetic moment value suggests that the structure of the copper complex is not tetrahedral. Therefore, a square planar structure can be assumed for this complex.

4.3.2 Electronic spectra

Solid state electronic spectra of the complexes are shown in Fig. 4.2, and the spectral data are given in Table IV.3. Because of the greater oxidising power of Fe(III), ligand to metal charge transfer bands often obscure the very low intensity d-d absorption. The electronic spectrum of the Fe(III) complex shows a broad absorption band with a maximum around 21000 cm^{-1} corresponding to a combination of $^6A_{1g} \longrightarrow {}^4T_{1g}$, $^6A_{1g} \longrightarrow {}^4T_{2g}$, and $^6A_{1g} \longrightarrow {}^4E_g$ forbidden transitions in the octahedral symmetry[219].

The Co(II) complex exhibits an absorption band around 16180 cm^{-1}, which can be assigned to $^4A_2 \longrightarrow {}^4T_1(P)$ electronic transition. It also exhibits a broad absorption band around 9300 cm^{-1} due to the $^4A_2 \longrightarrow {}^4T_1(F)$ transition. The transition, $^4A_2 \longrightarrow {}^4T_2$, is not observed in the spectrum of the present complex. In most instances it is seldom observed since it is inherently weak due to an orbital selection rule[208]. Thus electronic spectrum of the cobalt(II) complex is in agreement with the magnetic moment value to suggest a

Table IV. 3
Electronic spectral data

Compound	Abs.max. cm^{-1}	Tentative assignments
$[FeL(OH)_2(H_2O)_2].H_2O$	34800	Intraligand Transitions
	30000	Charge transfer transitions
	21200	Forbidden d-d transitions
$[CoL(OH)(H_2O)].H_2O$	35000	Intraligand transitions
	25000	Charge transfer transitions
	16180	$^4A_2 \longrightarrow {}^4T_1(P)$
	9300	$^4A_2 \longrightarrow {}^4T_1(F)$
$[NiL(OH)(H_2O)].H_2O$	40000	Intraligand transitions
	26100	Charge transfer transitions
	14500	$^3T_1(F) \longrightarrow {}^3T_1(P)$
	8730	$^3T_1(F) \longrightarrow {}^3A_2(F)$
$[CuL(OH)(H_2O)].H_2O$	34000	Intraligand transitions
	27450	Charge transfer transitions
	21000	$^2B_{1g} \longrightarrow {}^2A_{1g}$
	15300	$^2B_{1g} \longrightarrow {}^2B_{2g}$
	12500	$^2B_{1g} \longrightarrow {}^2E_{1g}$

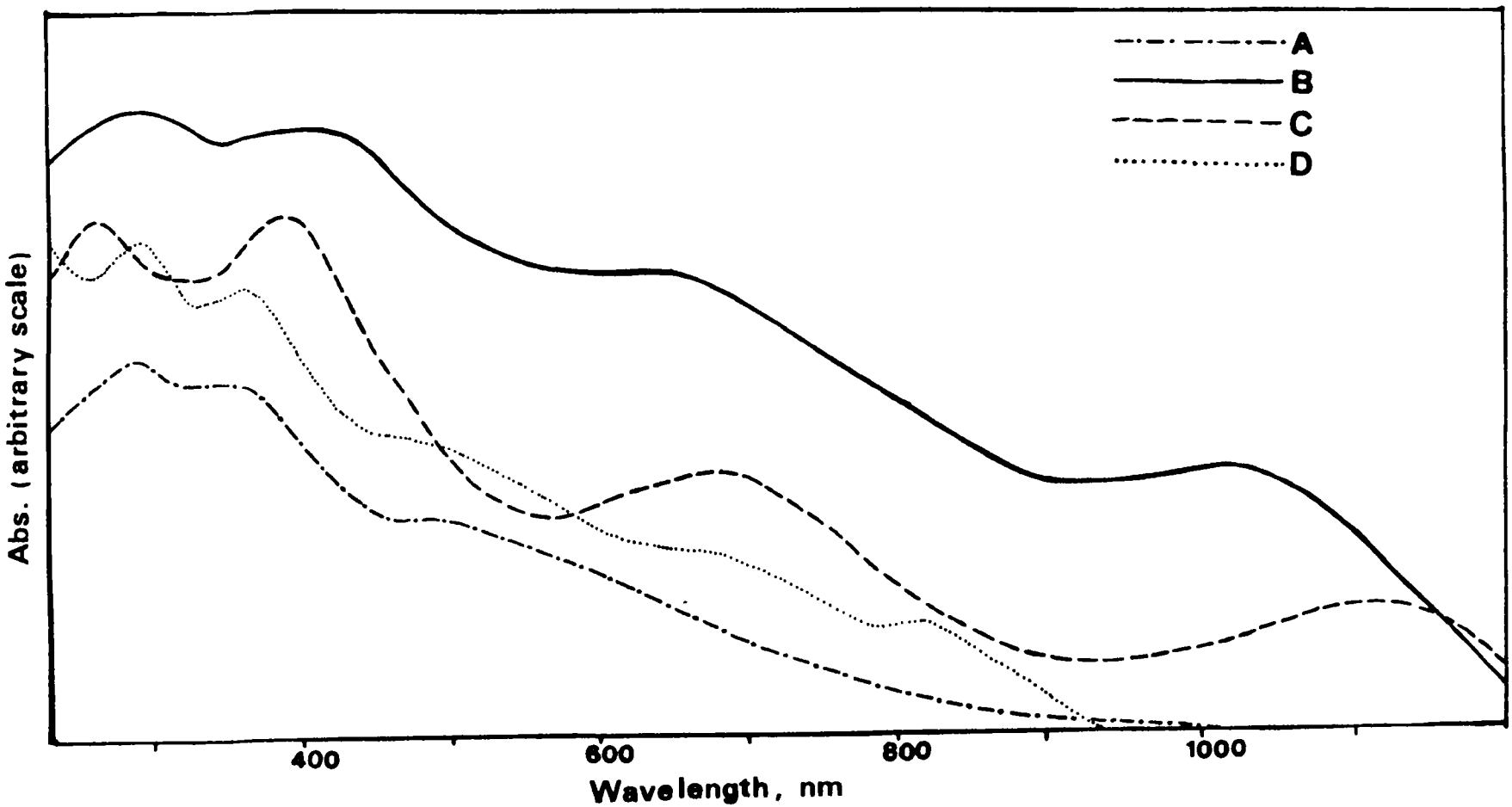

Fig. 4.2 Electronic spectra of the complexes

A = $[FeL(OH)_2(H_2O)_2].H_2O$, B = $[CoL(OH)(H_2O)].H_2O$

C = $[NiL(OH)(H_2O)].H_2O$, D = $[CuL(OH)(H_2O)].H_2O$

tetrahedral structure for the complex. The nickel(II) complex also displays absorption bands indicative of tetrahedral geometry[220]. It exhibits two bands, one at 14500 cm^{-1} and the other at 8730 cm^{-1}, which could be assigned to the $^3T_1(F) \longrightarrow {}^3T_1(P)$ and $^3T_1(F) \longrightarrow {}^3A_2(F)$ transitions respectively.

It is difficult to distinguish between a square planar and tetrahedral geometry for copper(II) ion. The electronic spectrum of the present Cu(II) complex shows a broad absorption band with shoulders at 12500 cm^{-1}, 15300 cm^{-1} and 21000 cm^{-1}. Assuming a square planar geometry, these could be assigned to $^2B_{1g} \longrightarrow {}^2A_{1g}$, $^2B_{1g} \longrightarrow {}^2B_{2g}$ and $^2B_{1g} \longrightarrow {}^2E_{1g}$ transitions respectively[221].

Furthermore, all the complexes exhibit a broad absorption band in the region 25000-30000 cm^{-1} which might be due to charge transfer transitions. The complexes also exhibit a band in the region 34000-40000 cm^{-1}, which can be attributed to the intraligand transitions.

4.3.3 Infrared spectra

All the complexes exhibit a very broad band in the region 3100-3500 cm^{-1} due to O-H stretching

vibrations[222]. Further a double hump around 3010 cm^{-1} and a sharp band at 840 cm^{-1} due to coordinated water molecules[223] are also seen in the spectra of the complexes. Evidences for the presence of one molecule of lattice water for all the complexes, one molecule of coordinated water for the cobalt(II), nickel(II) and copper(II) complexes and two molecules of coordinated water for the iron(III) complex are also obtained from the TG studies (*vide* discussions in Chapter V, page 128).

The band of medium intensity at 1500 cm^{-1} in the spectrum of the free HBHPBI ligand may be attributed to the C-N stretching vibrations. In the case of the present complexes this band is seen at 1490 cm^{-1}. The shifting of this band to a lower frequency suggests that bonding of the benzimidazole to the metal atom is through its N-3 atom.

In the spectra of free HBHPBI and its complexes, there is a band around 1280 cm^{-1} which can be assigned to the νC-O stretching vibration of the phenolic group[224]. The phenolic C-O bands of the uncoordinated ligand shifts to higher frequencies during complex formation[225]. An additional band at 1310 cm^{-1} is found in the case of all the complexes. Presence of this band and the retention of 1280 cm^{-1} band in the spectra of

Table IV. 4
Infrared absorption frequencies (cm^{-1})

L	I	II	III	IV	Assignments
3500m	3500m	3500m	3500m	3500m	ν(O-H)
3030m	3040m	3040m	3040m	3020m	
1585s	1590s	1590s	1590s	1590s	
1540m	1540m	1540m	1540m	1540m	
1500m	1490m	1490m	1490m	1490m	ν(C-N)
1450s	1450s	1450s	1450s	1450s	
1420m	1420s	1420s	1420m	1420s	
1390m	1390m	1390w	1390w	1390w	
-	1310m	1310m	1310m	1310m	ν(C-O)
1280s	1280s	1280m	1280w	1280m	
1260w	1260s	1260m	1260w	1260m	
1235w	1240s	1240s	1240w	1240m	
1150w	1150m	1150m	1150w	1150w	
-	1120m	1120m	1120m	1120m	δ(M-O-H)
1090m	1090w	1090m	1090m	1090m	
1030w	1030w	1030w	1030w	1030w	
980w	980w	980w	980w	980w	
920w	920w	920w	920w	920w	
-	840s	835m	840m	840m	δ(H-O-H)
800m	800s	800m	800m	800m	
745s	745m	750w	750w	750w	
710w	710w	715w	710w	710w	

Table IV.4 (continued)

560w	560w	550w	550w	560w	
520w	520w	520w	520w	520w	
470w	470w	470w	470w	470w	
425w	430w	430w	430w	430w	
-	420w	420w	415w	415w	ν(M-O)
370w	370w	370w	370w	370w	
330s	335m	330w	330w	330w	
-	320m	320m	320m	320m	ν(M-N)
305w	305w	300m	300w	310w	
270m	270m	270w	275w	270m	
230w	230w	230w	225w	230w	
205m	205m	210m	205w	210m	

Abbreviations: s = strong, m = medium, w = weak

L = HBHPBI, I = $[FeL(OH)_2(H_2O)_2].H_2O$,
II = $[CoL(OH)(H_2O)].H_2O$, III = $[NiL(OH)(H_2O)].H_2O$,
IV = $[CuL(OH)(H_2O)].H_2O$

all the present complexes suggest that only one of the phenolic oxygen atoms is coordinated to the metal atom. Furthermore, all the complexes exhibit M-O-H bending mode around 1120 cm^{-1}. A band around 320 cm^{-1} due to ν(M-N) and another band around 420 cm^{-1} due to ν(M-O) are also observed in all the cases[212].

CHAPTER V

THERMAL STUDIES OF SOME 1,2-DISUBSTITUTED BENZIMIDAZOLE COMPLEXES OF IRON(III), COBALT(II), NICKEL(II) AND COPPER(II)

5.1 INTRODUCTION

A literature search revealed that thermal decomposition behaviour of the BPBI and HBHPBI complexes described in Chapters III and IV respectively have not yet been reported. Thermal behaviour and the decomposition kinetics of these complexes have been studied and the results of these studies are presented in this chapter.

The thermal decomposition of solids is a very complicated process, involving the decomposition of one chemical compound and the formation of others, the destruction of initial crystal lattice, the formation of crystallization centres and their growth, the adsorption and desorption of gaseous products, the diffusion of gases, heat transfer and many other elemental processes. The overall process is influenced by many procedural variables such as heating rate, the heat conductivities of furnace atmosphere, the sample and the sample holder, the static or dynamic character of the atmosphere, the

physical state of the sample, particle size, compactness, sample weight etc. Owing to the complexity of thermal decomposition reactions, there is no chance of describing whole process theoretically at once. Therefore successive approaches are needed for understanding these processes. Application of formal kinetics of homogeneous reactions may be considered as a first approach. In fact, all the methods for deriving the kinetic parameters, n, E_a, ΔS and A, from TG curves recorded under dynamic temperature conditions are based on the relation taken from the formal kinetics of homogeneous reactions. In the present investigation, Coats and Redfern method[226] has been used for the calculation of the parameters, as it is simple and gives reliable results.

5.2 EXPERIMENTAL

Details about the instruments used and the treatment of data obtained are given in Chapter II.

Treatment of data

Thermogravimetry

The TG and DTG curves obtained were used as such. From the TG and DTG curves, the following information was obtained.: (1) temperature ranges of stability,

(2) decomposition peak temperature, (3) decomposition temperature ranges and (4) probable composition of the expelled groups.

For the evaluation of kinetic parameters, the Coats-Redfern equation was used in the form,

$$\log g(\alpha)/T^2 = \log (AR/\phi E) - E/2.303RT$$

(Details about the equation and the evaluation procedures are given in the Appendix of this chapter, page 133.) In the present study, the evaluation of the parameters was based on a computer program which was developed for use on a Busybee PC, PC/XT computer (HCL Ltd.).

Differential thermal analysis

The instrumental DTA curves were used as such. From these curves the following informations were obtained.

1. Endothermic and exothermic peak temperature
2. Peak base widths, *i.e.*, phase change or decomposition temperature ranges

These values have also been tabulated in every case along with the corresponding TG data.

5.3 RESULTS AND DISCUSSION

5.3.1 Thermal studies of the cobalt(II) complexes of BPBI

5.3.1a Thermal behaviour

The TG/DTG/DTA curves for all the complexes are shown in Fig. 5.1. Thermoanalytical data for the complexes are presented in Table V.1. The percentage mass loss and the probable compositions of the expelled groups are also given in this table.

All the complexes have a fairly wide stability range. The DTG curves show two peaks for the halogeno complexes and three peaks for the thiocyanato complex. All these DTG peaks have their parallel DTA peaks. The DTA peak corresponding to the first stage of decomposition is a very weak endothermic peak, followed immediately by a weak exothermic peak. The decomposition reactions should normally be endothermic: the exothermicity in this case could be due to the concomitant decomposition and oxidation processes taking place at this stage. The heat of decomposition released during the oxidation process might thus have swamped the endothermicity of the decomposition reactions.

Table V. 1
Thermal decomposition data of BPBI complexes

Compound	Peak temp. in DTA (°C)	Temp. range in DTA (°C)	Peak temp. in DTG (°C)	Temp. range in DTG (°C)	Stage	Loss(%) Found from TG (Calc.)	Probable composition of expelled group
	220 endo(m)	200-240					
	345 endo(vw)	340-350	355s	250-450	I	45.00 (40.70)	L
$[CoL_2Cl_2]$	355 exo(vw)	350-375					
	550 exo(vs)	400-620	560s	450-625	II	52.00 (50.86)	L & 2Cl
	230 endo(m)	225-240					
	310 endo(vw)	300-320	320vs	290-350	I	33.50 (36.10)	L
$[CoL_2Br_2]$	330 exo(vw)	320-350					
	490 exo(s)	360-530	510s	490-560	II	59.00 (56.41)	L & 2Br
	240 endo(m)	225-250					
	275 exo(vw)	260-290	265s	240-350	I	46.50 (46.65)	L & I
$[CoL_2I_2]$	390 exo(vs)	330-430	410vs	380-440	II	42.50 (46.65)	L & I
	195 endo(m)	190-210					
	305 endo(vw)	300-310					
	310 exo(vw)	310-320	320vs	210-350	I	57.00 (57.35)	1.5L
$[CoL_2(NCS)_2]$	470 exo(vw)	350-550	490s	425-550	II	26.00 (26.93)	0.5L & NCS
	720 exo(vw)	650-800	700w	650-750	III	7.00 (7.81)	NCS

Abbreviations: vs = very strong: s = strong: m = medium: w = weak: vw = very weak: endo = endothermic: exo = exothermic
L = BPBI

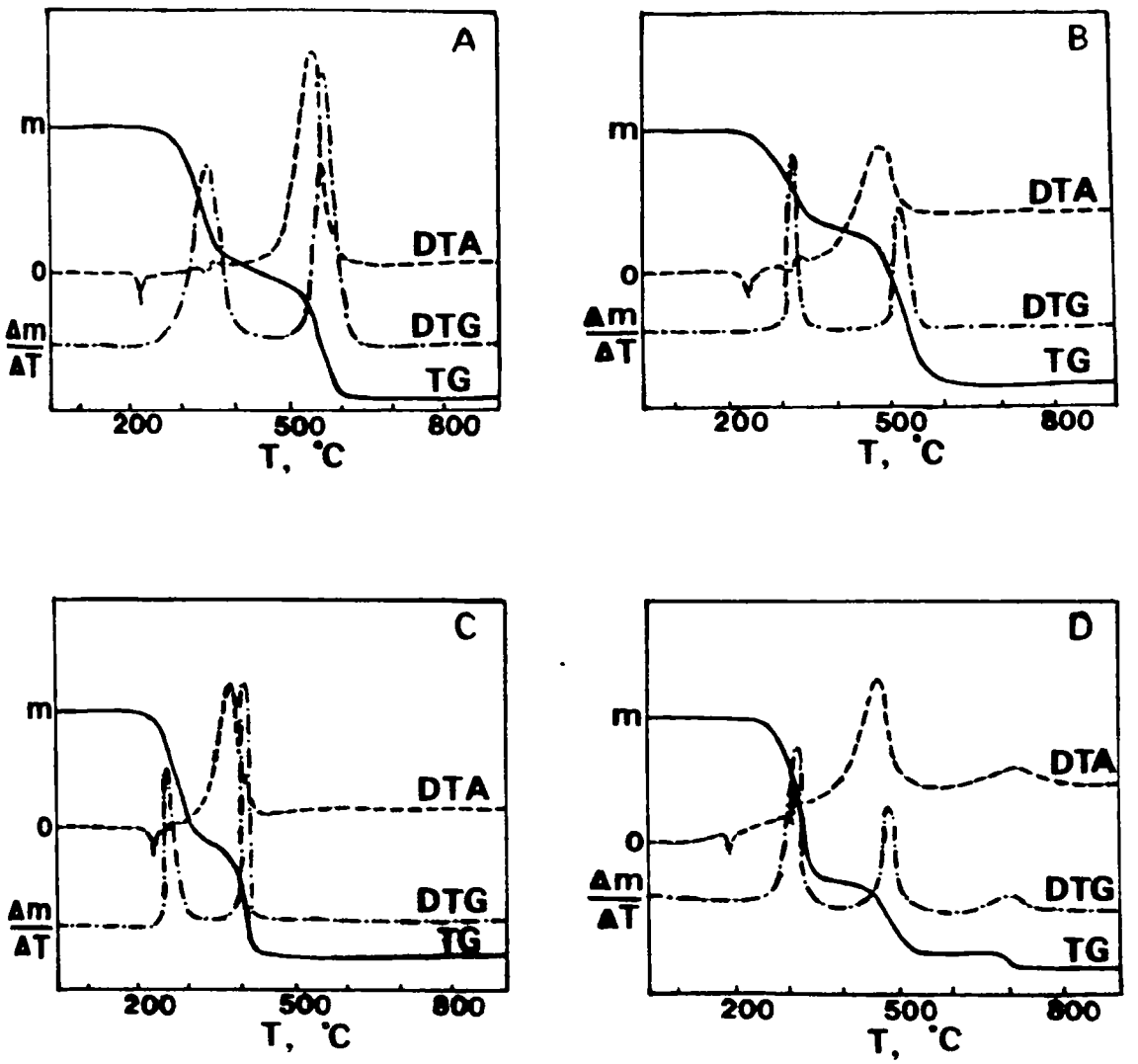

Fig. 5.1 TG/DTG/DTA traces of BPBI complexes

A = $[Co(BPBI)_2Cl_2]$, B = $[Co(BPBI)_2Br_2]$

C = $[Co(BPBI)_2I_2]$, D = $[Co(BPBI)_2(NCS)_2]$

The mass loss at the first stage corresponds to the expulsion of one BPBI molecule in the case of the chloro and bromo complexes, one BPBI molecule and one iodine atom in the case of the iodo complex and 1.5 BPBI molecule in the case of the thiocyanato complex. The IR spectra of the residues after this stage showed the presence of the BPBI ligand in all cases, indicating only a partial removal of the BPBI ligand at this stage. The elemental analyses (for Co and the anion) of the residue after the first stage indicated the approximate composition of the intermediate complexes to be $[Co(BPBI)Cl_2]$, $[Co(BPBI)Br_2]$, $[Co(BPBI)I]$ and $[Co(BPBI)_{0.5}(NCS)_2]$.

In all the complexes, the first DTG peak is followed by a very strong DTG peak. The mass loss at this stage corresponds to the removal of one BPBI molecule and two chlorine atoms in the case of the chloro complex, one BPBI molecule and two bromine atoms in the case of the bromo complex, one BPBI molecule and one iodine atom in the case of the iodo complex, and 0.5 BPBI molecule and one thiocyanate group in the case of the thiocyanato complex. This DTG peak is paralleled by a very strong exothermic DTA peak. The exothermicity of these peaks, here also, may be due to the concomitant oxidation processes. The thiocyanato complex shows one

more DTG peak, and the mass loss for this stage seems to agree with the expulsion of one NCS group. In all cases, the residue after the final stage of decomposition was found to be CoO.

In addition to the DTA peaks mentioned above, a sharp endothermic peak appeared just before the decomposition of the complexes. This DTA peak, which has no parallel in DTG, represents melting. Independent determination of the melting points of the complexes confirmed this.

5.3.1b Decomposition kinetics

The kinetic parameters n, E_a, ΔS and A for two clear-cut decomposition stages of each of the BPBI complexes have been calculated using the Coats-Redfern equation, and are presented in Table V.2. The order, n, of the reaction in these cases does not provide any meaningful information about the mechanism of decomposition of the complexes. However, the parameters E_a and ΔS may be employed for the comparison of a given decomposition process for similar compounds[227]. In the present investigation these values have been evaluated using the same equation for nearly the same experimental conditions (same heating rate, furnace atmosphere,

Table V. 2
Kinetic data of BPBI complexs

Compound	Stage	Order(n)	E_a(kJ mol^{-1})	ΔS(kJ mol^{-1} K^{-1})	A (S^{-1})
$[CoL_2Cl_2]$	I	0.85	92.50	-147.14	$2.694*10^5$
	II	1.40	373.85	-35.67	$0.241*10^{12}$
$[CoL_2Br_2]$	I	0.73	91.16	-141.56	$4.977*10^5$
	II	0.70	105.82	-169.42	$2.318*10^4$
$[CoL_2I_2]$	I	1.54	152.82	-14.69	$0.189*10^{13}$
	II	1.42	302.50	158.00	$0.255*10^{22}$
$[CoL_2(NCS)_2]$	I	0.40	113.65	-105.82	$3.658*10^7$
	II	1.38	198.60	-33.65	$0.278*10^{12}$

sample weight, etc.), and hence can be used conveniently for comparison purposes.

The activation energy for the first stage of decomposition of the chloro and bromo complexes was found to have nearly the same value, suggesting a similar type of mechanism for the decomposition reaction, $[Co(BPBI)_2X_2] \longrightarrow [Co(BPBI)X_2] + BPBI$ (where X = Cl or Br). The iodo and thiocyanato complexes, however, have different E_a values, indicating a mechanism different from that for the chloro and bromo complexes. Moreover, the differences in stoichiometry of the intermediate iodo and thiocyanato complexes formed after the first stage of decomposition (Table V.1) also indicate a difference in behaviour.

The E_a values for the first stage are much lower than those for the second stage in the case of all the complexes except the bromo complex, indicating the rate of decomposition for the first stage to be greater than that for the second stage. It is generally observed that stepwise formation constants decrease with an increase in the number of ligands attached to the metal ion[217]. It can therefore be expected that the rate of removal of the remaining ligands will be smaller after the expulsion of one or two ligands. Moreover, in the

present case, steric strain caused by the bulky BPBI ligands would further enhance the rate of decomposition in the first stage.

The negative ΔS values for the first stage show that all the complexes are more ordered in the activated state[228]. This may be due to the chemisorption of gases, probably oxygen present in the air, by these complexes. The ΔS values for the second stage are larger than those for the first stage, suggesting more disorder during this stage, which can be expected from the decreased association of molecules at elevated temperatures. For the iodo complex, ΔS values were found to be much higher than those of the other BPBI complexes for both the stages of decomposition, which might be due to the release of iodine during the first stage itself.

The E_a and ΔS values for the second stage of decomposition of the bromo complex were found to be anomalously low. The lower value of E_a indicates increased rate at this stage, and might be due to the catalytic effect of the intermediate $[Co(BPBI)Br_2]$ complex in the oxidation of the ligands and other decomposition products. This possibility is also reflected in the negative ΔS value, indicating more chemisorption of oxygen molecules by the complex during

this stage. Catalytic activity can be expected in such complexes with vacant coordination sites. Indeed systems containing cobalt(II) and bromide ions are known catalysts for oxidation reactions involving molecular oxygen or air[229-231].

5.3.2 Thermal studies of the Fe(III), Co(II), Ni(II) and Cu(II) complexes of HBHPBI

5.3.2a Thermal behaviour

The TG/DTG/DTA curves for all the complexes are shown in Fig. 5.2. Thermoanalytical data for the complexes are presented in Table V.3. The percentage mass loss and the probable composition of the expelled groups and residues are also given in this table.

The DTG curves show three peaks for Fe(III), Co(II) and Cu(II) complexes and two peaks for the Ni(II) complex. All these DTG peaks have their parallel DTA peaks. It is evident from DTA curves that the loss of lattice water in all the cases is an endothermic process, while the subsequent reactions appear to be exothermic in nature. The exothermicity in these cases is due to the concomitant decomposition and oxidation processes taking place at these stages. The high heat of decomposition released during the oxidation process

Table V. 3
Thermal decomposition data of HBHPBI complexes

Compound	Peak temp. in DTA (°C)	Temp. range in DTA (°C)	Peak temp. in DTG (°C)	Temp. range in DTG (°C)	Stage	Loss(%) Found from TG (Calc.)	Probable composition of expelled group
	80 endo(w)	50-110	65w	50-95	I	4.20 (3.80)	H_2O
A	295 exo(m)	220-370	300m	260-340	II	15.22 (15.10)	2OH, and $2H_2O$
	485 exo(s)	400-550	490s	460-540	III	67.10 (68.90)	L
	70 endo(w)	40-120	40w	30-80	I	4.50 (4.10)	H_2O
B	410 exo(m)	300-440	320m	290-360	II	32.50 (33.10)	OH,H_2O, and 0.3L
	510 exo(s)	450-620	560s	520-610	III	48.50 (49.40)	0.7L
C	65 endo(w)	30-100	60w	40-75	I	4.60 (4.17)	H_2O
	300 exo(s)	260-400	320s	280-350	II	81.81 (82.23)	OH,H_2O, and L
	80 endo(w)	50-120	70w	50-90	I	4.50 (4.13)	H_2O
D	280 exo(m)	170-310	265m	200-290	II	10.48 (8.04)	OH, and H_2O
	460 exo(s)	350-550	485s	400-550	III	69.45 (73.20)	L

Abbreviations: s=strong: m=medium: w=weak: endo=endothermic: exo=exothermic

L = HBHPBI, A = $[FeL(OH)_2(H_2O)_2].H_2O$, B = $[CoL(OH)(H_2O)].H_2O$,

C = $[NiL(OH)(H_2O)].H_2O$, D = $[CuL(OH)(H_2O)].H_2O$

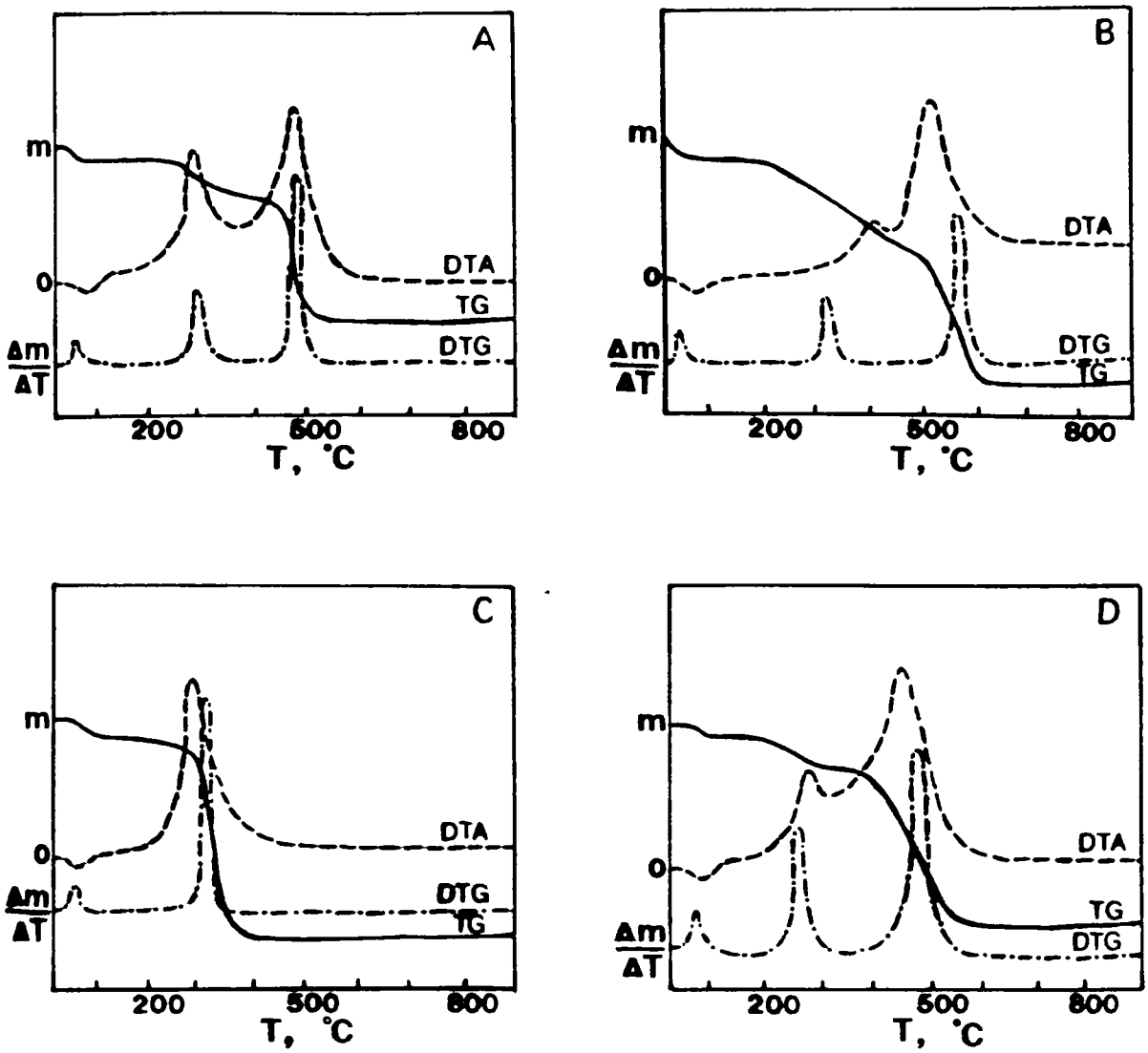

Fig. 5.2 TG/DTG/DTA traces of HBHPBI complexes

A = $[FeL(OH)_2(H_2O)_2].H_2O$, B = $[CoL(OH)(H_2O)].H_2O$
C = $[NiL(OH)(H_2O)].H_2O$, D = $[CuL(OH)(H_2O)].H_2O$

might have masked the endothermicity of the decomposition reactions.

In all the complexes, first stage of decomposition begins around 40°C and is complete at 120°C. The mass loss at this stage corresponds to the removal of one molecule of water. This water is not coordinated to the metal, as it is lost below 120°C, and probably be lattice water. The evidence for lattice water is present in the IR spectra of these complexes which show a broad band in the region 3100-3500 cm^{-1}.

The first DTG peak is followed by a medium DTG peak in the case of the Fe(III), Co(II) and Cu(II) complexes and a strong DTG peak in the case of the Ni(II) complex. The mass loss at this stage corresponds to the removal of coordinated water molecules and OH groups in the case of Fe(III) and Cu(II) complexes, and coordinated water molecules, OH groups and 0.3 HBHPBI molecule in the case of the Co(II) complex. The IR spectra of the residues after this stage showed the presence of HBHPBI ligand. For the Ni(II) complex, mass loss at this stage corresponds to the removal of coordinated water molecule, OH group and one HBHPBI molecule.

Except the Ni(II)complex, all the other complexes show one more strong DTG peak which corresponds to the

removal of one HBHPBI molecule in the case of the Fe(III) and Cu(II) complexes, and 0.7 HBHPBI molecule in the case of the Co(II) complex. In all the cases, the residue after the final stage of decomposition was found to be the metal oxide.

5.3.2b Decomposition kinetics

The kinetic parameters, n, E_a, ΔS and A for all decomposition stages have been calculated using the Coats-Redfern equation, and are presented in Table V.4.

It can be seen from Table V.4 that the order parameter for different decomposition stages is a decimal number. It is known from the literature that this order, n, need not be an integer[232,233]. The energy of activation for the decomposition of lattice interacted water is in the range 23-44 kJ mol^{-1} which is much lower than that for the coordinated water. These values are closer to the activation energy values for dehydration reactions reported by earlier workers[234].

The E_a and ΔS values for the second stage of decomposition of all the complexes, except the Ni(II) complex, were found to be much lower than that for the third stage of decomposition. The lower value of E_a

Table V. 4
Kinetic data of HBHPBI complexs

Compound	Stage	Order(n)	E_a (kJ mol^{-1})	ΔS (kJ mol^{-1} K^{-1})	A (S^{-1})
	I	0.23	34	-190	$8.279*10^{2}$
A	II	1.06	79	-164	$3.580*10^{4}$
	III	1.91	406	269	$1.806*10^{27}$
	I	1.75	43	-149	$1.086*10^{5}$
B	II	0.33	48	-223	$0.281*10^{2}$
	III	1.18	170	-91	$2.955*10^{8}$
C	I	0.38	23	-218	$0.283*10^{2}$
	II	1.83	148	-45	$5.680*10^{10}$
	I	0.90	32	-239	$2.381*10^{2}$
D	II	1.49	20	-288	$0.105*10^{0}$
	III	0.77	97	-172	$1.729*10^{4}$

L = HBHPBI, A = $[FeL(OH)_2(H_2O)_2].H_2O$, B = $[CoL(OH)(H_2O)].H_2O$,

C = $[NiL(OH)(H_2O)].H_2O$, D = $[CuL(OH)(H_2O)].H_2O$

indicates increased rate at this stage, and might be due to the catalytic effect of the metal complexes in the oxidation of the ligands and other decomposition products. The negative ΔS value indicates more ordered activated state through chemisorption of oxygen and other decomposition products[228]. For all catalysis reactions chemisorption of the reactants is the prime requirement.

The E_a and ΔS values for the third stage of decomposition for the Fe(III), Co(II) and Cu(II) complexes were found to be much higher than those for the other stages, indicating that the rate of decomposition for this stage to be lower than that for the other stages. It is generally observed that stepwise formation constants decrease with an increase in the number of ligands attached to the metal ion. It can therefore be expected that the rate of removal of the remaining ligands will be smaller after the expulsion of one or two ligands.

For the Ni(II) complex, second stage of decomposition is the final stage, and the decomposition is complete at a lower temperature of 350°C. For the other metal complexes, the decomposition is complete only after 540°C. The faster decomposition for the

Ni(II) complex at this stage might be due to the catalytic effect of nickel oxide formed during the decomposition. This is also indicated from the lower E_a and the negative ΔS value for this complex at this stage. Oxygen adsorption is found to occur far more extensively on p-type oxides than on n-type oxides. NiO is known to be a p-type oxide, and hence works as a better catalyst for oxidation reactions[235].

Thus the decomposition at the final stage seems to have a bearing on the catalytic effect of the oxides formed at this stage. The lower value of E_a and the negative ΔS value for Cu(II) complex suggests that oxide formed might be p-type Cu_2O (this will be ultimately oxidised to CuO). The E_a value for Co(II) complex is slightly higher than that for the Ni(II) complex. Here also involvement of a p-type oxide, CoO, is indicated, as the ΔS value is negative. However, for the Fe(III) complex, formation of n-type Fe_2O_3 is suspected at the final stage of decomposition, as the E_a and ΔS values are very much higher for this stage.

APPENDIX

Kinetic parameters from nonisothermal thermogravimetry

The kinetic equations for solid state decomposition reactions have usually been developed by invoking the concept of homogeneous kinetics into heterogeneous systems.

Thus the specific rate equation for the thermal decomposition of a single solid giving another solid and a volatile product:

$$A(solid) \longrightarrow B(solid) + C(gas)$$

can be written in the form,

$$d\alpha/dt = kf(\alpha) \qquad (1)$$

where α is the fraction decomposed at time t, $f(\alpha)$ is a function of α and k is the specific reaction rate. Actually, $f(\alpha)$ can have various forms. In the derivation of almost all the well known kinetic equations developed for evaluating kinetic parameters, simplified form of $f(\alpha)$: $f(\alpha) = (1-\alpha)^n$ is used. Eventhough, n can be identified as the order of the reaction, it does not have much physical significance in solid state reactions, which are usually heterogeneous[236-239]. However, n can be treated as a useful parameter.

For the decomposition reaction with a constant linear heating rate, ϕ, (where $\phi = dT/dt$) equation (1) can be rewritten as

$$d\alpha/dT = (k/\phi)\ f(\alpha) = (k/\phi)\ (1-\alpha)^n \qquad (2)$$

Substituting the Arrhenius equation, *i.e.*,

$$k = A\ e^{-E_a/RT} \qquad (3)$$

into the equation (2), we get,

$$d\alpha/dT = (A/\phi)\ e^{-E_a/RT}\ (1-\alpha)^n \qquad (4)$$

where A is the pre-exponential factor and E_a is the energy of activation. Equation (4) is the fundamental equation employed in non-isothermal TG.

Various attempts have been made by several workers to obtain convenient forms of equation (4). Depending upon the type of equation used, the methods for evaluating the kinetic parameters can be broadly classified into three groups[240]: (1) differential methods (2) approximation methods and (3) integral methods. Integral methods are considered to be most accurate and give quite reliable values[241,242]. Among them, Coats-Redfern method is the most reliable one and in the present investigation this method has been used for the evaluation of kinetic parameters. Therefore

only details about the Coats-Redfern method are given here.

The Coats-Redfern method

This method employs the integrated form of the equation (4). Coats and Redfern used the equation (4) in the following form:

$$d\alpha/(1-\alpha)^n = (A/\phi)\ e^{-E_a/RT}\ dT \qquad (5)$$

The integration of the left hand side (LHS) of equation (5) with limits 0 to α is direct, but the integration of the right hand side (RHS) with limits 0 to T poses some difficulty, as it has no exact solution. The integral of LHS, denoted by the function $g(\alpha)$, can be written as:

$$g(\alpha) = [1-(1-\alpha)^{1-n}]/(1-n) \qquad (6)$$

when $n \neq 1$, and

$$g(\alpha) = -\ln(1-\alpha) \qquad (7)$$

when $n = 1$. Coats and Redfern evaluated the RHS of equation (5), *i.e.*, the temperature integral, with the aid of the Rainville function[243]. The final form of the equation derived by them was:

$$\log g(\alpha)/T^2 = (\log AR/\phi E_a)(1-2RT/E_a) - E_a/2.303RT \qquad (8)$$

They have suggested that the term $2RT/E_a$ is negligible in comparison with unity and can therefore be neglected. Therefore equation (8) can be written in the form,

$$\log g(\alpha)/T^2 = \log AR/\phi E_a - E_a/2.303RT \qquad (9)$$

A plot of $\log g(\alpha)/T^2$ vs $1/T$ will be linear and the slope of this plot will give the value of $-E_a/2.303R$ from which activation energy value (E_a) can be calculated. Knowing E_a, the value of pre-exponential factor (A) can be found out from the intercept.

The entropy of activation, ΔS is calculated using the relation, $A = (kT/h)e^{\Delta S/R}$, where k is the Boltzmann constant, h is the Plank's constant and R is the gas constant. The DTG peak temperature is usually taken as the value of temperature term T in the above equation.

The disadvantage of the Coats-Redfern method is the prior determination of the value of order, n. To determine the best value of n, the following procedure is adopted. First a value of n is selected. The best values of intercept (a) and slope (b) for this value of n are found out by the method of least squares. Using these values of a and b, the $g(\alpha)$ values are calculated

employing the equation (9). Then, the sum of the squares of deviation of these values from the experimental values, S, is calculated and the whole procedure is repeated for various values of n until S is a minimum. The value of n which gives the minimum value of S is taken as the best value.

CHAPTER VI

LANTHANIDE(III) COMPLEXES OF 1-(2'-HYDROXYBENZYL)-2-(2'-HYDROXYPHENYL)BENZIMIDAZOLE

6.1 INTRODUCTION

It is becoming increasingly apparent that the coordination chemistry of lanthanides is of importance to a wide variety of chemical, biological and applied problems[244]. A search through the literature revealed that not much work has been done on the lanthanide complexes of benzimidazole ligands. In this chapter, we report the synthesis and structural studies of La(III), Pr(III), Nd(III), Sm(III), Eu(III), Gd(III), Tb(III), Dy(III) and Y(III) complexes of 1-(2'-hydroxybenzyl)-2-(2'-hydroxyphenyl)benzimidazole, abbreviated as HBHPBI (Fig. 4.1).

6.2 EXPERIMENTAL

6.2.1 Materials

Details about the preparation of the ligand, and all other reagents and solvents employed are given in Chapter II.

6.2.2 Synthesis of the complexes

The ligand, HBHPBI (0.01 mol, 3.15 g)), was dissolved in 1% NaOH solution (80 mL). The solution was neutralized with a few drops of 2N acetic acid, and to this was added metal chloride (0.005 mol - 1.63 g of La_2O_3, 5.08 g of Pr_6O_{11}, 1.68 g of Nd_2O_3, 1.74 g of Sm_2O_3, 1.76 g of Eu_2O_3, 1.81 g of Gd_2O_3, 2.15 g of Tb_4O_7, 1.87 g Dy_2O_3 or 1.13 g of Y_2O_3 is dissolved in concentrated HCl and evaporated to dryness on a water bath.) solution in water (25 mL). The complex separated out was filtered, washed with 1N acetic acid and several times with water, and dried *in vacuo* over P_2O_5.
(Yield = 70-80%)

6.2.3 Analytical methods

Details about the analytical methods and other characterization techniques are given in Chapter II.

6.3 RESULTS AND DISCUSSION

All the complexes are microcrystalline, non-hygroscopic and stable to aerial oxidation. The complexes are insoluble in ethanol, methanol, acetone, chloroform and benzene, and are fairly soluble in DMF and DMSO. The analytical data (Table VI.1) show that

Table VI. 1
Analytical Data

Compound (Empirical formula)	C(%) Found (Calc.)	H(%) Found (Calc.)	N(%) Found (Calc.)	Ln(%) Found (Calc.)	Cl(%) Found (Calc.)
$[LaLCl(OH)(H_2O)_4]$	41.30	3.85	4.80	24.66	6.08
$(LaC_{20}H_{24}N_2O_7Cl)$	(41.51)	(4.18)	(4.85)	(24.06)	(6.14)
$[PrLCl(OH)(H_2O)_4]$	41.39	3.91	4.82	24.51	6.04
$(PrC_{20}H_{24}N_2O_7Cl)$	(41.43)	(4.17)	(4.83)	(24.32)	(6.12)
$[NdLCl(OH)(H_2O)_4]$	41.02	3.83	4.78	24.81	6.03
$(NdC_{20}H_{24}N_2O_7Cl)$	(41.19)	(4.14)	(4.81)	(24.75)	(6.08)
$[SmLCl(OH)(H_2O)_4]$	40.71	3.76	4.71	25.80	5.99
$(SmC_{20}H_{24}N_2O_7Cl)$	(40.70)	(4.10)	(4.76)	(25.54)	(6.02)
$[EuLCl(OH)(H_2O)_4]$	40.60	3.94	4.74	25.68	5.80
$(EuC_{20}H_{24}N_2O_7Cl)$	(40.59)	(4.09)	(4.75)	(25.78)	(6.01)
$[GdLCl(OH)(H_2O)_4]$	40.23	3.85	4.68	26.39	5.93
$(GdC_{20}H_{24}N_2O_7Cl)$	(40.29)	(4.05)	(4.70)	(26.40)	(5.95)
$[TbLCl(OH)(H_2O)_4]$	39.98	3.79	4.60	26.84	5.87
$(TbC_{20}H_{24}N_2O_7Cl)$	(40.12)	(4.04)	(4.69)	(26.54)	(5.93)
$[DyLCl(OH)(H_2O)_4]$	39.38	3.86	4.62	27.12	6.03
$(DyC_{20}H_{24}N_2O_7Cl)$	(39.88)	(4.02)	(4.66)	(27.04)	(6.00)
$[YLCl(OH)(H_2O)_4]$	45.18	4.17	5.29	16.92	6.68
$(YC_{20}H_{24}N_2O_7Cl)$	(45.51)	(4.58)	(5.31)	(16.81)	(6.72)

the complexes have the general empirical formula $[LnLCl(OH)(H_2O)_4]$ (where Ln = La(III), Pr(III), Nd(III), Sm(III), Eu(III), Gd(III), Tb(III), Dy(III) or Y(III), and L = HBHPBI). The complexes act as non-electrolytes in DMF solutions. Their room temperature magnetic moment values showed very little deviation from the Van Vleck values[245], indicating little participation of 4f electrons in bond formation (Table VI.2).

6.3.1 Electronic spectra

All the present complexes exhibit a broad absorption band with high intensity around the region 35000-36000 cm^{-1}. This band is found to be sensitive with the change of the metal ions, and hence can be attributed to charge transfer transition. Furthermore, the complexes show intraligand transition around 42000 cm^{-1}.

The electronic absorption spectra of lanthanide ions have been subject of several investigations[246-248]. The spectral data of the Pr(III), Nd(III) and Sm(III) complexes along with various calculated parameters are given in Table VI.3. In the case of other lanthanide complexes, the bands due to f-f transitions could not be identified as these are presumably masked by the ligand

Table VI.2
Molar conductance and magnetic moment data

Compound	Molar conductance $ohm^{-1}\ cm^{2}\ mol^{-1}$	Magnetic moment BM
$[LaLCl(OH)(H_2O)_4]$	0.72	diamagnetic
$[PrLCl(OH)(H_2O)_4]$	0.63	3.5
$[NdLCl(OH)(H_2O)_4]$	0.68	3.7
$[SmLCl(OH)(H_2O)_4]$	0.58	1.7
$[EuLCl(OH)(H_2O)_4]$	0.78	3.6
$[GdLCl(OH)(H_2O)_4]$	0.49	7.9
$[TbLCl(OH)(H_2O)_4]$	0.65	9.4
$[DyLCl(OH)(H_2O)_4]$	0.81	10.4
$[YLCl(OH)(H_2O)_4]$	0.66	diamagnetic

Table VI. 3
Electronic spectral data

Compound	Abs.max. cm^{-1}	Tentative assignments	Parameters calculated
$[PrLCl(OH)(H_2O)_4]$	22320 (22490)	$^3H_4 \longrightarrow {}^3P_2$	β = 0.992
	21190 (21320)	$^3H_4 \longrightarrow {}^3P_1$	$b^{1/2}$ = 0.063
	20580 (20740)	$^3H_4 \longrightarrow {}^3P_0$	δ% = 0.806
	16840 (17000)	$^3H_4 \longrightarrow {}^1D_2$	η = 0.004
$[NdLCl(OH)(H_2O)_4]$	19470 (19520)	$^4I_{9/2} \longrightarrow {}^4G_{9/2}$	β = 0.993
	19000 (19200)	$^4I_{9/2} \longrightarrow {}^4G_{7/2}$	$b^{1/2}$ = 0.059
	17260 (17370)	$^4I_{9/2} \longrightarrow {}^4G_{5/2}$	δ% = 0.705
	13610 (13660)	$^4I_{9/2} \longrightarrow {}^4S_{3/2}$	η = 0.004
	13410 (13510)	$^4I_{9/2} \longrightarrow {}^4F_{7/2}$	
	12340 (12470)	$^4I_{9/2} \longrightarrow {}^4F_{5/2}$	
$[SmLCl(OH)(H_2O)_4]$	21010 (21100)	$^6H_{5/2} \longrightarrow {}^4I_{11/2}$	β = 0.996
			$b^{1/2}$ = 0.047
			δ% = 0.402
			η = 0.002

* Values given in brackets are for the aquo complexes.

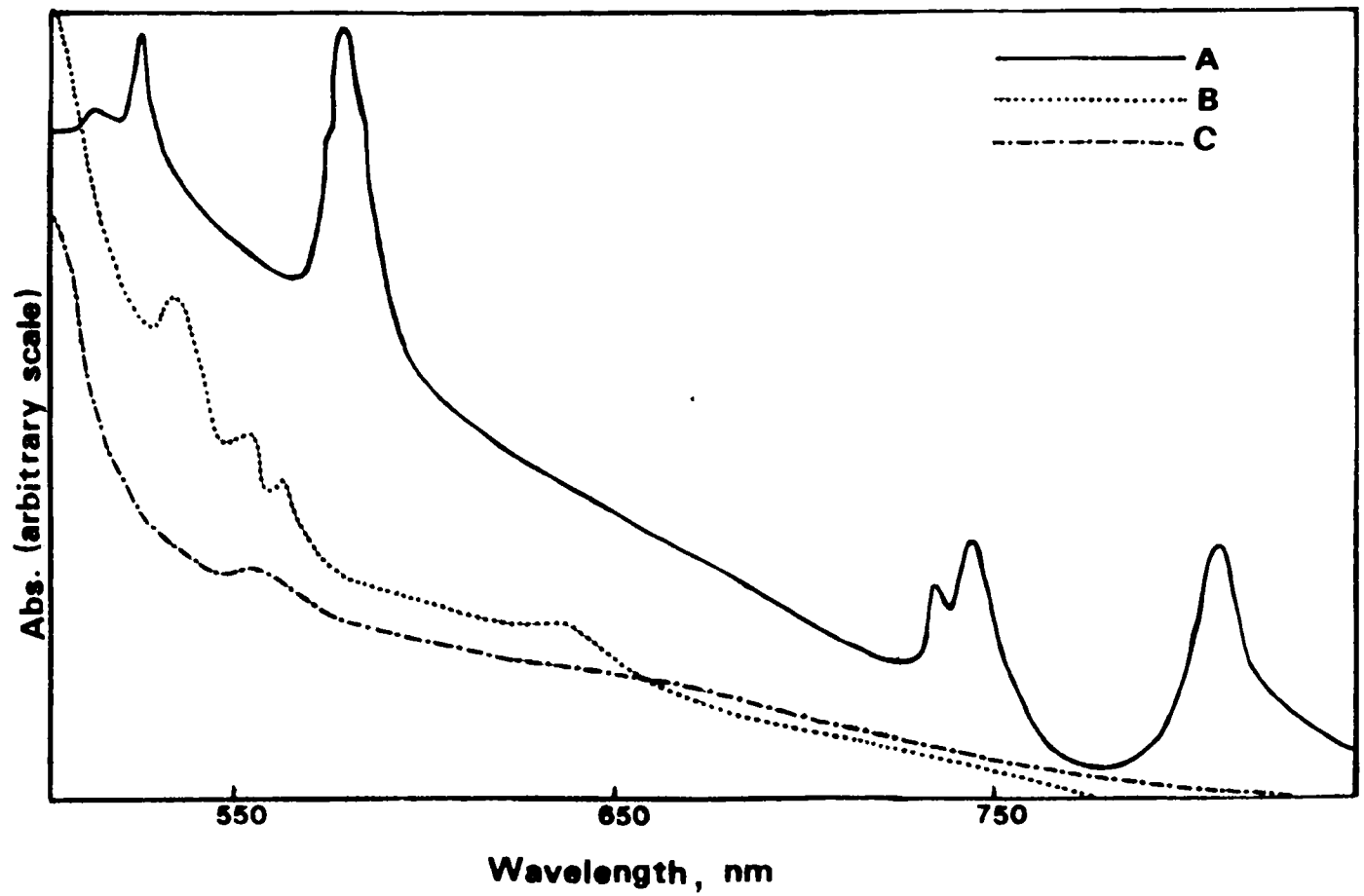

Fig. 6.1 Electronic spectra of the complexes

A = $[NdLCl(OH)(H_2O)_4]$, B = $[PrLCl(OH)(H_2O)_4]$

C = $[SmLCl(OH)(H_2O)_4]$

charge transfer transitions[249]. The spectral features of the complexes are similar in both the solid as well as in DMF solution, indicating that the complexes maintain identical stereochemistry and coordination number in the solid and in the solution phases.

The interelectronic repulsion parameter (β), percentage covalency (δ%), the bonding parameter ($b^{1/2}$) and the covalency angular overlap parameter (η) have been calculated from solid state spectrum for the Pr(III), Nd(III) and Sm(III) complexes (Fig. 6.1) using the expressions:

$$\beta = n^{-1} \Sigma \nu_{complex} / \nu_{aquo}$$

$$\delta(\%) = [(1-\beta)/\beta]x100$$

$$b^{1/2} = 1/2[(1-\beta)^{1/2}]$$

$$\eta = (1-\beta^{1/2})/\beta^{1/2}$$

Interelectronic repulsion parameter, β, is the average value of the ratio of absorption maxima of the complex to that of the aquo ion, taking into account as many (n) transitions as possible. Depending upon the ligands, δ(%) values may either be positive for covalent bonding or negative for ionic bonding. The value of β is found to be less than unity and the $b^{1/2}$ and δ (%)

values are positive indicating the covalency in the metal-ligand bonding[250]. However, δ (%) values of the complexes are below 1.5 which indicate weak covalent bonding in the complexes. Although the absolute values of δ (%) are of less importance, they may be conveniently used in assessing the relative covalent character of the complexes[251]. The covalent character in the present cases is seen to decrease in the order: Pr(III) > Nd(III) > Sm(III). Ligand to metal charge transfer bands are expected to undergo a red shift with increase of ionic character and mask the hypersensitive bands in the visible region. Absence of hypersensitive bands in the spectra of higher lanthanide metal complexes of HBHPBI might be due to their increased ionic character.

Further, the hypersensitive bands of the present Nd(III) complex have striking resemblances with that of the eight coordinated complexes reported earlier[252]; hence an eight coordinated structure can be presumed in these cases.

6.3.2 Infrared spectra

The infrared spectral data of the ligand and the complexes are given in Table VI.4. All the complexes exhibit a very broad band around the region 3100-3500

Table VI.4

Infrared absorption frequencies (cm^{-1})

L	I	II	III	IV	V	VI	VII	VIII	IX	Assign-ments
3500m	3300m	3300m	3300m	3300m	3300m	3300m	3300m	3300m	3300m	ν(O-H)
3030m	3030m	3030m	3030m	3030m	3030m	3030m	3030m	3030m	3030m	
1585s	1585m	1585m	1585w	1585m	1585m	1585w	1585m	1585w	1585m	
1540m	1540w	1540w	1540w	1540w	1540w	1540w	1540w	1540w	1540w	
1500m	1490w	1490w	1490w	1490w	1490w	1490w	1490w	1490w	1490w	ν(C-N)
1450s	1450s	1450s	1450s	1450s	1450s	1450s	1450s	1450s	1450s	
1420m	1420m	1420m	1420m	1420m	1420m	1420m	1420m	1420m	1420m	
1390m	1390m	1390m	1390m	1390m	1390m	1390m	1390m	1390m	1390m	
-	1290m	1290m	1290m	1290m	1290m	1290m	1290m	1290m	1290m	ν(C-O)
1280s	1280m	1280m	1280m	1280m	1280m	1280m	1280m	1280m	1280m	
1260w	1260m	1260m	1260m	1260m	1260m	1260m	1260m	1260m	1260m	
1235w	1235w	1235w	1235w	1235w	1235w	1235w	1235w	1235w	1235w	
1150w	1155w	1150w	1150m	1145w	1150w	1150w	1145w	1155w	1150w	

Table VI.4 (continued)

-	1115w	1120w	1115w	1115w	1115w	1115w	1115w	1120w	1115w	δ(M-O-H)
1090m	1090w	1090w	1090w	1090w	1090w	1090w	1090w	1090w	1090w	
1030w	1030w	1030w	1030w	1030w	1030w	1030w	1030w	1030w	1030w	
980w	975w	980w	975w	970w	980w	975w	980w	980w	975w	
920w	920w	920w	920w	920w	920w	920w	920w	920w	920w	
-	840m	840m	840m	840m	840m	840m	840m	840m	840m	δ(H-O-H)
800m	800m	800m	800m	800m	800m	800m	800m	800m	800m	
745s	740w	745w	750w	750m	745m	750w	745w	750m	745w	
710w	710w	710w	710w	710w	710w	710w	710w	710w	710w	
560w	550w	560w	560w	550w	565w	560w	560w	565w	560w	
520w	525m	520w	520w	525m	520w	525m	520w	525m	520w	
-	490m	485m	470m	460w	465w	470w	460w	445w	440w	ν(M-O)
470w	470w	470w	470w	470w	470w	470w	470w	470w	470w	
425w	430w	425w	430w	435w	425w	430w	435w	425w	430w	
370w	375w	375w	375w	375w	375w	375w	375w	375w	375w	
-	365m	360w	365w	350w	350m	340w	345m	340w	340w	ν(M-N)

Table VI.4 (continued)

330s	330s	330s	330s	330s	330s	330s	330s	330s	330s	
305w	310w	310m	310w	310m	310w	310w	315w	310m	310w	
270m	270m	270m	270m	270m	270m	270m	270m	270m	270m	
230w	230w	230w	230w	230w	230w	230w	230w	230w	230w	
-	220s	220m	220m	215w	215w	215w	215w	220m	215w	ν(M-Cl)
205m	210m	210m	210m	210m	210m	210m	210m	210m	210m	

Abbreviations: s = strong, m = medium, w = weak

L = HBHPBI, I = $[LaLCl(OH)(H_2O)_4]$, II = $[PrLCl(OH)(H_2O)_4]$, III = $[NdLCl(OH)(H_2O)_4]$, IV = $[SmLCl(OH)(H_2O)_4]$, V = $[EuLCl(OH)(H_2O)_4]$, VI = $[GdLCl(OH)(H_2O)_4]$, VII = $[TbLCl(OH)(H_2O)_4]$VIII = $[DyLCl(OH)(H_2O)_4]$, IX = $[YLCl(OH)(H_2O)_4]$

cm^{-1} due to O-H stretching vibrations. A sharp band at 840 cm^{-1} is also seen in the spectra of the complexes due to coordinated water molecules[223]. Furthermore, the complexes exhibit M-O-H bending mode around 1120 cm^{-1}.

The band of medium intensity observed at 1500 cm^{-1} in the spectrum of the free HBHPBI ligand may be assigned to the C-N stretching vibration. The shifting of this band to a lower frequency was observed by earlier workers in the case of some transition metal complexes of benzimidazoles and has been attributed to the involvement of the N-3 atom of benzimidazole in bonding to the metal atom[209,211].

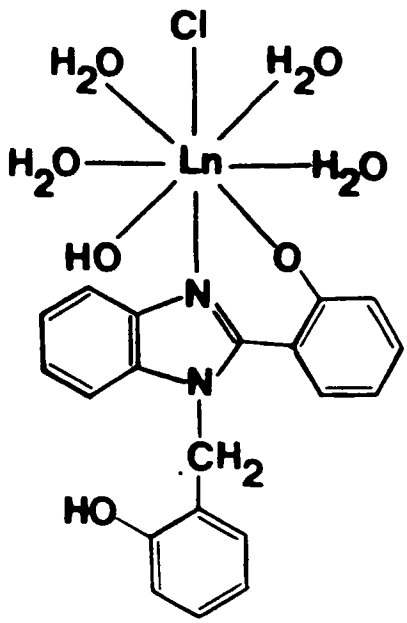

Fig.6.2 Proposed structure of the complexes

In the spectra of free HBHPBI, there is a band around 1280 cm^{-1} which can be assigned to the νC-O stretching vibration of the phenolic group[224]. This band is seen to shift towards higher frequencies during complex formation[225]. The present complexes exhibit a new band at 1290 cm^{-1}, while retaining the band at 1280 cm^{-1}, which suggests that only one of the phenolic oxygen atoms of the HBHPBI ligand is coordinated to the metal atom.

In the far IR spectra of metal chelates, the bands observed around 490 cm^{-1}, 360 cm^{-1} and 220 cm^{-1} can be assigned to ν(M-O), ν(M-N) and ν(M-Cl) stretching modes respectively, and are in agreement with those values reported for other lanthanide complexes[253-255]. These bands are absent in the spectrum of the ligand.

Based on the elemental analyses and various physico-chemical studies, the structure shown in Fig. 6.2 may be tentatively proposed for the present complexes.

CHAPTER VII

STUDIES ON SOME POLYMER BOUND COBALT COMPLEXES

7.1 INTRODUCTION

A polymer-metal complex is usually composed of a synthetic polymer and metal ions. Its synthesis represents an attempt to give an organic polymer inorganic functions. Numerous chelating macromolecular ligands with various chemically active groups fixed on different supports are known today[256,257]. Substantial difference has been observed in the complexation behaviour of macromolecular ligands and simple ligands, probably due to the macroenvironment that is created at the coordination centre. The macroenvironment around the metal complex affects the coordination sphere and causes steric, electrostatic, hydrophobic and conformational effects. It has been shown that in metalloenzymes such as oxidase and hemoglobin, where the metal complex is the active site, the macromolecular protein part plays a significant role, or even controls the reactivity of the metal complex.

The introduction of specific complexing groups into the polymeric matrix gives them the capacity to bind metal ions. The groups taking part in the formation of

metal complexes usually include nitrogen, oxygen and sulphur atoms. The selectivity of the complexing ligand is due to the difference in stabilities of its complexes under the same conditions. The delayed development of the coordination chemistry of the polymer-metal complex appears to be due to the strong influence of analytical chemistry and the tendency to exploit the polymeric ligands as selective metal ion binders and the lack of theoretical background and instrumentation for studying the physico-chemical aspects of metal complexes.

A wide variety of investigations have been carried out on polymeric metal complexes; these include studies of semiconductivity, thermostability, redox reactions, collection of metal ions, biomedical effects, and so on. Study of polymer-metal complex is still a new field, and not all possible applications of metal complexes have been explored yet. Further demonstrations of new, unique applications of the polymer-metal complexes offering advantages over the conventional properties of both polymers and metal complexes are to be expected in the near future.

We have synthesized a new polymer-bound Schiff base by the condensation of polystyrene-bound benzaldehyde with 2-aminobenzimidazole. This polymer ligand was made to react with $[Co(BPBI)_2X_2]$ or [CoTPP]

(where BPBI = 1-benzyl-2-phenylbenzimidazole, TPP = *meso*-tetraphenylporphyrin and X = Cl. Br or NCS), and the corresponding polymer-metal complexes were obtained. Studies on these complexes are described in this chapter.

7.2 EXPERIMENTAL

7.2.1 Materials

Details of the preparation of polymer-bound Schiff base, 1-benzyl-2-phenylbenzimidazole, *meso*-tetraphenylporphyrin and other reagents and solvents employed are given in Chapter II. Cobalt(II) complexes of 1-benzyl-2-phenylbenzimidazole were prepared using the procedure given in Chapter III. Cobalt(II) tetraphenylporphyrin was prepared by a literature procedure[258] with slight modifications, and the details of preparation are described below.

A three-necked R. B. flask fitted with a sealed stirrer and water condenser was used for the simultaneous stirring and refluxing of the reaction mixture, and nitrogen is continuously passed through the system in order to create an inert atmosphere. Reagent grade DMF is brought to reflux in the flask and to this *meso*-tetraphenylporphyrin (0.01 mol, 6.12 g) was added. Allowed for complete solution to occur and $CoCl_2.6H_2O$

(0.01 mol, 2.72 g) was added and reaction was allowed to proceed. After 5 h the reaction vessel is removed from the hot plate and cooled in ice for 15 minutes. Then deoxygenated water (500 mL) was added and kept for 2 h. The resulting partially crystalline precipitate is filtered, washed with deoxygenated water and then dried *in vacuo* over anhydrous calcium chloride. All the operations were done in a glove bag. (Yield = 60%)

7.2.2 Synthesis of the complexes

All the polymer bound cobalt(II) complexes were prepared by the same general procedure. Polymer bound Schiff base (1 g) was swollen in deoxygenated chloroform for 2 h. An excess of solid $[Co(BPBI)_2X_2]$ or [CoTPP] was added in one portion and the reaction vessel is sealed. The mixture is shaken for 5 h using a mechanical shaker. The resulting polymer bound cobalt(II) complexes were filtered, washed with deoxygenated chloroform and dried *in vacuo* over anhydrous calcium chloride. All the operations were done in an inert atmosphere to prevent oxidation of cobalt(II) to cobalt(III) in the presence of air.

7.2.3 Analytical methods

Details about the analytical methods and other characterization techniques are given in Chapter II.

7.3 RESULTS AND DISCUSSION

Before going into details of the present discussion, a few remarks have to be made concerning the structure of the polymer bound metal complexes. Indeed, detailed information about the structure of the complexes formed with polymeric ligands is generally more difficult to obtain. Elemental analysis of the complexes is of only limited value. Most often, the structures for supported complexes were proposed essentially on the basis of previously gathered data for unsupported similar species. However detailed information about the micro and macroenvironment of the metal atom, the nature of other ligands present and structural changes of polymer support during complexation is usually not known.

In the present study, chloromethylated polystyrene (2% crosslinked with divinylbenzene, 12.9% Cl) beads were used as the starting material for the synthesis of the polymer bound Schiff base. The chlorine content in the chloromethylated polystyrene is compared with the percentage of chlorine calculated for all possible repeating units. This comparison indicates that only alternate rings are chloromethylated. Thus the repeating unit can be shown as below.

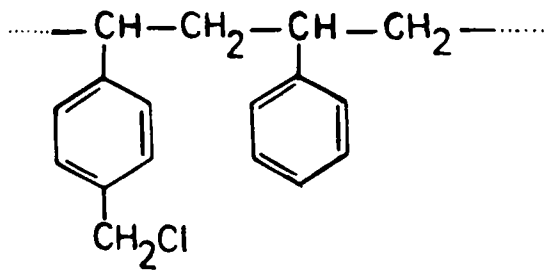

The beads on treating with DMSO and $NaHCO_3$ yielded polymer bound benzaldehyde. This is evidenced by a positive test with Borsche's reagent. The loading of aldehyde groups on the polymer support was determined by estimating the chlorine content of the beads. The chlorine content in the polymer bound benzaldehyde was found to be 0.3% which shows that almost all chloromethylene groups have been converted into the aldehyde. The polymer bound benzaldehyde was then condensed with 2-aminobenzimidazole to give polymer bound Schiff base (L) as shown in Scheme I.

The nitrogen analysis of this sample suggests that only 14% of the aldehyde groups have been converted to the Schiff base units. This might be due to the large size of the benzimidazole moiety.

The polymeric ligand (L) forms complexes on treatment with chloroform solutions of [CoTPP] or

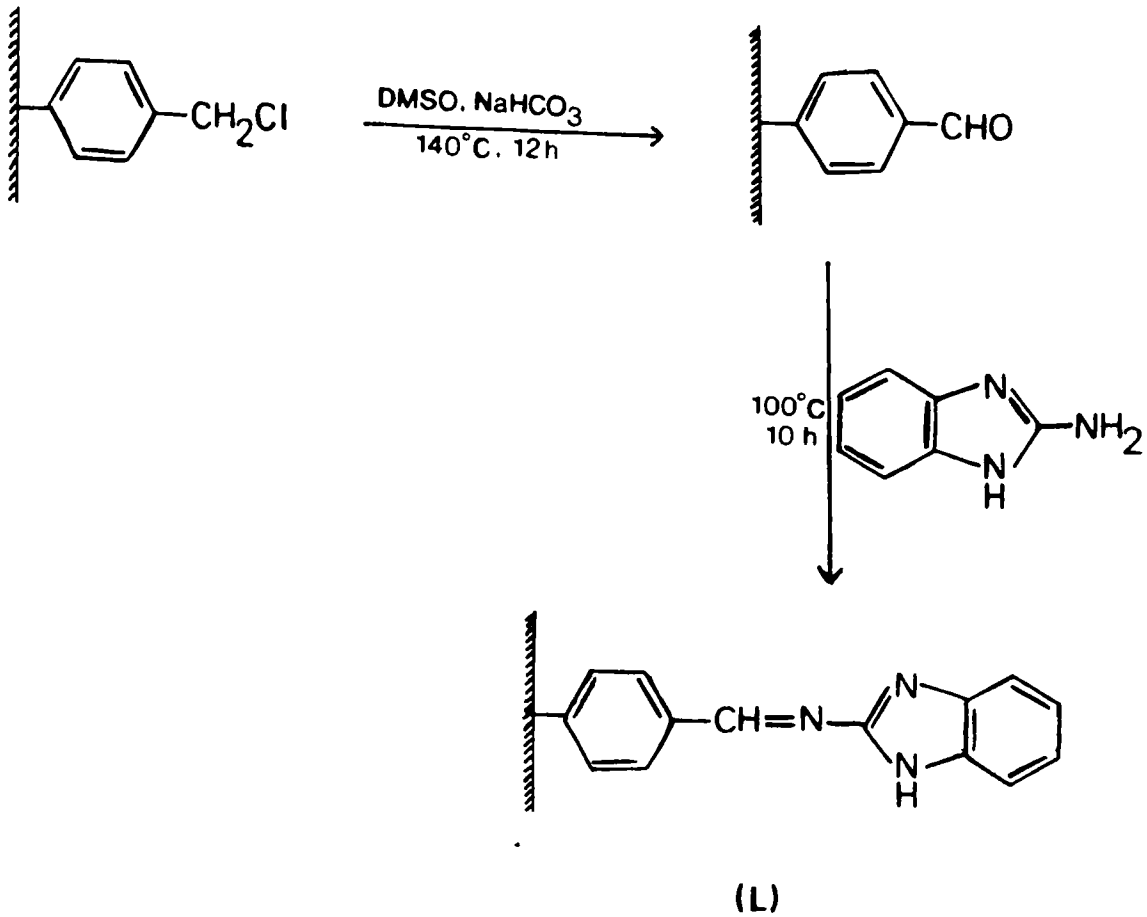

Scheme I

$[Co(BPBI)_2X_2]$. The percentages of cobalt and that of nitrogen (Table VII.1) in the complexes show that only one Schiff base unit is coordinated to cobalt. However, as pointed out by other workers, microanalytical data for polymeric samples can be taken as a qualitative rather than a quantitative guide.

7.3.1 Magnetic susceptibility measurements

For the calculation of magnetic susceptibility of the complexes, VSM measurements were used. All the

Table VII.1
Analytical data

Compound	%C Found (Calc.)	%H Found (Calc.)	%N Found (Calc.)	%Co Found (Calc.)	%Cl/Br/S Found (Calc.)
L	85.12 (85.70)	6.54 (6.46)	2.50 (2.38)	-	-
$[CoL(BPBI)_2Cl_2]$	80.86 (80.90)	6.08 (5.93)	3.78 (3.90)	2.28 (2.38)	2.70 (2.88)
$[CoL(BPBI)_2Br_2]$	78.80 (78.09)	5.80 (5.72)	2.40 (2.19)	2.15 (2.30)	6.51 (6.26)
$[CoL(BPBI)_2(NCS)_2]$	80.25 (80.42)	5.80 (5.82)	3.00 (3.35)	2.20 (2.34)	2.05 (2.55)
[CoL(TPP)]	83.08 (83.59)	5.15 (5.83)	3.90 (4.03)	2.08 (2.41)	-

complexes show negative magnetic susceptibility values (Table VII.2) due to the low concentration of the cobalt and the very large diamagnetic susceptibility of the atoms present in the polymer complex. Unfortunately, these measurements do not provide any clue about the structure of the complexes, as the molecular weight and diamagnetic contributions could not be found out. However, approximate molecular weight and empirical formula of the repeating complex unit containing one cobalt atom were found out from the analytical data. The diamagnetic correction was also calculated based on this empirical formula. When these values were used for the calculation of magnetic moment, μ_{eff} values around 2.1 BM were obtained. Hence a low-spin state for the cobalt(II) ion is indicated in these complexes.

7.3.2 EPR spectra

Further evidence for the low-spin nature of the complexes is obtained from their EPR spectra. All the present complexes exhibit reasonably good spectra at room temperature. If the complexes were in the high spin state, they would have three unpaired electrons and very short spin-lattice relaxation time in all the common stereochemistry so that the spectra would not be observed at room temperature. Very low temperatures are needed to detect any EPR signals in these cases.

Table VII.2
Magnetic susceptibility and elctronic spectral data

Compound	Magnetic susceptibility $cm^3\ mol^{-1}$	Abs. max. cm^{-1}
$[CoL(BPBI)_2Cl_2]$	-1529.81×10^{-6}	25300
$[CoL(BPBI)_2Br_2]$	-1534.20×10^{-6}	24800
$[CoL(BPBI)_2(NCS)_2]$	-1526.10×10^{-6}	25600
[CoL(TPP)]	-1501.81×10^{-6}	26900

The EPR parameters of the complexes are given in Table VII.3. The spectra show intense perpendicular direction signals at g = ~2.2 and the parallel ones at g = ~2.0. Both the signals are seen to split into hyperfine lines due to the interactions with ^{59}Co nucleus (I = 7/2). Many of the parallel signals show superhyperfine splittings due to the nitrogen nuclei. Further, the EPR parameters indicate that the complexes have square pyramidal geometry[72]. The spectra were also recorded at very low temperature (-140°C); but, the low temperature spectra did not show any deviation from those taken at room temperature.

7.3.3 Electronic spectra

The electronic spectral data are given in Table VII.2. The data do not provide any conclusive evidence to assign the structure of these complexes. The [CoTPP] complex shows characteristic electronic spectral bands[259] at 24510 cm^{-1}, 18940 cm^{-1}, 16950 cm^{-1} and 15270 cm^{-1}. In the polymer supported [CoTPP] complex, a very broad absorption band is observed in the visible region which shows that the stereochemistry around cobalt(II) has been changed. The polymer supported BPBI complexes also show a broad band around the region 24000-26000 cm^{-1} which can be assigned to the charge

Table VII.3
EPR parameters of the complexes

Compound	$g_{\parallel}$	$g_{\perp}$	$A_{\parallel}$*	$A_{\perp}$*
$[CoL(BPBI)_2Cl_2]$	2.02	2.21	80.1	9.8
$[CoL(BPBI)_2Br_2]$	2.01	2.20	80.1	10.0
$[CoL(BPBI)_2(NCS)_2]$	2.02	2.20	80.2	10.1
[CoL(TPP)]	2.02	2.21	80.1	9.5

*values in $cm^{-1} \times 10^{-4}$

transfer transition. Probably all the low intensity bands expected for square pyramidal complexes might have been obscured by the strong charge transfer transitions[220].

7.3.4 Infrared spectra

The infrared spectral data are given in Table VII.4. A strong band at 1610 cm^{-1} in the spectrum of the free ligand may be attributed to the C=N(azomethine) stretching vibration[260]. This band is seen at the same position in the spectra of the complexes which reveals non-participation of the azomethine nitrogen in coordination. The band of medium intensity at 1580 cm^{-1} in the spectrum of the polymer ligand may be attributed to the C-N stretching vibration of the benzimidazole ring system[224]. In the spectra of all the complexes, this band is seen at 1570 cm^{-1}. The shifting of this band to a lower frequency has been suggested as being due to the coordination of the nitrogen atom of benzimidazole. The disappearance of the band at 1580 cm^{-1} and the appearance of a new band at 1570 cm^{-1} suggests that all the Schiff base units take part in coordination through the nitrogen atom of the benzimidazole. The band at 1710 cm^{-1} due to the C=O stretching vibration of the aldehyde[261] is also observed

Table VII.4
Infrared absorption frequencies (cm^{-1})

L	I	II	III	IV	Assignments
2930s	2930s	2930s	2930s	2930s	ν(N-H)
2880s	2880s	2880s	2880s	2880s	
-	-	-	2090m	-	ν(C-N) (thiocyanate)
1710s	1710s	1710s	1710s	1710s	ν(C=O)
1690m	1685m	1690m	1685m	1685m	
1660w	1665w	1660w	1665w	1660w	
1650w	1650w	1650w	1650w	1650w	
1640w	1640w	1640w	1640w	1640w	
1620m	1625m	1620m	1625m	1625m	
1610s	1610s	1610s	1610s	1610s	ν(C=N) (azomethine)
1580m	1570m	1570m	1570m	1570m	ν(C-N) (benzimidazole)
1540w	1540w	1540w	1540w	1540w	
1515w	1520w	1515w	1520w	1520w	
1495m	1495m	1495m	1495m	1495m	
1470w	1470w	1470w	1470w	1470w	
1420m	1420m	1420m	1420m	1420m	
1390w	1395w	1390w	1395w	1390w	
1385w	1385w	1385w	1385w	1380w	
1360w	1360w	1360w	1360w	1360w	
-	-	-	-	1350m	ν(C-N) (porphyrin)
1310w	1310w	1310w	1310w	1310w	
1270w	1270w	1270w	1270w	1270w	
1210m	1210m	1210m	1210m	1210m	

Table VII.4 (continued)

1170m	1170w	1170w	1170w	1170w	
1110w	1110m	1110w	1110w	1110m	
1025w	1020w	1025w	1020w	1020w	
-	-	-	-	1000s	π(C-H) (porphyrin)
840w	840w	840w	840w	840w	
820w	825w	825w	820w	825w	
760w	760w	760w	760w	760w	
700m	700m	700m	700m	700m	
670w	665w	670w	670w	665w	
650w	650w	650w	650w	650w	
640w	640w	640w	640w	640w	
610w	620w	620w	610w	620w	

Abbreviations: s = strong, m = medium, w = weak
I = $[CoL(BPBI)_2Cl_2]$, II = $[CoL(BPBI)_2Br_2]$
III = $[CoL(BPBI)_2(NCS)_2]$, IV = [CoL(TPP)]

in the complexes, suggesting that unreacted repeating units of aldehyde remain in the complexes.

In the spectrum of the polymer supported [CoTPP] complex, most of the bands due to the *meso*-tetraphenylporphyrin[262] are also seen. The complex shows the characteristic absorption band of the TPP chelates near 1000 cm^{-1}. This intense band has been attributed to a rocking vibration of the porphyrin ring or the pyrrole units[263]. A medium band is also seen at 1350 cm^{-1} which can be assigned to ν(C-N). This band is seen in the spectrum of free TPP at 1340 cm^{-1}. The shift of this ν(C-N) band to higher frequency during the complexation indicates greater double bond character of the C-N bond in the complex[263]. No significant change was observed

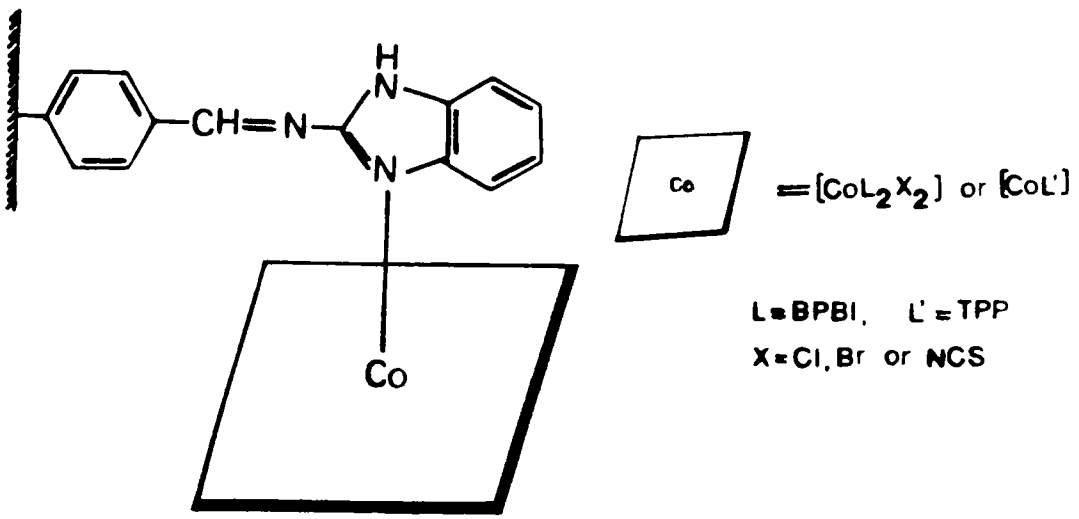

Fig. 7.1 Schematic structure of the complexes

for the numerous C=C stretching vibrations of the phenyl rings. A few bands due to TPP are not seen in the spectra of the complexes, probably they might have been masked by the strong absorptions of the polystyrene support.

Furthermore, definite assignments could not be made for metal-ligand vibrations in the far IR spectra of polymer supported complexes, due to the presence of the difference bands of the polymer ligand in this region.

Schematic diagram of the structure of the complexes presumed from the results obtained are given in Fig. 7.1. However, no conclusive evidence has been obtained to assign the exact structure of these complexes.

CHAPTER VIII

COMPLEXES OF IRON(III), COBALT(II), NICKEL(II) AND COPPER(II) WITH THE SCHIFF BASE DERIVED FROM QUINOXALINE-2-CARBOXALDEHYDE AND GLYCINE

8.1 INTRODUCTION

Schiff bases have gained importance because of the physiological and pharmacological activities associated with them[264-266]. They constitute an interesting class of chelating agents capable of coordination with one or more metal ions and giving mononuclear as well as polynuclear metal complexes which would serve as models for metallo-proteins[267].

In this chapter, the results of our studies on the synthesis and characterization of some new transition metal complexes of the Schiff base derived from glycine and quinoxaline-2-carboxaldehyde are presented. The complexes of this ligand were not studied before. These complexes may be of biological interest, as the glycyl residue is an important and versatile binding site of some proteins and the quinoxalinoyl residues are present in several biologically active polypeptides such as levomycin, actinoleukin and echinomycin[268]. Moreover,

quinoxaline derivatives play an important role in the synthesis of antibiotic peptide, triostin[269].

8.2 EXPERIMENTAL

8.2.1 Materials

Details about the preparation of quinoxaline-2-carboxaldehyde, and all other reagents and solvents employed are given in Chapter II.

8.2.2 Synthesis of the complexes

All the complexes were prepared by the same general procedure. Glycine (0.01 mol, 0.75g) is dissolved in the minimum quantity of 6N NaOH solution. It is mixed with a solution of quinoxaline-2-carboxaldehyde in 25 mL (0.01 mol, 1.58g) ethanol (25 mL). After an hour, the mixture is added to a saturated ethanolic solution of metal chloride (0.01 mol - 1.62g of $FeCl_3$, 2.37g of $CoCl_2.6H_2O$, 2.37g of $NiCl_2.6H_2O$ or 1.70g of $CuCl_2.2H_2O$) and is stirred magnetically for 10 h at room temperature. The complex separated out was filtered, washed several times with ethanol and dried *in vacuo* over anhydrous calcium chloride.
(Yield = 80-90%)

8.2.3 Analytical methods

Details about the analytical methods and other characterization techniques are given in Chapter II.

8.3 RESULTS AND DISCUSSION

The reaction of aldehyde and glycine was carried out in the presence of sodium hydroxide (6N). A semisolid substance was separated, to which addition of an ethanolic solution of metal chlorides yielded complexes with definite stoichiometry.

All the complexes are dark brown, non-hygroscopic and are quite stable to aerial oxidation. The complexes are very slightly soluble in methanol, ethanol, dimethylformamide and dimethyl sulphoxide and therefore, NMR spectra and molar conductance of these complexes could not be recorded. The analytical data (Table VIII.1) show that the complexes have the general empirical formulae $[M_2(QCG)Cl(OH)_2(H_2O)_4]$ for the cobalt(II), nickel(II) and copper(II) complexes and $[Fe_2(QCG)(OH)_4(H_2O)_2]$ for the iron(III) complex. Magnetic susceptibility measurements, analysis of TG curves and examination of electronic and infrared spectra furnish enough clues to suggest a dimeric structure for these complexes. A schematic diagram of the structure of the complexes is shown in Fig. 8.1.

Table VIII.1
Analytical data

Compound (Empirical formula)	C(%) Found (Calc.)	H(%) Found (Calc.)	N(%) Found (Calc.)	M(%) Found (Calc.)	Cl(%) Found (Calc.)
$[Fe_2(QCG)Cl(OH)_4(H_2O)_2]$	28.20	3.40	9.01	24.00	7.59
$(C_{11}H_{16}ClFe_2N_3O_8)$	(28.38)	(3.44)	(9.03)	(24.01)	(7.62)
$[Co_2(QCG)Cl(OH)_2(H_2O)_4]$	27.10	3.78	8.83	24.50	7.31
$(C_{11}H_{18}ClCo_2N_3O_8)$	(27.89)	(3.80)	(8.87)	(24.90)	(7.49)
$[Ni_2(QCG)Cl(OH)_2(H_2O)_4]$	27.30	3.77	8.82	24.20	7.14
$(C_{11}H_{18}ClNi_2N_3O_8)$	(27.90)	(3.80)	(8.88)	(24.82)	(7.50)
$[Cu_2(QCG)Cl(OH)_2(H_2O)_4]$	27.00	3.70	8.69	26.10	7.20
$(C_{11}H_{18}ClCu_2N_3O_8)$	(27.36)	(3.73)	(8.70)	(26.33)	(7.35)

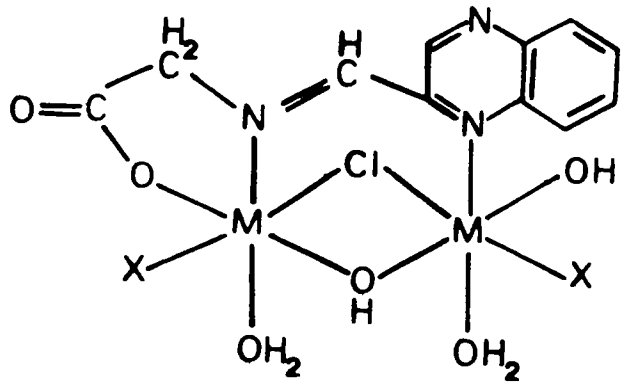

Fig. 8.1 Proposed structure of the complexes

8.3.1 Mangnetic susceptibility measurements

The magnetic moment values of the complexes are given in Table VIII.2. In all the cases, magnetic moments are lower than the usual values for spin-free octahedral complexes. This may be attributed to the antiferromagnetic exchange interaction between the neighbouring metal ions through the bridging chlorine atom and hydroxo group, which also indicates a dimeric structure for the complexes[199].

8.3.2 Electronic spectra

Solid state electronic spectra of the complexes are shown in Fig. 8.2, and the spectral data are given in Table VIII.2. In high spin Fe(III) octahedral complexes, all the d-d transitions are Laporte and spin

Table VIII.2
Magnetic moment and electronic spectral data

Compound	Magnetic moment $\mu_{eff.}$(B.M.)	Abs. max. cm^{-1}	Tentative assignments
$[Fe_2(QCG)Cl(OH)_4(H_2O)_2]$	5.7	24390	Charge transfer
$[Co_2(QCG)Cl(OH)_2(H_2O)_4]$	5.0	30950	Charge transfer
		25000	$^4T_{1g}(F) \longrightarrow {}^4T_{1g}(P)$
		18180	$^4T_{1g}(F) \longrightarrow {}^4A_{2g}(F)$
		8790	$^4T_{1g}(F) \longrightarrow {}^4T_{2g}(F)$
$[Ni_2(QCG)Cl(OH)_2(H_2O)_4]$	2.6	30580	Charge transfer
		25640	$^3A_{2g} \longrightarrow {}^3T_{1g}(P)$
		20830	$^3A_{2g} \longrightarrow {}^3T_{1g}(F)$
		15620	$^3A_{2g} \longrightarrow {}^3T_{2g}(F)$
$[Cu_2(QCG)Cl(OH)_2(H_2O)_4]$	1.6	25000	Charge transfer

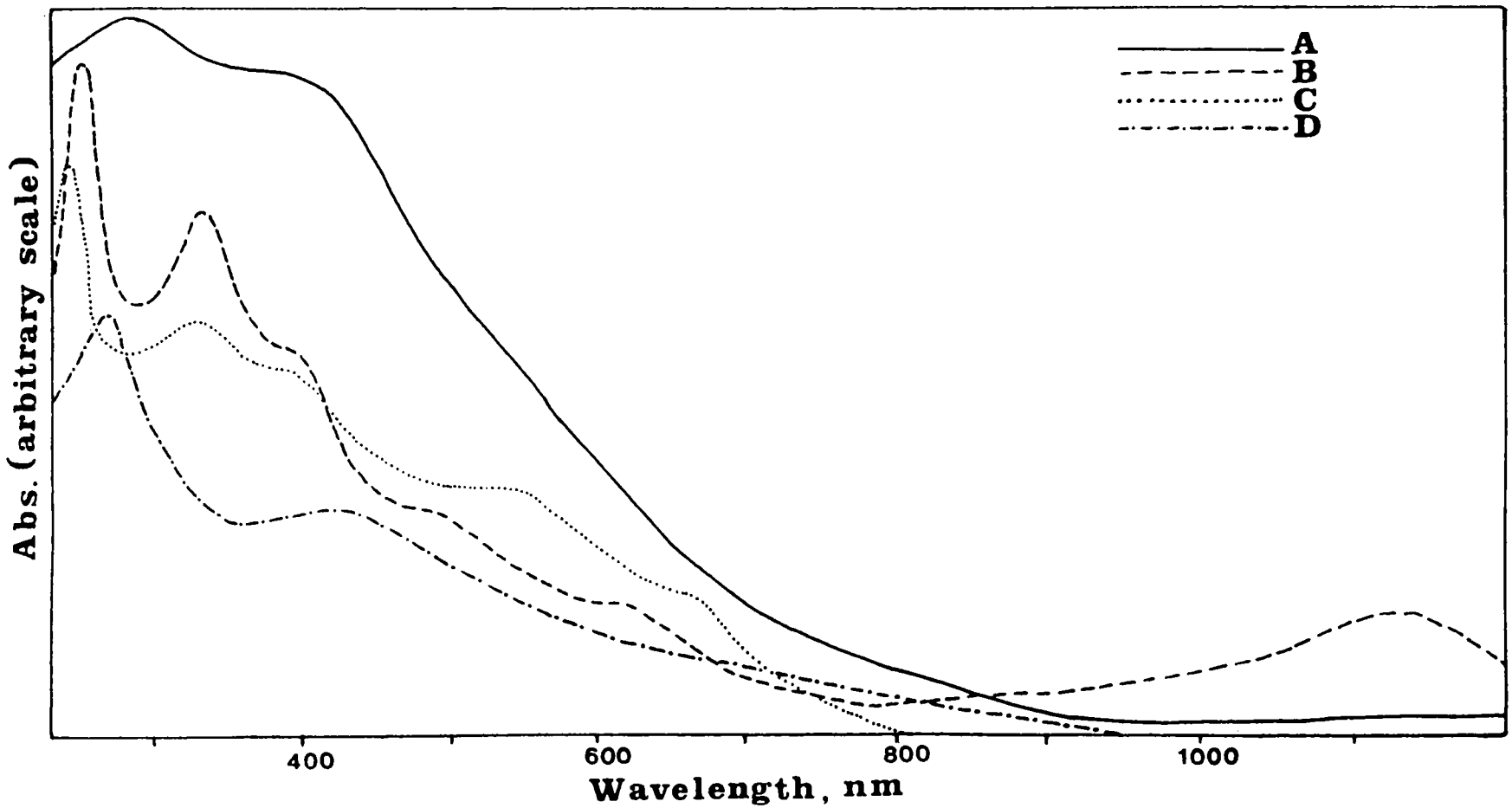

Fig. 8.2 Electronic spectra of the complexes

A = $[Fe_2(QCG)Cl(OH)_4(H_2O)_2]$, B = $[Co_2(QCG)Cl(OH)_2(H_2O)_4]$
C = $[Ni_2(QCG)Cl(OH)_2(H_2O)_4]$, D = $[Cu_2(QCG)Cl(OH)_2(H_2O)_4]$

forbidden and are not observed normally. In the present case only one broad band is observed in the uv-visible region which can be assigned to the charge transfer transition and is sufficiently strong to obscure almost completely the very weak forbidden d-d bands[220].

The cobalt(II) complex shows bands indicative of a high spin octahedral complex[270]. The absorption band observed at 8790 cm^{-1} for this complex can be attributed to the $^4T_{1g}(F) \longrightarrow {}^4T_{2g}(F)$ transition, and the very weak shoulder band at 18180 cm^{-1} can be assigned to the $^4T_{1g}(F) \longrightarrow {}^4A_{2g}(F)$ transition. The $^4T_{1g}(F) \longrightarrow {}^4T_{1g}(P)$ transition appears at 25000 cm^{-1}. The band observed at 30950 cm^{-1} might be due to charge transfer transition.

Three spin allowed transitions are expected for octahedral Ni(II) complexes[271]. These transitions are observed as shoulder bands at 15620 cm^{-1}, 20830 cm^{-1} and 25640 cm^{-1} and are attributed to $^3A_{2g} \longrightarrow {}^3T_{2g}(F)$, $^3A_{2g} \longrightarrow {}^3T_{1g}(F)$ and $^3A_{2g} \longrightarrow {}^3T_{1g}(P)$ transitions respectively. The band observed at 30580 cm^{-1} is due to the charge transfer transition. For the Cu(II) complex, there is a very broad charge transfer band with a maximum around 25000 cm^{-1} which might have obscured all the expected transitions supporting octahedral configuration[272]. The band observed around 40000 cm^{-1}

in all the complexes is due to the electronic transitons within the ligand.

8.3.3 Infrared spectra

As we were not able to isolate the free ligand, the assignments of the infrared bands of the complexes are done based on the infrared spectra of the glycine and quinoxaline-2-carboxaldehyde. Most of the bands due to the glycine and the aldehyde are present in the spectra of the complexes (Table VIII.3). However, as expected, the band due to CHO group of the aldehyde at 1680 cm^{-1} is absent in the spectra of all the complexes.

All the complexes exhibit a very broad band around 3400 cm^{-1} due to OH stretching vibrations. Further, a double hump around 3010 cm^{-1} and a sharp band at 850 cm^{-1} are seen in the spectra of the complexes due to coordinated water molecules[273].

The C=N (ring) stretching vibrations appear as a medium band around 1595 cm^{-1} in quinoxaline-2-carboxaldehyde[224]. In the complexes this band is lowered to 1580 cm^{-1} showing that nitrogen atom of the quinoxaline ring is coordinated to the metal atom. The medium band appearing at 1640 cm^{-1}, which is absent in the spectra of both glycine and the aldehyde, can be

Table VIII.3
Infrared absorption frequencies (cm^{-1})

I	II	III	IV	V	VI	Assignments
3200s	-	3400s	3390s	3400s	3410s	ν(O-H)
-	-	3010m	3010m	3010m	3010m	
-	-	2940m	2920m	2920m	2920m	
-	-	2840w	2840m	2840s	2840m	
-	-	1960m	1955m	1960m	1950m	
-	-	1930m	1930w	1930w	1930m	
-	-	1810w	1810w	1815m	1810w	
-	1680s	-	-	-	-	ν(C=O)
-	-	1640m	1640m	1635m	1640m	ν(C=N)
1610m	-	1600m	1600m	1600m	1600m	ν_a(COO)
-	1595m	1580m	1580w	1580w	1580w	ν(C=N) (ring)
-	1560w	1560w	1560w	1560w	1560w	
-	1480m	1475w	1470w	1480w	1480w	
1445m	-	1445m	1445w	1450w	1450w	
1413m	-	1405m	1405w	1405w	1405w	ν_s(COO)
-	1370w	1370w	1370w	1370w	1370w	
-	1350s	1350m	1350m	1350m	1350m	
1330m	-	1330m	1330m	1330m	1330m	
-	1270m	1270m	1270m	1270w	1275w	
1240s	-	1240m	1240w	1235w	1235m	
-	-	1180m	1180m	1180m	1180m	δ(M-O-H)
1030w	-	1030w	1030w	1030w	1030w	

Table VIII.3 (continued)

-	-	980m	980m	980m	980m	δ(M-O-M)
-	960m	960m	960m	960m	960m	
910w	-	910w	910w	910w	910w	
890m	-	890m	890m	890m	890m	
-	-	850m	850m	850w	850m	δ(H-O-H)
-	840w	835w	840w	835w	835w	
-	750s	750s	750s	750s	750s	
695s	-	700s	700m	700s	700m	
600m	-	600m	605m	605w	600w	
515w	-	515w	515w	515w	515w	
500w	-	500w	505w	500w	500w	
-	-	490m	495m	485m	490m	ν(M-N)
-	-	465m	460m	460m	460m	ν(M-O)
-	430m	430m	430m	425w	430w	

Abbreviations: s = strong, m = medium, w = weak
I = Quinoxaline-2-carboxaldehyde, II = Glycine
III = $[Fe_2(QCG)Cl(OH)_4(H_2O)_2]$, IV = $[Co_2(QCG)Cl(OH)_2(H_2O)_4]$
IV = $[Ni_2(QCG)Cl(OH)_2(H_2O)_4]$, V = $[Cu_2(QCG)Cl(OH)_2(H_2O)_4]$

assigned to the stretching vibrations of the azomethine group of the Schiff base.

In free glycine, asymmetric COO stretching band occurs at 1610 cm^{-1}. This band is almost seen at the same position in the spectra of other Schiff bases derived from glycine[274]. In the present metal complexes, this band appears as a strong band at 1600 cm^{-1}. The band due to the symmetric COO stretching vibration at 1413 cm^{-1} is lowered to 1405 cm^{-1} in these metal complexes. All these indicate participation of COO^- group of the ligand in coordination.

A new band appears in all the complexes around 980 cm^{-1} and 1180 cm^{-1} which might be due to the bridging OH bending and due to M-O-H bending vibrations respectively[212]. A band around 490 cm^{-1} due to ν(M-N) and another band around 460 cm^{-1} due to ν(M-O) are also observed in all the complexes.

8.3.4 Thermal analysis

The thermal behaviour of the complexes of Fe(III), Co(II), Ni(II), and Cu(II) follows almost the same pattern (Fig.8.3). All the complexes are stable upto 120°C and show two DTG peaks. The first DTG peak occurs at 293°C for the iron complex, 330°C for the cobalt and

Table VIII.4
Thermal decomposition data

Compound	DTG peak temp. (°C)	Temp. range in DTG (°C)	Loss(%) from TG found (Calcd.)	Probable composition of expelled group	Composition of the residue
$[Fe_2(QCG)Cl(OH)_4(H_2O)_2]$	293	130-400	27.05(29.90)	$2H_2O$,4OH,1Cl	$Fe_2(QCG)$
	670	468-794	42.49(46.00)	QCG	Fe_2O_3
$[Co_2(QCG)Cl(OH)_2(H_2O)_4]$	330	130-460	25.90(29.88)	$4H_2O$,2OH,1Cl	$Co_2(QCG)$
	518	462-760	43.90(45.20)	QCG	Co_2O_3
$[Ni_2(QCG)Cl(OH)_2(H_2O)_4]$	330	130-410	27.82(29.91)	$4H_2O$,2OH,1Cl	$Ni_2(QCG)$
	534	420-670	40.20(45.25)	QCG	NiO
$[Cu_2(QCG)Cl(OH)_2(H_2O)_4]$	228	120-370	25.96(29.30)	$4H_2O$,2OH,1Cl	$Cu_2(QCG)$
	645	380-850	39.00(44.30)	QCG	CuO

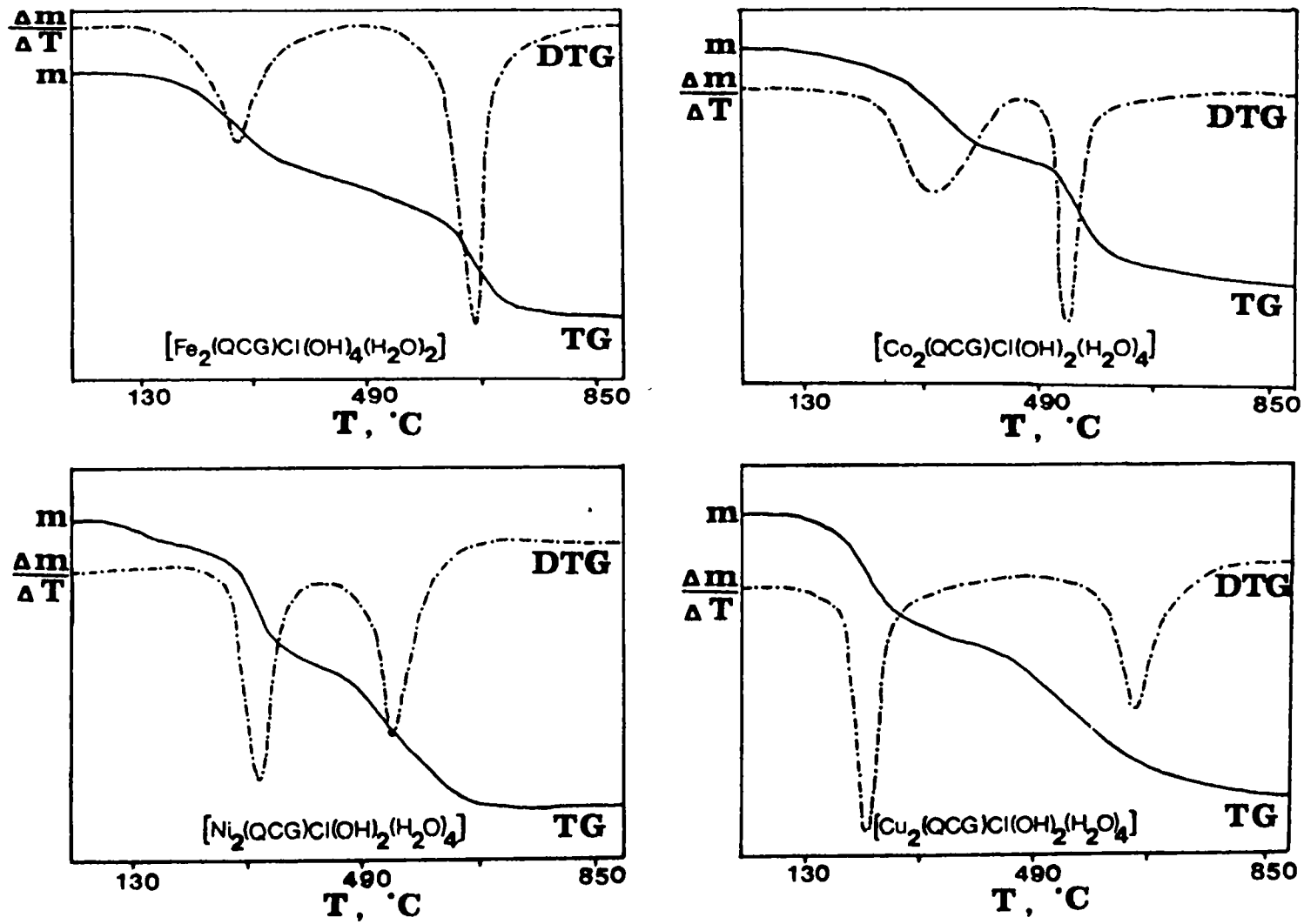

Fig. 8.3 TG and DTG traces of the complexes

nickel complexes, and 228°C for the copper complex (Table VIII.4). The mass loss data for this stage corresponds to the loss of two water molecules, four hydroxyl groups and one chlorine atom for the iron complex, and four water molecules, two hydroxyl groups and one chlorine atom for the rest of the complexes. The TG studies thus agree with the conclusion arrived from IR studies and elemental analyses for the presence of water and hydroxyl groups. A second DTG peak is found at 670°C for the iron complex, 518°C for the cobalt complex, 534°C for the nickel complex and 645°C for the copper complex. Mass loss data suggest that the Schiff base ligand has been expelled during this stage. The product at the end of the decomposition in all the cases was found to be the metal oxides.

CHAPTER IX

COMPLEXES OF COBALT(III), NICKEL(II) AND COPPER(II) WITH QUINOXALINE-2-CARBOXALDEHYDE THIOSEMICARBAZONE

9.1 INTRODUCTION

One of the most fruitful classes of new anticancer drugs that have been examined are heterocyclic thiosemicarbazones. Many thiosemicarbazones derived from compounds with carbonyl group in a position α to a heteroaromatic nitrogen atom have been synthesized and were found to be active against experimental neoplasms[275-277]. Pronounced anticancer activity is seen for the thiosemicarbazones which have a nitrogen heterocyclic ring system and are capable of NNS coordination with a metal ion[278]. It was therefore considered worthwhile to synthesize a thiosemicarbazone ligand with these qualities and study the physico-chemical properties of its complexes. We have synthesized and characterized cobalt(III), nickel(II) and copper(II) complexes with such a ligand, quinoxaline-2-carboxaldehyde thiosemicarbazone (QTSC). The ligand exists probably as an equilibrium mixture of thione (1) and thiol (2) tautomers as shown in Fig. 9.1

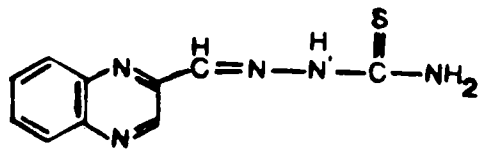

(1)

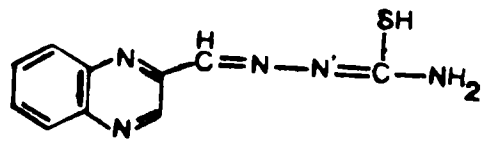

(2)

Fig. 9.1 Tautomeric structures of QTSC

Thione form can act as a neutral ligand, while the deprotonated thiol form can act as a singly charged ligand.

9.2 EXPERIMENTAL

9.2.1 Materials

Details about the preparation of the ligand QTSC, and all other reagents and solvents employed are given in Chapter II.

9.2.2 Synthesis of the complexes

For the preparation of the cobalt complexes, a template synthetic procedure was adopted. Thiosemicarbazide (0.01 mol, 0.91 g), quinoxaline-2-carboxaldehyde (0.01 mol, 1.58 g) and cobaltous halide (0.005 mol- 1.19 g of $CoCl_2.6H_2O$ or 1.08 g of $CoBr_2$)

were dissolved in minimum ethanol and was refluxed on a water bath for 5 h. The precipitated product was filtered, washed with ethanol and dried *in vacuo* over P_2O_5.

Nickel and copper complexes were prepared by a common procedure: A solution of metal halide (0.005 mol- 1.19 g of $NiCl_2.6H_2O$, 1.08 g of $NiBr_2$ or 0.85 g of $CuCl_2.2H_2O$) in DMF (25 mL) was added to a solution of QTSC (0.01 mol, 2.31 g) in DMF (25 mL). The mixture was heated on a water bath for 20 h. Then 10 mL of saturated sodium acetate solution was added to the mixture and was kept aside for 5 h. The complex separated out was filtered off, washed with distilled water containing DMF and dried *in vacuo* over P_2O_5. (Yield = 60-70%)

9.2.3 Analytical methods

Details about the analytical methods and other characterization techniques are given in Chapter II.

9.3 RESULTS AND DISCUSSION

The ligand, QTSC, is soluble in DMF and DMSO and is only very slightly soluble in other solvents. Therefore the complexation was tried in DMF. The complexes could not be isolated from the solution containing QTSC and

the metal salts even after heating it for 24 h. However, the nickel complexes and the copper complexes could be separated by adding acetate solution to such a system. Even this procedure was not successful in the case of the cobalt complexes. Hence a template synthetic procedure was adopted in these cases.

All the complexes are coloured, crystalline, non-hygroscopic and are quite stable to aerial oxidation. The cobalt and the nickel complexes are soluble in methanol, ethanol, acetone, DMF and DMSO; while the copper complex is insoluble in almost all organic solvents. Only the cobalt complexes are soluble in water.

Analytical data and molar conductance data are given in Tables IX.1 and IX.2 respectively. The molar conductivities of 10^{-3} M solutions of the cobalt complexes in methanol at room temperature are in the range 80-90 $ohm^{-1}cm^{2}mol^{-1}$ which suggest that the complexes are 1:1 electrolytes[279]. The values measured for the nickel complexes are in agreement with their non-electrolytic nature. Because of the insolubility, molar conductance of the copper complex could not be measured.

Table IX.1

Analytical data

Compound (Empirical formula)	C(%) Found (Calc.)	H(%) Found (Calc.)	N(%) Found (Calc.)	S(%) Found (Calc.)	X(%) Found (Calc.)	M(%) Found (Calc.)
$[Co(QTSC)_2]Cl$	42.60	3.00	26.10	11.58	6.54	10.65
$(C_{20}H_{16}N_{10}CoS_2Cl)$	(43.29)	(2.89)	(25.25)	(11.54)	(6.39)	(10.63)
$[Co(QTSC)_2]Br$	40.01	2.98	23.60	10.71	13.41	9.75
$(C_{20}H_{16}N_{10}CoS_2Br)$	(40.08)	(2.67)	(23.38)	(10.69)	(13.34)	(9.84)
$[Ni(QTSC)_2(OAc)Cl]$	42.27	3.67	23.59	10.63	6.00	9.57
$(C_{22}H_{21}N_{10}NiS_2O_2Cl)$	(42.92)	(3.73)	(22.76)	(10.40)	(5.76)	(9.54)
$[Ni(QTSC)_2(OAc)Br]$	40.32	3.41	21.90	9.87	12.49	9.04
$(C_{22}H_{21}N_{10}NiS_2O_2Br)$	(40.02)	(3.48)	(21.23)	(9.70)	(12.07)	(8.90)
$[Cu(QTSC)(OAc)(H_2O)]_2$	37.98	3.76	18.53	8.42	-	17.30
$(C_{24}H_{26}N_{10}Cu_2S_2O_4)$	(38.86)	(3.78)	(18.89)	(8.64)		(17.15)

Table IX.2
Molar conductance and magnetic moment data

Compound	Molar conductance $ohm^{-1}\ cm^{2}\ mol^{-1}$	Magnetic moment BM
$[Co(QTSC)_2]Cl$	89	diamagnetic
$[Co(QTSC)_2]Br$	82	diamagnetic
$[Ni(QTSC)_2(OAc)Cl]$	0.6	3.3
$[Ni(QTSC)_2(OAc)Br]$	0.4	3.3
$[Cu(QTSC)(OAc)(H_2O)]$	-	1.5

Analytical data and molar conductance data suggest that the cobalt and the nickel complexes have the general formulae, $[Co(QTSC)_2]X$ and $[Ni(QTSC)_2(OAc)X]$ respectively, while the data for the copper complex are in agreement with the formula, $[Cu(QTSC)(OAc)(H_2O)]_2$ (where QTSC = quinoxaline-2-carboxaldehyde thiosemicarbazone, X = Cl or Br and OAc = acetate).

9.3.1 ^1H NMR spectra

The ^1H NMR spectra of the cobalt complexes were recorded in D_2O. Spectra of the other complexes could not be recorded due to their insufficient solubilities in the common deuterated solvents. In the spectrum of the complex, $[Co(QTSC)_2]Br$, signals due to aromatic protons on the benzene ring appear as a multiplet at δ 7.80-8.40 ppm, whereas the signal due to the proton present in the heterocyclic ring appears as a singlet at δ 9.50 ppm. The corresponding signals appear at δ 7.50-7.75 ppm (multiplet) and δ 9.00 ppm respectively for the complex, $[Co(QTSC)_2]Cl$. The signals due to the azomethine proton appear at δ 9.30 ppm and δ 8.75 ppm for the bromo and chloro complexes respectively. In both the complexes, the $-NH_2$ proton signals appear in the region δ 4.80-5.00 ppm. The integrated areas of the signals are in agreement with the number of protons responsible for these signals.

All the signals of the chloro complexes are seen to experience a downfield shift with respect to those of the bromo complexes, and this might be due to the strong electron withdrawing nature of the chlorine atom.

9.3.2 Magnetic susceptibility measurements

The magnetic moment values of the complexes are given in Table IX.2. The cobalt complexes are found to be diamagnetic which suggests that the complexes are in the +3 oxidation state and have low-spin octahedral structures. Eventhough we have used cobalt(II) salts for the synthesis, we got only cobalt(III) complexes. This suggests that oxidation of the metal has taken place during the complexation reaction. Such type of oxidations are possible during the interaction of cobalt(II) salts with thiosemicarbazones in the presence of air[280].

In the case of the nickel(II) complexes also the magnetic moment value (3.3 BM) is in favour for an octahedral structure[200]. The copper(II) complexes have a magnetic moment value of 1.5 BM which may be attributed to the antiferromagnetic exchange interaction between the neighbouring metal ions. This further indicates a dimeric structure for the copper complex.

9.3.3 Electronic spectra

The electronic spectra of the complexes are shown in Fig. 9.2 and the spectral data are given in Table IX.3. The cobalt(III) complexes show bands indicative of a low-spin, distorted octahedral structure. The absorption bands observed around 10300 cm^{-1}, 20000 cm^{-1} and 24000 cm^{-1} may be attributed to $^1A_{1g} \longrightarrow {}^1A_{2g}$, $^1A_{1g} \longrightarrow {}^1E_g$ and $^1A_{1g} \longrightarrow {}^1T_{2g}$ transitions respectively[220].

Three spin allowed transitions are expected for octahedral nickel(II) complexes[281]. The absorption band observed around 11800 cm^{-1} for the present nickel(II) complexes can be attributed to the $^3A_{2g} \longrightarrow {}^3T_{2g}$ transition and another band around 20000 cm^{-1} can be assigned to the $^3A_{2g} \longrightarrow {}^3T_{1g}(F)$ transition. The $^3A_{2g} \longrightarrow {}^3T_{1g}(P)$ transition appears around 25900 cm^{-1}.

Tetragonal copper(II) complexes are expected to show the transitions $^2B_{1g} \longrightarrow {}^2A_{1g}$, $^2B_{1g} \longrightarrow {}^2B_{2g}$ and $^2B_{1g} \longrightarrow {}^2E_g$, but bands due to these transitions usually overlap to give one broad absorption band[282]. The broad band observed in the present complex around 20000 cm^{-1} suggests that it has tetragonal configuration around copper(II) ion. Further, the electronic spectra of all the complexes exhibit an intense absorption band in the

Table IX.3
Electronic spectral data

Compound	Abs.max. cm^{-1}	Tentative assignments
$[Co(QTSC)_2]Cl$	10330	$^1A_{1g} \longrightarrow {}^1A_{2g}$
	20000	$^1A_{1g} \longrightarrow {}^1E_g$
	23920	$^1A_{1g} \longrightarrow {}^1T_{2g}$
	33000	Charge transfer
$[Co(QTSC)_2]Br$	10280	$^1A_{1g} \longrightarrow {}^1A_{2g}$
	19820	$^1A_{1g} \longrightarrow {}^1E_g$
	24000	$^1A_{1g} \longrightarrow {}^1T_{2g}$
	33000	Charge transfer
$[Ni(QTSC)_2(OAc)Cl]$	11760	$^3A_{2g} \longrightarrow {}^3T_{2g}$
	20280	$^3A_{2g} \longrightarrow {}^3T_{1g}(F)$
	25910	$^3A_{2g} \longrightarrow {}^3T_{1g}(P)$
	31300	Charge transfer
$[Ni(QTSC)_2(OAc)Br]$	11720	$^3A_{2g} \longrightarrow {}^3T_{2g}$
	20000	$^3A_{2g} \longrightarrow {}^3T_{1g}(F)$
	25900	$^3A_{2g} \longrightarrow {}^3T_{1g}(P)$
	30300	Charge transfer
$[Cu(QTSC)(OAc)(H_2O)]$	20000	d-d transitions
	34800	Charge transfer

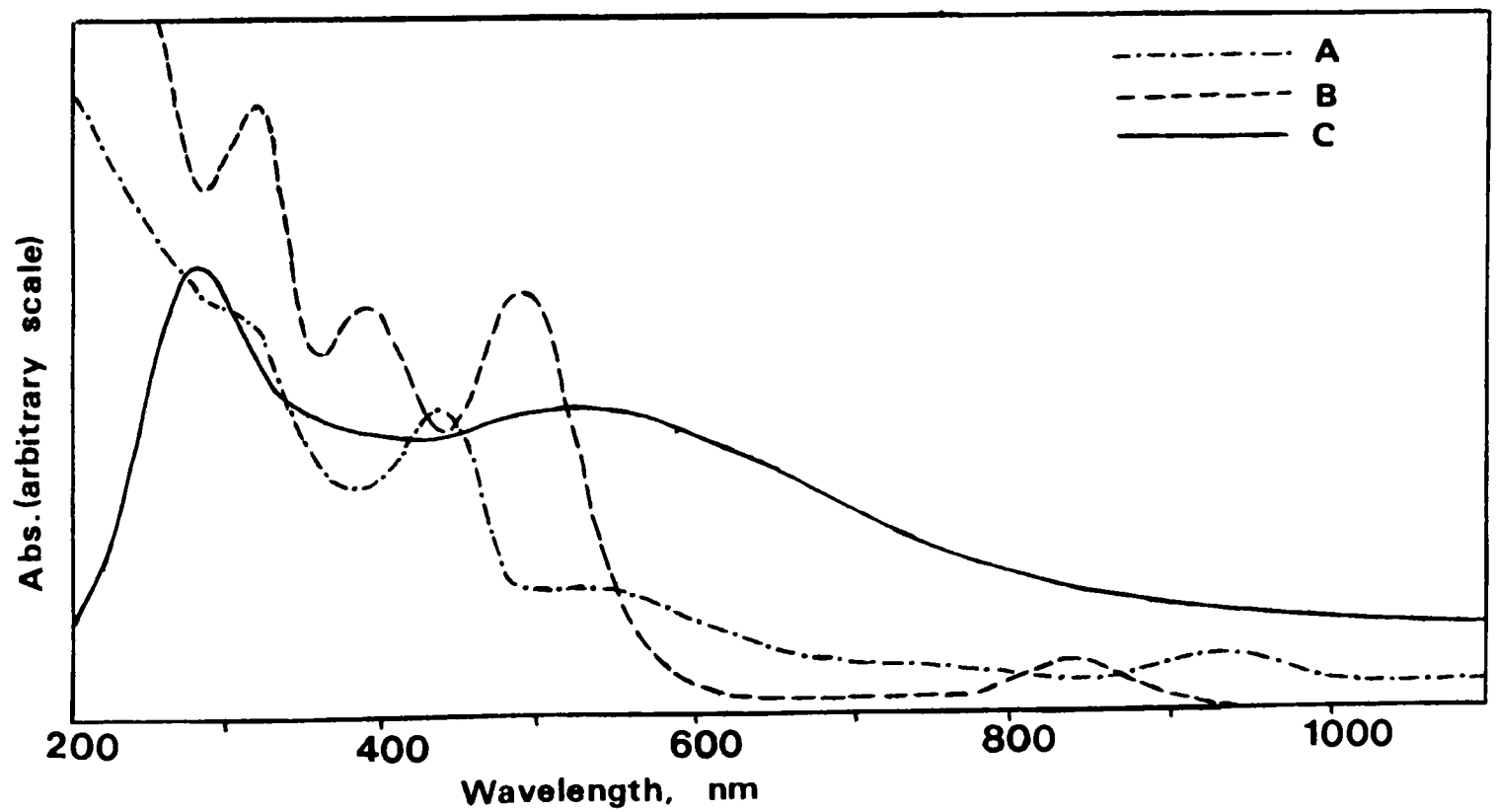

Fig. 9.2 Electronic spectra of the complexes

A = $[Co(QTSC)_2]Cl$, B = $[Ni(QTSC)_2(OAc)Cl]$

C = $[Cu(QTSC)(OAc)(H_2O)]$

region 31000-35000 cm^{-1} which might be due to charge transfer processes.

9.3.4 Infrared spectra

The infrared spectral data (Table IX.4) show that QTSC acts as a uninegative tridentate or a neutral bidentate ligand depending on the metal salt used and the medium of the reaction. Band due to ν(S-H) is not observed in the free ligand indicating that the ligand exists mainly as the thione form in the solid state. The spectra of the ligand and complexes show two bands in the range 3100-3300 cm^{-1} which can be assigned to ν(N-H) vibrations[122]. The ligand exhibits bands around 1640 cm^{-1} and 1010 cm^{-1} which might be due to ν(C=N) of the azomethine linkage and ν(N-N') vibrations respectively[283]. In the spectra of all the present complexes, ν(C=N) band appears at 1625 cm^{-1}. This red shift clearly suggests the involvement of azomethine nitrogen atom in bonding to the metal ion. In the spectrum of the free ligand, ν(C=S) appears as a medium band at 780 cm^{-1}. On complexation, this band is seen to be shifted to 730-700 cm^{-1} indicating participation of the sulphur atom in coordination[284]. The non-ligand band in the region 360-300 cm^{-1} in the far infrared spectra of the complexes can be assigned tentatively to ν(M-N) (azomethine)[285].

Table IX.4
Infrared absorption frequencies (cm^{-1})

L	I	II	III	IV	V	Assignments
-	-	-	-	-	3400s	ν(O-H)
3280s	3300s	3300s	3290s	3280s	3300s	ν(N-H)
3100s	3100s	3100s	3100s	3100s	3100s	
2930s	2910s	2940s	2940m	2930m	3060s	
2345m	2340w	2340w	2340m	2340m	2345m	
1860w	1860w	1860w	1870w	1865w	1870w	
1660w	1660w	1650m	1650m	1650m	1650m	
1640m	1625s	1630s	1625s	1625s	1625s	ν(C=N) (azomethine)
-	-	-	1605s	1605s	-	ν_a(COO)
-	1610s	1610s	-	-	1610s	ν(C=N')
1600s	1580m	1580m	1600s	1600m	1580m	ν(C-N) (quinoxaline)
-	-	-	-	-	1570m	ν_a(COO)
1520s	1525m	1520m	1525m	1520m	1520s	
1485m	1485m	1480m	1480s	1485s	1480s	
1450m	1450w	1455w	1445w	1450w	1455w	
1430w	1425w	1430w	1425w	1430w	1430w	
-	-	-	-	-	1410s	ν_s(COO)
1345m	1350m	1345m	1340s	1340s	1340s	
-	-	-	1315m	1315m	-	ν_s(COO)
1270s	1270w	1270w	1270w	1270w	1270w	
1255s	1255w	1260m	1260m	1260w	1260w	

Table IX.4 (continued)

1210s	1210m	1210m	1210m	1210m	1210m	
1110s	1110s	1110m	1110w	1110w	1110m	
1010m	1015m	1015m	1010m	1010m	1015m	ν(N-N')
970w	965m	970w	975w	970w	970w	
930w	935m	935m	930w	930w	930m	
-	-	-	-	-	870m	$\delta(H_2O)$
865w	860w	860w	860w	860w	860w	
-	-	-	765m	765m	-	δ(COO)
780m	710m	710m	730m	730m	710m	ν(C=S)
660w	660w	660w	660w	660w	660w	
620w	625m	620w	620m	620m	620m	
560s	560m	560m	560w	560w	560m	
470s	470m	470s	470m	470m	470m	
415s	415m	415m	415m	415m	415m	
380w	380w	380w	380w	380w	380w	
370w	370w	370w	370w	370w	370w	ν(M-N)

Abbreviations: s = strong, m = medium, w = weak
L = QTSC, I = $[Co(QTSC)_2]Cl$, II = $[Co(QTSC)_2]Br$
III = $[Ni(QTSC)_2(OAc)Cl]$, IV = $[Ni(QTSC)_2(OAc)Br]$
V = $[Cu(QTSC)(OAc)(H_2O)]_2$

A new band is seen at 1610 cm^{-1} in the spectra of the copper complex and the cobalt complexes which can be attributed to ν(C=N'). Further in these complexes, a blue shift of ν(N-N') band to 1015 cm^{-1} is also observed, which suggests the involvement of thiol form of the ligand in coordination[284]. The band due to the ν(C-N) of the quinoxaline ring[224] shifts to a lower frequency, 1580 cm^{-1}, (This band is observed at 1600 cm^{-1} in the case of the free ligand) suggesting the coordination of this nitrogen atom. Thus, in these complexes, QTSC acts as a uninegative tridentate NNS donor. However, in the case of the copper complex, additional bands are seen at 1570 cm^{-1} and 1410 cm^{-1} which may be due to the asymmetric and symmetric stretching vibrations of the bridging acetate groups,[286] which further supports the magnetic behaviour of the copper complex. The spectrum also exhibits additional bands due to coordinated water[222,223] at 3400 cm^{-1} and 870 cm^{-1}.

The acetate group in the nickel complexes acts as a unidentate ligand and this is supported by the appearance of two new bands at 1605 cm^{-1} and 1315 cm^{-1}, which may be attributed to ν_a(COO) and ν_s(COO) respectively[287]. Further the nickel(II) complexes exhibit δ(COO) at 765 cm^{-1} which is unique for

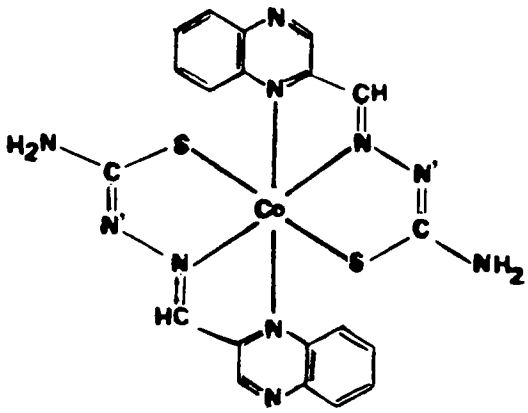

$[Co(QTSC)_2]^+$

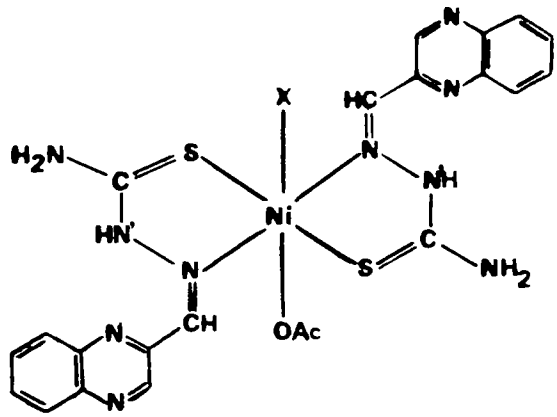

$[Ni(QTSC)_2(OAc)X]$

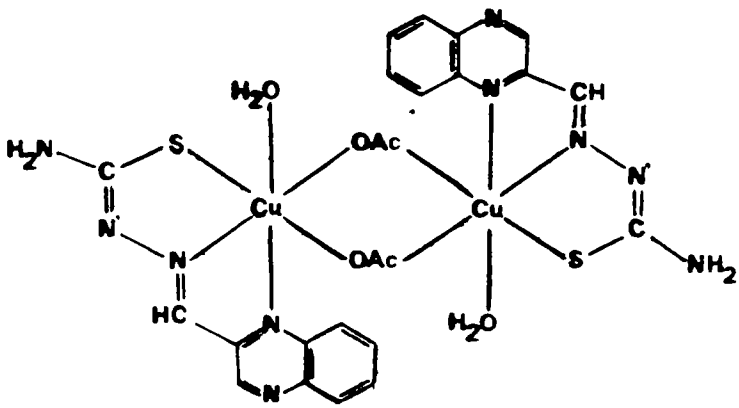

$[Cu(QTSC)(OAc)(H_2O)]_2$

Fig. 9.3 Schematic structures of the complexes

unidentate acetates[212]. The retention of ν(C-N) band of the quinoxaline ring at 1600 cm^{-1} indicates that the nitrogen atom of the ring is not taking part in coordination. Thus in the nickel complexes, the ligand QTSC acts as a neutral bidentate NS donor.

Based on the chemical composition and physico-chemical studies, the schematic structures shown in Fig. 9.3 may be tentatively assigned to these complexes.

SUMMARY

The thesis deals with the synthesis and characterization of some metal complexes of biologically important ligands such as benzimidazoles, Schiff bases derived from amino acids, and thiosemicarbazones.

The thesis is divided into nine chapters. Chapter I presents a discussion on the iron, cobalt, nickel and copper complexes of the above mentioned ligands. The scope of the present investigation is also outlined in this chapter. Chapter II gives detailed information concerning the actual experimental procedures involved.

Chapter III deals with the synthesis and characterization of 1-benzyl-2-phenylbenzimidazole (BPBI) complexes of cobalt(II). The empirical formulae of the complexes agree with $[Co(BPBI)_2X_2]$ (where X = Cl, Br, I or NCS). The complexes are non-electrolytes in nitrobenzene. Electronic spectra and magnetic behaviour suggest that the complexes have a tetrahedral structure. Infrared spectra reveal that the N-3 atom of BPBI is involved in bonding.

Chapter IV is a discussion on the synthesis and characterization of iron(III), cobalt(II), nickel(II) and copper(II) complexes of 1-(2'-hydroxybenzyl)-2-(2'-

hydroxyphenyl)benzimidazole (HBHPBI). The general formula for the cobalt(II), nickel(II) and copper(II) complexes is $[ML(OH)(H_2O)].H_2O$, and for the iron(III) complex, it is $[FeL(OH)_2(H_2O)_2].H_2O$. Octahedral and square planar structures have been assigned for the iron(III) and copper(II) complexes respectively, while the cobalt(II) and nickel(II) complexes have tetrahedral structures. The bonding of the ligand is through the N-3 atom and one of the phenolic OH groups.

In Chapter V, the thermal behaviour of the complexes mentioned in Chapters III and IV are described. All the complexes were subjected to a systematic TG/DTG/DTA analysis. The main decomposition steps in TG were studied further with a view to evaluating the kinetic parameters of decomposition. All the BPBI complexes decompose just after melting, and the decomposition process consists essentially of two stages. The final residue was found to be CoO. The mass loss data indicate the formation of intermediate complexes with approximate compositions $[Co(BPBI)Cl_2]$, $[Co(BPBI)Br_2]$, $[Co(BPBI)I]$, and $[Co(BPBI)_{0.5}(NCS)_2]$ at the end of the first stage of decomposition. The kinetic parameters were calculated using the Coats-Redfern equation. In all the BPBI complexes except the bromo complex, the E_a values for the second

stage of decomposition were found to be much higher than those for the first stage. The anomalously smaller E_a and ΔS values exhibited by the bromo complex for the second stage of decomposition indicate catalytic activity for the intermediate bromo complex. In the case of HBHPBI complexes, the decomposition process consists of two stages for the nickel(II) complex, and three stages for the other complexes. Kinetic parameters were evaluated for each of these stages using Coats-Redfern equation. The rate of decomposition at the final stage seems to have a bearing on the oxygen chemisorption capabilities of the metal oxides formed during this stage.

Synthesis and characterization of HBHPBI complexes of La(III), Pr(III), Nd(III), Sm(III), Eu(III), Gd(III), Tb(III), Dy(III) and Y(III) are presented in Chapter VI. The complexes are of the type, $[LnLCl(OH)(H_2O)_4]$, where Ln = La(III), Pr(III), Nd(III), Sm(III), Eu(III), Gd(III), Tb(III), Dy(III) or Y(III), and L = HBHPBI. The spectral parameters β, $b^{1/2}$, δ(%) and η have been calculated from the solid state electronic spectra of Pr(III), Nd(III) and Sm(III) complexes and these values suggest a weak covalent metal-ligand bond formation. Infrared spectra indicate coordination through one of the phenolic oxygen atoms and N-3 atom of the ligand.

An eight coordinated structure has been proposed for the complexes.

Chapter VII deals with the synthesis and characterization of some polymer bound cobalt(II) complexes of a Schiff base ligand derived from crosslinked polystyrene bound benzaldehyde and 2-aminobenzimidazole. The polymer-metal complexes were obtained when the polymer ligand swollen in $CHCl_3$ was made to react with $[Co(BPBI)_2X_2]$ or [Co(TPP)] (where TPP = *meso*-tetraphenylporphyrin and X = Cl/Br/NCS). The percentages of cobalt and nitrogen in the complexes show that only one Schiff base unit is coordinated to cobalt. Infrared spectra suggest that the bonding of the polymer ligand to cobalt is through the N-3 atom of the benzimidazole moiety. The EPR spectra indicate that the complexes are in the low-spin state and have a square pyramidal environment around cobalt(II).

New complexes of Fe(III), Co(II), Ni(II) and Cu(II) with a Schiff base (L) derived from quinoxaline-2-carboxaldehyde and glycine have been synthesized and characterized. Various studies on these complexes are given in Chapter VIII. The complexes have the general formulae, $[M_2LCl(OH)_2(H_2O)_4]$ for the cobalt(II), nickel(II) and copper(II), and $[Fe_2LCl(OH)_4(H_2O)_2]$ for

the iron(III) complex. A dimeric octahedral structure involving Cl and OH bridges has been proposed for these complexes.

Chapter IX of the thesis deals with the synthesis and characterization of new quinoxaline-2-carboxaldehyde thiosemicarbazone (QTSC) complexes of cobalt(III), nickel(II) and copper(II). Analytical and molar conductance data suggest that the complexes have the empirical formulae, $[Co(QTSC)_2]X_2$, $[Ni(QTSC)_2(OAc)X]$, and $[Cu(QTSC)(OAc)(H_2O)]_2$ (where X = Cl/Br and OAc = acetate). The magnetic and spectral data suggest a distorted octahedral geometry for the complexes. The copper complex appears to be dimeric with bridging acetate groups. The ligand, QTSC, acts as a uninegative tridentate NNS donor in the cobalt and copper complexes, while it acts as a neutral bidentate NS donor in the nickel complexes.

REFERENCES

1. M. N. Hughes, "The Inorganic Chemistry of Biological Processes", 2nd Ed., Wiley, London, 1981.

2. R. W. Hay, "Bio-inorganic Chemistry", Ellis Horwood Limited, England, 1984.

3. H. C. Freeman, "Inorganic Biochemistry", G. L. Eichhorn, Ed., Elsevier, Amsterdam, 1973.

4. J. M. Wood, *Naturewissenschaften*, 62, 357(1975).

5. B. L. Vallee and W. E. C. Wacker, "The Proteins", H. Neurath, Ed., Academic Press, New York, Vol. 5, 1970.

6. T. L. Blundell and J. A. Jenkins, *Chem. Soc. Rev.*, 6, 139(1977).

7. N. Farrell, D. Dolphin and B. R. James, *J. Am. Chem. Soc.*, 100, 324(1978).

8. W. S. Brinigar, C. K. Chang, J. Geibel and T. G. Traylor, *J. Am. Chem. Soc.*, 96, 5597(1974).

9. F. Basolo, B. M. Hoffman and J. A. Ibers, *Acc. Chem. Res.*, 8, 384(1975).

10. J. C. Stevens, P. J. Jackson, W. P. Schammel, G. C. Christoph and D. H. Busch, *J. Am. Chem. Soc.*, 102, 3283(1980).

11. J. P. Collman and K. S. Suslick, *Pure Appl. Chem.*, 50, 951(1978).

12. F. R. N. Gurd and P. E. Wilcox, *Adv. Protein Chem.*, 11, 311(1956).

13. J. E. Falk, "Porphyrins and Metalloporphyrins", Elsevier, Amsterdam, 1964.

14. P. S. Braterman, R. C. Davies and R. J. P. Williams, *Adv. Chem. Phys.*, 7, 359(1964).

15. E. B. Fleischer, *Acc. Chem. Res.*, 3, 105(1970).

16. J. N. Philips, *Rev. Pure Appl. Chem.*, 10, 35(1960).

17. H. H. Inhoffen, *Rev. Pure Appl. Chem.*, 17, 443(1968).

18. R. D. Jones, D. A. Summerville and F. Basolo, *Chem. Rev.*, 79, 139(1979).

19. D. D. Perrin, "Topics in Current Chemistry", Springer-Verlag, New York, Vol. 64, 1976.

20. S. Kirshner, Y. K. Wei, D. Francis and J. G. Bergman, *J. Med. Chem.*, 9, 369(1966).

21. A. J. Thomson, R. J. P. Williams and S. Reslova, "Structure and Bonding", Springer-Verlag, New York, Vol. 11, 1972.

22. P. M. Harrison and R. J. Hoare, "Metals in Biochemistry", Chapman and Hall, London, 1980.

23. A. Albert, "Selective Toxicity", 5th Ed., Chapman and Hall, London, 1973.

24. M. B. Chenoweth, *Pharmacol. Rev.*, 8, 57(1956).

25. M. J. Seven and L. A. Johnson, "Metal Binding in Medicine", J. B. Lippincott Co., Philadelphia, 1960.

26. A. C. Sartorelli and W. A. Creasey, *Ann. Rev. Pharmacol.*, 9, 51(1969).

27. T. N. Pullman, A. R. Lavender and M. Forland, *Ann. Rev. Med.*, 14, 175(1963).

28. M. B. Chenoweth, *Clin. Pharmacol. Therap.*, 3, 365(1968).

29. M. M. Jones, "Metal Ions in Biological Systems", H. Sigel, Ed., Marcel Dekker, Inc., New York, Vol. 16, 1980.

30. P. M. May and R. A. Bulman, *Prog. Med. Chem.*, 20, 225(1983).

31. P. N. Preston, *Chem. Rev.*, 74, 279(1974).

32. A. D. Mighell and S. Santoro, *Acta Crystallogr.*, 27B, 2084(1971).

33. L. G. Marzilli and P. A. Marzilli, *Inorg. Chem.*, 11, 457(1972).

34. R. J. Sundberg and R. B. Martin, *Chem. Rev.*, 74, 471(1974).

35. M. F. Belichi, G. F. Gasparri, C. Pelizzi and P. Tarasconi, *Transition Met. Chem.*, 10, 295(1985).

36. Q. Chen, L. G. Marzilli, N. B. Pahor, L. Randaccio and E. Zangrando, *Inorg. Chim. Acta*, 144, 241(1988).

37. S. Juen, L. Xueyi, C. Liarong and L. Baoshen, *Inorg. Chim. Acta*, 153, 5(1988).

38. M. Goodgame, S. D. Holt, B. Piggott and D. J. Williams, *Inorg. Chim. Acta*, 107, 49(1985).

39. M. V. Capparelli, M. Goodgame, A. C. Skapski and B. Piggott, *Inorg. Chim. Acta*, 92, 15(1984).

40. J. V. Daddigian, V. Mc Kee and C. A. Reed, *Inorg. Chem.*, 21, 1332(1982).

41. P. J. M. W. L. Birker, J. Helder, G. Henkel, B. Krebs and J. Reedijk, *Inorg. Chem.*, 21, 357(1982).

42. A. Toth, C. Floriani, A. Chiesi-Villa and C. Guastini, *Inorg. Chem.*, 26, 3897(1987).

43. J. van Rijn, J. Reedijk, M. Dartmann and B. Krebs, *J. Chem. Soc. Dalton Trans.*, 2579(1987).

44. Y. Nishida and K. Takahashi, *J. Chem. Soc. Dalton Trans.*, 691(1988).

45. S. B. Sanni, H. J. Behm, P. T. Beurskens, G. A. van Albada, J. Reedijk, A. T. H. Lenstra, A. W. Addison and M. P. Palaniandavar, *J. Chem. Soc. Dalton Trans.*, 1429(1988).

46. N. Matsumoto, T. Akui, J. Kanesaka, A. Ohyoshi and H. Okawa, *J. Chem. Soc. Dalton Trans.*, 1021(1988).

47. M. Bukowska-Strzyzewska and A. Tosik, *Acta Crystallogr.*, 39C, 203(1983).

48. N. B. Pahor, W. M. Attia, L. Randaccio, C. Lopez and J. P. Charland, *Acta Crystallogr.*, 43C, 1484(1987).

49. D. M. L. Goodgame, M. Goodgame and M. J. Weeks, *J. Chem. Soc.* A, 1125, 1676(1967).

50. M. G. B. Drew, D. H. Templeton and A. Zalkin, *Inorg. Chem.*, 7, 2618(1968).

51. M. C. Browning, J. R. Mellor, D. J. Morgan, S. A. J. Pratt, L. E. Sutton and L. M. Venanzi, *J. Chem. Soc.*, 693(1962).

52. W. Ludwig and G. Wittmann, *Helv. Chim. Acta*, 47, 1265(1964).

53. M. D. Glonek, C. Curran and J. V. Quagliano *J. Am. Chem. Soc.*, 84, 2014(1962).

54. B. J. Kennedy and K. S. Murray, *Inorg. Chim. Acta*, 134, 249(1987).

55. M. Massacessi, R. Pinna, G. Devoto, E. Barni, P. Savarino and L. S. Erre, *Transition Met. Chem.*, 9, 351(1984).

56. L. K. Thompson, S. K. Mandal, L. Rosenberg, F. L. Lee and E. J. Grabe, *Inorg. Chim. Acta*, 133, 81(1987).

57. A. Maslejova, J. Kohout and J. Gazo, *Inorg. Chim. Acta*, 63, 125(1982).

58. A. W. Addison, H. M. J. Hendriks, J. Reedijk and L. K. Thompson, *Inorg. Chem.*, 20, 103(1981).

59. G. C. Wellon, D. V. Bautista, L. K. Thompson and F. W. Hartstock, *Inorg. Chim. Acta*, 75, 271(1983).

60. N. Shashikala, E. G. Leelamani and G. K. N. Reddy, *Indian J. Chem.*, 21A, 743(1982).

61. M. R. Chaurassia, S. K. Saxena and S. D. Khattri, *Indian J. Chem.*, 20A, 741(1981).

62. K. V. Patel and P. K. Bhattacharya, *Indian J. Chem.*, 21A, 674(1982).

63. N. N. Ghosh, *J. Inorg. Nucl. Chem.*, 36, 1909(1974).

64. A. Furuhashi, T. Nomura, T. Nozawa and S. Edanami, *J. Inorg. Nucl. Chem.*, 37, 1417(1975).

65. N. N. Ghosh and B. Bhattacharya, *J. Inorg. Nucl. Chem.*, 35, 517(1973).

66. B. J. Kennedy, G. D. Fallon, B. M. K. C. Gatehouse and K. S. Murray, *Inorg. Chem.*, 23, 580(1984).

67. A. W. Addison, S. Burman, C. G. Wahlgren, O. A. Rajan, T. M. Rowe and E. Sivin, *J. Chem. Soc. Dalton Trans.*, 11, 2621(1987).

68. J. R. Sams, J. C. Scott and T. B. Tsin, *Chem. Phys. Lett.*, 18, 451(1973).

69. J. R. Sams and T. B. Tsin, *J. Chem. Soc. Dalton Trans.*, 488(1976).

70. K. H. Sugiyarto and H. A. Goodwin, *Aust. J. Chem.*, 40, 775(1987).

71. T. Sakurai, H. Oi and A. Nakahara, *Inorg. Chim. Acta*, 92, 131(1984).

72. A. Bencini and D. Gatteschi, "Transition Metal Chemistry", G. A. Melson and B. N. Figgis, Eds., Marcel Dekker, Inc., New York, Vol. 8, 1965.

73. B. J. Hathway and D. E. Billing, *Coord. Chem. Rev.*, 5, 143(1970).

74. Y. Nakao, M. Onoda, T. Sakurai, A. Nakahara, I. Kinoshita and S. Ooi, *Inorg. Chim. Acta*, 151, 55(1988).

75. M. F. Cabral, J. D. O. Cabral, J. V. Rijn and J. Reedijk, *Inorg. Chim. Acta*, 87, 87(1984).

76. K. Takahashi, E. Ogawa, N. Oishi, Y. Nishida and S. Kida, *Inorg. Chim. Acta*, 66, 97(1982).

77. P. J. M. W. L. Birker, J. Helder and J. Reedijk, *Recl. Trav. Chim. Pays-Bas*, 99, 367(1980).

78. K. J. Morgan, *J. Chem. Soc.*, 2343(1961).

79. D. G. O'Sullivan, *Spectrochim. Acta*, 16, 764(1960).

80. D. J. Rabiger and M. M. Joullie, *J. Org. Chem.*, 29, 476(1964).

81. D. J. Rabiger and M. M. Joullie, *J.Chem. Soc.*, 915(1964).

82. G. Vasilev and K. Davarski, *Dokl. Bolg. Akad. Nauk.*, 35, 1717(1982).

83. M. A. Pujar, T. D. Dharmagouder, S. M. Gaddad and Y. F. Neelgund, *Indian J. Microbiol.*, 27, 75(1987).

84. R. Milanino, E. Concari, A. Conforti, M. Marrella, L. Franco, M. Moretti, G. Velo, K. D. Rainsford and M. Bressan, *Eur. J. Med. Chem.*, 23, 217(1988).

85. J. F. Drake and R. J. P. Williams, *Nature*, 182, 1084(1958).

86. A. H. Corwin and Z. Reyes, *J. Am. Chem. Soc.*, 78, 2437(1956).

87. A. H. Corwin and S. D. Bruck, *J. Am. Chem. Soc.*, 80, 4736(1958).

88. C. R. Chang and T. G. Traylor, *J. Am. Chem. Soc.*, 95, 8475(1973).

89. G. N. Shrauzer, *Acc. Chem. Res.*, 1, 97(1968).

90. T. Sasaki and F. Matsunaga, *Bull. Chem. Soc. Japan*, 42, 1308(1969).

91. R. H. Holm, G. W. Everett, Jr. and A. Chakravorthy, "Progress in Inorganic Chemistry", Interscience, New York, Vol. 7, 1966.

92. E. E. Snell, P. M. Fasella, A. Braunstein and A. Rossi-Fanelli, "Chemical and Biological Aspects of Pyridoxal Catalysis", Macmillan, New York, 1963.

93. T. C. Bruice and S. J. Benkovic, "Bio-organic Mechanisms", Benjamin, New York, Vol. II, 1966.

94. E. E. Snell, A. E. Braunstein, E. S. Severin and Y. M. Torchinsky, "Pyridoxal Catalysis: Enzymes and Model Systems", Wiley, New York, 1968.

95. R. H. Holm, "Inorganic Biochemistry", G. L. Eichhorn, Ed., Elsevier, Amsterdam, 1973.

96. D. Dolphin, R. Poulson and A. Avramovic, "Vitamin B_6 Pyridoxal Phosphate: Chemical, Biochemical and Medicinal Aspects", Wiley, New York, 1986.

97. N. Thankarajan and K. Mohanan, *J. Indian Chem. Soc.*, 63, 861(1986).

98. N. Thankarajan and K. Mohanan, *Indian J. Chem.*, 27A, 360(1988).

99. P. R. Shukla and O. P. Pandey, *J. Indian Chem. Soc.*, 60, 397(1983).

100. H. Okawa, Y. Numata, A. Mio and S. Kida, *Bull. Chem. Soc. Japan*, 53, 2248(1980).

101. Y. N. Belokon, V. M. Belikov, S. V. Vitt, T. F. Saveleva, V. M. Burbelo, V. I. Bakhmutov, G. G. Aleksandrov and Y. T. Struchkov, *Tetrahedron*, 33, 2551(1977).

102. A. M. A. Hassaan, E. M. Soliman and M. El-Shabasy, *Synth. React. Inorg. Met.-Org. Chem.*, 19, 773(1989).

103. M. R. Mahmoud, S. A. El-Gyar, A. A. Moustafa and A. Shaker, *Polyhedron*, 6, 1017(1987).

104. V. V. Ramanujam and B. Sivasankar, *J. Indian Chem. Soc.*, 62, 734(1985).

105. F. Jursik and B. Hajek, *Inorg. Chim. Acta*, 13, 169(1975).

106. L. G. Mac Donald, D. H. Brown and W. E. Smith, *Inorg. Chim. Acta*, 63, 213(1982).

107. L. G. Mac Donald, D. H. Brown, J. H. Morris and W. E. Smith, *Inorg. Chim. Acta*, 67, 7(1982).

108. L. Casella, M. Gullotti, A. Pasini, G. Ciani, M. Manassero and A. Sironi, *Inorg. Chim. Acta*, 26, L1(1978).

109. M. E. Ahmed and E. M. Soliman, *Synth. React. Inorg. Met.-Org. Chem.*, 18, 797(1988).

110. Y. N. Belokon, I. E. Zel'tzer, V. I. Bakhmulov, M. B. Saporovskaya, M. G. Ryzhov, A. I. Yanovsky, Y. T. Struchkov and V. M. Belikov, *J. Am. Chem. Soc.*, 105, 2010(1983).

111. W. L. Kwik and A. W. N. Tay, *Polyhedron*, 9, 1293(1990).

112. F. Paveleik and J. Majer, *Acta Crystallogr.*, 36B, 1645(1980).

113. K. Korhonen and R. Hamalainen, *Acta Crystallogr.*, 37B, 829(1981).

114. T. Ueki, T. Ashida, Y. Sasada and M. Kakudo, *Acta Crystallogr.*, 25B, 328(1969).

115. T. Ueki, T. Ashida, Y. Sasada and M. Kakudo, *Acta Crystallogr.*, 22, 870(1967).

116. T. Ueki, T. Ashida, Y. Sasada and M. Kakudo, *Acta Crystallogr.*, 24B, 1361(1968).

117. D. L. Leussing, *Met. Ions Biol. Syst.*, 5, 1(1976).

118. G. Wilkinson (Ed.), "Comprehensive Coordination Chemistry; The Synthesis, Reactions, Properties and Applications of Coordination Compounds", Pergamon Press, New York, Vol. 6, 1987.

119. L. Casella and M. Gullotti, *Inorg. Chem.*, 25, 1293(1986).

120. Y. N. Belokon, V. I. Bakhmutov, N. I. Chernoglazoa, K. A. Kochetkov, S. V. Vitt, N. S. Garbalinskaya and V. M. Belikov, *J. Chem. Soc. Perkin Trans.*, 2, 305(1988).

121. S. Padhye and G. B. Kauffman, *Coord. Chem. Rev.*, 63, 127(1985).

122. M. J. M. Campbell, *Coord. Chem. Rev.*, 15, 279(1975).

123. S. E. Livingstone, *Q. Rev. Chem. Soc.*, 19, 386(1965).

124. R. B. Singh, B. S. Garg and R. P. Singh, *Talanta*, 25, 619(1978).

125. A. G. Asuero and M. G. Balairon, *Microchem. J.*, 25, 14(1980).

126. V. Divjakovic and V. Leovac, *Cryst. Struct. Commun.*, 7, 689(1978).

127. J. A. McCleverty, N. A. Bailey, S. E. Hull and C. J. Jones, *Chem. Commun.*, 124(1970).

128. M. Mathew and G. J. Palenik, *J. Am. Chem. Soc.*, 91, 4923(1969).

129. M. Mathew and G. J. Palenik, *Inorg. Chim. Acta*, 5, 349(1971).

130. M. Mathew and G. J. Palenik, *J. Am. Chem. Soc.*, 91, 6310(1969).

131. G. W. Bushnell and A. Y. M. Tasang, *Can. J. Chem.*, 57, 603(1979).

132. M. B. Ferrari, G. G. Fava, C. Pelizzi, P. Tarasconi and G. Tosi, *J. Chem. Soc. Dalton Trans.*, 227(1987).

133. A. G. Bingham, H. Bogge, A. Muller, E. W. Ainscough and A. M. Brodie, *J. Chem. Soc. Dalton Trans.*, 493(1987).

134. M. F. Belicchi, G. F. Gasparri, E. Leporati, C. Pelizzi, P. Tarasconi and G. Tosi, *J. Chem. Soc. Dalton Trans.*, 2455(1986).

135. G. Dessy, V. Fares and L. Scaramuzza, *Cryst. Struct. Commun.*, 5, 605(1976).

136. M. Bonamico, G. Dessy, V. Fares and L. Scaramuzza, *Cryst. Struct. Commun.*, 4, 629(1975).

137. N. A. Ryabova, V. I. Ponomarev, L. O. Atomayan, V. V. Zelentzov and V. I. Shipilov, *Sov. J. Coord. Chem.*, 4, 95(1976).

138. N. A. Ryabova, V. I. Ponomarev, L. O. Atomayan, V. V. Zelentzov and V. I. Shipilov, *J. Struct. Chem. U. S. S. R.*, 2, 234(1981).

139. Y. K. Bhoon, *Polyhedron*, 5, 365(1983).

140. K. H. Reddy, *Current Science*, 57, 776(1988).

141. T. T. Bamgboye and O. A. Bamgboye, *Inorg. Chim. Acta*, 133, 247(1987).

142. M. M. S. K. Prakash, L. D. Prabhakar and D. V. Reddy, *Inorg. Chim. Acta*, 141, 179(1988).

143. M. F. Iskander, M. M. Mishrikcy, L. El-Sayed and A. El-Toukhy, *J. Inorg. Nucl. Chem.*, 41, 815(1979).

144. M. Mohan, M. Kumar, A. Kumar, P. H. Madhuranath and N. K. Jha, *J. Inorg. Biochem.*, 32, 239(1988).

145. R. Cao, G. Viciedo and H. Berty, *Rev. Roum. Chim.*, 30, 639(1985).

146. H. B. Singh, S. Maheshwary, N. Wasi and H. Om, *Synth. React. Inorg. Met.-Org. Chem.*, 15, 335(1985).

147. K. Mukkanti, K. B. Pandeya and R. P. Singh, *Synth. React. Inorg. Met.-Org. Chem.*, 15, 613(1985).

148. S. Chandra and K. K. Sharma, *Synth. React. Inorg. Met.-Org. Chem.*, 13, 559(1983).

149. K. Mukkanti, K. B. Pandeya and R. P. Singh, *Synth. React. Inorg. Met.-Org. Chem.*, 16, 229(1986).

150. K. K. Sharma, S. Chandra and A. Jaggi, *Synth. React. Inorg. Met.-Org. Chem.*, 16, 565(1986).

151. S. Chandra and R. Singh, *Synth. React. Inorg. Met.-Org. Chem.*, 17, 869(1987).

152. A. A. El-Asmy, Y. M. Shaibi, I. M. Shedaiwa and M. A. Khattab, *Synth. React. Inorg. Met.-Org. Chem.*, 18, 331(1988).

153. B. Singh and U. Srivastava, *Synth. React. Inorg. Met.-Org. Chem.*, 18, 515(1988).

154. T. T. Bamgboye and O. A. Bamgboye, *Inorg. Chim. Acta*, 105, 223(1985).

155. M. Mohan, P. Sharma and N. K. Jha, *Inorg. Chim. Acta*, 107, 91(1985).

156. K. K. Aravindakshan, *Indian J. Chem.*, 26A, 241(1987).

157. C. J. Jones and J. A. McCleverty, *J. Chem. Soc. A*, 2829(1970).

158. M. J. M. Campbell, R. Grzeskowiak, C. G. Jenkinson and I. D. M. Turner, *Analyst*, 97, 70(1972).

159. W. E. Blumberg and J. Peisach, *J. Chem. Phys.*, 49, 1793(1968).

160. R. Raina and T. S. Srivastava, *Indian J. Chem.*, 22A, 701(1983).

161. L. E. Warren, J. M. Flowers and W. E. Hatfield, *J. Chem. Phys.*, 51, 1270(1969).

162. D. Getz and B. L. Silver, *J. Chem. Phys.*, 52, 6449(1970).

163. C. F. Bell, K. A. K. Lott and N. Hearn, *Polyhedron*, 6, 39(1987).

164. A. El-Dissouky, *Spectrochim. Acta*, 43A, 1177(1987).

165. M. J. M. Campbell and R. Grzekowiak, *J. Chem. Soc. A*, 396(1967).

166. B. A. Gingras, R. W. Hornal and C. H. Bayley, *Can. J. Chem.*, 38, 712(1960).

167. B. A. Gingras, R. L. Somerjai and C. H. Bayley, *Can. J. Chem.*, 39, 973(1961).

168. B. A. Gingras, T. Suprunchuk and C. H. Bayley, *Can. J. Chem.*, 40, 1053(1962).

169. B. A. Gingras and A. F. Siriani, *Can. J. Chem.*, 42, 17(1964).

170. D. M. Wiles, B. A. Gingras and T. Suprunchuk, *Can. J. Chem.*, 45, 469(1967).

171. D. M. Wiles, B. A. Gingras and T. Suprunchuk, *Can. J. Chem.*, 45, 1735(1967).

172. M. Goldstein, E. F. Mooney, A. Anderson and H. A. Gebbie, *Spectrochim. Acta*, 21, 105(1965).

173. G. Domagk, R. Behnisch, F. Mietzsch and H. Schmidt, *Naturwissenschaften*, 33, 315(1946).

174. N. N. Orlova, V. A. Aksenova, D. A. Selidovkin, N. S. Bogdanova and G. N. Pershin, *Russ. Pharm. Toxic.*, 348(1968).

175. D. J. Bauer, L. St. Vincent, C. H. Kempe and A. W. Downe, *Lancet*, 2, 494(1963).

176. H. G. Petering, H. H. Buskirk and G. E. Underwood, *Cancer Res.*, 64, 367(1964).

177. C. W. Johnson, J. W. Joyner and R. D. Perry, *Antibiotics and Chemotherapy*, 2, 636(1952).

178. B. G. Benns, B. A. Gingras and C. H. Bayley, *Appl. Microbiol.*, 8, 353(1961).

179. K. Leibermeister, *Z. Naturforsch. B*, 5, 79(1950).

180. J. A. Crim and H. G. Petering, *Cancer Res.*, 27(1967).

181. H. G. Petering and G. J. van Geissen, "The Biochemistry of Copper", Academic Press, New York, 1966.

182. N. E. Springarn and A. C. Sartorelli, *J. Med. Chem.*, 22, 1314(1979).

183. J. S. Oxford and D. D. Perrin, *Gen. Virol.*, 23, 59(1974).

184. D. L. Klayman, J. P. Scovill and C. F. Franchino, *J. Med. Chem.*, 25, 1261(1982).

185. Y. K. Bhoon, S. Mitra, J. P. Scovill and D. L. Klayman, *Transition Met. Chem.*, 7, 264(1982).

186. L. A. Saryan, K. Mailer, C. Krishnamurti, W. Antholine and D. H. Petering, *Biochem. Pharmacol.*, 30, 1595(1981).

187. G. W. Bushnell and A. Y. M. Tasang, *Can. J. Chem.*, 57, 603(1979).

188. J. S. Oxford and D. D. Perrin, *J. Gen. Virol.*, 23, 59(1974).

189. W. Levison, W. Rhode, P. Mikelens, A. Antony, T. Ramakrishna, *Ann. N. Y. Acad. Sci.*, 284, 525(1977).

190. D. S. Auld, H. Kawaguchi, D. M. Livingstone, B. L. Valle, *Proc. Natl. Acad. Sci. U. S. A.*, 71, 2091(1974).

191. C. L. Leese and H. N. Rydon, *J. Chem. Soc.*, 303(1955).

192. J. M. J. Frechet and K. E. Haque, *Macromolecules*, 8, 130(1975).

193. A. Weissberger, P. S. Proskauer, J. A. Riddick and E. E. Troops, "Organic Solevnts", Interscience, New York, 1956.

194. N. V. Subba Rao and C. V. Ratnam, *Proc. Indian Acad. Sci.*, 43A, 174(1956).

195. A. D. Adler, F. R. Longo, J. D. Finarelli, J. Goldmacher, J. Assour and L. Korsakoff, *J. Org. Chem.*, 32, 476(1967).

196. A. I. Vogel, "A Text Book of Quantitative Inorganic Analysis", Longmans-Green, London, 1978.

197. B. N. Figgis and R. S. Nyholm, *J. Chem. Soc.*, 4190(1958).

198. B. N. Figgis and J. Lewis, "Modern Cordination Chemistry", J. Lewis and R. G. Wilkins, Eds., Interscience, New York, 1960.

199. P. W. Selwood, "Magnetochemistry", Interscience, New York 1958.

200. A. Earnshaw, "Introduction to Magnetochemistry", Academic Press, New York, 1968.

201. B. N. Figgis and J. Lewis, "Progress in Inorganic Chemistry", F. A. Cotton, Ed., Interscience, New York, Vol. 4, 1964.

202. G. Dyer, J. G. Hartley and L. M. Venanzi, *J. Chem. Soc.*, 1293(1965).

203. S. Bahadur, A. K. Gori and R. S. Varma, *J. Indian Chem. Soc.*, 53, 1163(1976).

204. V. M. Reddy, M. A. S. Chary and S. M. Reddy, *Indian Drugs*, 15, 7(1980).

205. R. L. Thompson, *J. Immunol.*, 55, 345(1947).

206. W. R. Doderick, C. W. Nordeen, A. M. von Esdh and H. N. Appell, *J. Med. Chem.*, 15, 655(1972).

207. M. Goodgame and F. A. Cotton, *J. Am. Chem. Soc.*, 84, 1543(1962).

208. R. S. Drago, "Physical Methods in Chemistry", Saunders Company, Philadelphia, 1974.

209. K. S. Bose and C. C. Patel, *J. Inorg. Nucl. Chem.*, 32, 1141(1970).

210. K. S. Bose and C. C. Patel, *J. Inorg. Nucl. Chem.*, 33, 755(1971).

211. P. T. Joseph, C. Pavithran and K. G. K. Warrier, *Transition Met. Chem.*, 3, 286(1978).

212. K. Nakamoto, "Infrared and Raman Spectra of Inorganic and Coordination Compounds", Wiley-Interscience, New York, 1986.

213. A. Sabatini and I. Bertini, *Inorg. Chem.*, 4, 1665(1965).

214. D. M. Adams, "Metal-Ligand and Related Vibrations", Arnold, London, 1967.

215. L. D. Prabhakar, K. M. M. S. Prakash and M. C. Chowdary, *Inorg. Chim. Acta*, 133, 233(1987).

216. L. D. Prabhakar, K. M. M. S. Prakash and M. C. Chowdary, *Synth. React. Inorg. Met.-Org. Chem.*, 19, 937(1987).

217. F. A. Cotton and G. Wilkinson, "Advanced Inrganic Chemistry", Wiley, New York, 1980.

218. M. Baral, B. K. Kanungo and B. Pradhan, *J. Indian Chem. Soc.*, 63, 1018(1986).

219. S. A. Cotton, *Coord. Chem. Rev.*, 8, 184(1972).

220. A. B. P. Lever, "Inorganic Electronic Spectroscopy", Elsevier, New York, 1984.

221. B. V. Patel, K. Desai and B. T. Thaker, *Synth. React. Inorg. Met.-Org. Chem.*, 19, 391(1989).

222. J. R. Ferraro and W. R. Wacker, *Inorg. Chem.*, 4, 1382(1965).

223. I. Gamo, *Bull. Chem. Soc. Japan*, 34, 760(1961).

224. K. Nakanishi and P. H. Solomon, "Infrared Absorption Spectroscopy", Holden-Day, San Fransisco, 1977.

225. T. M. Aminabhavi, N. S. Biradar, V. L. Roddabasanagoudar, W. E. Rudzinski and D. E. Hoffman, *Inorg. Chim Acta*, 121, L45(1986).

226. A. W. Coats and J. P. Redfern, *Nature*, 68, 201(1964).

227. G. T. Natu, S. B. Kulkarni and P. S. Dhar, *J. Therm. Anal.*, 23, 101(1982).

228. P. M. Madhusudanan, K. K. M. Yusuff and C. G. R. Nair, *J. Therm. Anal.*, 8, 31(1975).

229. D. E. Burney, G. H. Weisemann and N. Fragen, *Petrol. Refiner*, 38, 186(1959).

230. D. A. S. Ravens, *Trans. Faraday Soc.*, 55, 1768(1959).

231. M. Yamamoto, T. Minoda, H. Nishino and T. Imoto, *J. Appl. Chem.*, 17, 293(1967).

232. D. Blecic and Z. D. Zivkovic, *Thermochim. acta*, 60, 68(1983).

233. A. C. Norris, M. I. Pope and M. Selwood, *Thermochim. Acta*, 41, 357(1980).

234. A. Srivastava, P. Singh, V. G. Gunjkar and A. P. B. Sinha, *Thermochim. Acta*, 86, 77(1985).

235. G. C. Bond, "Heterogeneous Catalysis: Principles and Applications", Oxford University Press, London, 1974.

236. W. B. Hillig, "Kinetics of High Temerature Processes", W. D. Kingery, Ed., Wiley, New York, 1959.

237. W. Gomes, *Nature*, 192, 865(1961).

238. T. A. Clarke and J. M. Thomas, *Nature*, 219, 1149(1968).

239. T. A. Clarke, E. L. Evans, K. G. Robins and J. M. Thomas, *Chem. Commun.*, 266(1969).

240. J. Sestak, A. Brown, V. Rihak and G. Berggren, "Thermal Analysis", R. F. Schwenker, Jr. and P. D. Garn, Eds., Academic Press, New York, Vol. 2, 1969.

241. J. P. Redfern, "Differential Thermal Analysis", R. C. Mackenzie, Ed., Academic Press, New York, Vol. 1, 1970.

242. J. Sestak, *Talanta*, 13, 567(1966).

243. D. Rainville, "Special Functions", Macmillan & Co., New York, 1960.

244. *Inorg. Chim. Acta*, 139(1987), a special volume containing the papers presented at the 2nd International Conference on the Basic and Applied Chemistry of f-Transition and Related Elements, Lisbon, Portugal, April 6-10, 1987.

245. J. H. Van Vleck and N. Frank, *Phys. Rev.*, 34, 1494(1929).

246. W. T. Carnall, P. R. Fields and K. Rajnak, *J. Chem. Phy.*, 49, 4413(1968).

247. S. S. L. Surana, M. Singh and S. N. Misra, *J. Inorg. Nucl. Chem.*, 42, 610(1980).

248. R. D. Peacock, *J. Chem. Soc. A*, 2028(1971).

249. S. P. Sinha, "Complexes of Rare Earths", Pergamon Press, New York, 1966.

250. S. P. Tandon and P. C. Mehta, *J. Chem. Phys.*, 52, 4313(1970).

251. S. P. Sinha, *Spectrochim. Acta*, 22, 57(1966).

252. D. G. Karraker, *Inorg. Chem.*, 6, 1863(1967).

253. M. M. Mostapa, A. M. Shallaby and A. A. El Asmy, *J. Inorg. Nucl. Chem.*, 43, 2992(1981).

254. B. Dash and S. K. Mahapatra, *J. Inorg. Nucl. Chem.*, 37, 271(1975).

255. S. K. Agarwal and J. P. Tandon, *Monatsh. Chem.*, 110, 401(1979).

256. E. Tsuchida and H. Nishide, "Advances in Polymer Science", Springer-Verlag, Berlin, Vol. 24, 1977.

257. D. Wohrle, "Advances in Polymer Science", Springer-Verlag, Berlin, Vol. 50, 1983.

258. A. D. Adler, F. R. Longo, F. Kampas and J. Kim, *J. Inorg. Nucl. Chem.*, 32, 2443(1970).

259. G. D. Dorough, J. R. Miller and F. M. Huennekens, *J. Am. Chem. Soc.*, 73, 4315(1951).

260. A. K. Saxena, P. Raj and S. K. Dixit, *Synth. React. Inorg. Met.-Org. Chem.*, 20, 199(1990).

261. A. K. Saxena, S. Saxena and A. K. Rai, *Synth. React. Inorg. Met.-Org. Chem.*, 20, 21(1990).

262. D. W. Thomas and A. E. Martell, *J. Am. Chem. Soc.*, 80, 5111(1958).

263. D. W. Thomas and A. E. Martell, *J. Am. Chem. Soc.*, 78, 1338(1956).

264. P. H. Wang, J. G. Keck, E. J. Lien and M. M. C. Lai, *J. Med. Chem.*, 33, 608(1990).

265. A. E. Tai, E. J. Lien, M. M. C. Lai and T. A. Khwaja, *J. Med. Chem.*, 27, 236(1984).

266. X. M. Gao and J. Rhodes, *J. Immunol.*, 144, 2883(1990).

267. A. E. Martell and M. Calvin, "Chemistry of the Metal Chelate Compounds", Prentice-Hall, Inc., Englewood Cliffs, New Jersey, 1952.

268. K. Sato, O. Shiratori and K. Katagiri, *J. Antibiotic., Ser. A*, 20, 270(1967).

269. Y. Tadashi, K. Yasuo and K. Ken, *Progr. Antimicrob. Anticancer Chemother., Proc. Int. Congr. Chemother.*, 2, 1160(1969).

270. S. B. Sharma, *Synth. React. Inorg. Met.-Org. Chem.*, 20, 223(1990).

271. L. L. Martin, R. L. Martin, K. S. Murray and A. M. Surgeson, *Inorg. Chem.*, 29, 1387(1990).

272. S. Ferrer, J. Borras, C. Miratvilles and A. Fuertes, *Inorg. Chem.*, 29, 206(1990).

273. K. S. Siddiqi, S. Tabassum, R. I. Kureshy, N. H. Khan and S. A. A. Zaidi, *Synth. React. Inorg. Met.-Org. Chem.*, 20, 133(1990).

274. D. Heinert and A. E. Martell, *J. Am. Chem. Soc.*, 84, 3257(1962).

275. F. A. French and E. J. Blanz, *Cancer Res.*, 26, 1638(1966).

276. A. J. Lin, K. C. Agrawal and A. C. Sartorelli, *J. Med. Chem.*, 15, 615(1972).

277. E. J. Blanz and F. A. French, *Cancer Res.*, 28, 2419(1968).

278. F. A. French and E. J. Blanz, *J. Med. Chem.*, 9, 585(1966).

279. W. J. Geary, *Coord. Chem. Rev.*, 7, 81(1971).

280. K. K. W. Sun and R. A. Haines, *Can. J. Chem.*, 46, 3241(1968).

281. W. Rosen and D. H. Busch, *Inorg. Chem.*, 9, 262(1970).

282. Y. Nishida and S. Kida, *Coord. Chem. Rev.*, 27, 275(1979).

283. A. Braibanti, F. Delvalla, M. A. Pellinghelli and E. Leporati, *Inorg. Chem.*, 7, 1430(1968).

284. A. A. El-Asmy, Y. M. Shaibi, I.M. Shedaiwa and M. A. Khattab, *Synth. React. Inorg. Met.-Org. Chem.*, 20, 461(1990).

285. R. C. Aggarwal and C. S. Vallabhaneni, *Transition Met. Chem.*, 3, 309(1978).

286. T. A. Stephenson and G. Wilkinson, *J. Inorg. Nucl. Chem.*, 29, 2122(1967).

287. S. D. Robinson and M. F. Uttley, *J. Chem. Soc.*, 1912(1973).